ТЕХНІКА ТА ЕНЕРГЕТИКА

Засновник:
Національний університет біоресурсів і природокористування України

Рік заснування: 2010

*Рекомендовано до друку та поширення
через мережу Інтернет Вченою радою
Національного університету біоресурсів і природокористування України
(протокол № 7 від 23 лютого 2022 р.)*

**Свідоцтво про державну реєстрацію
друкованого засобу масової інформації**
серії КВ № 25126-15066 ПР

Журнал входить до переліку наукових фахових видань України

Категорія «Б». Галузь наук – Технічні.
Спеціальності: 131 – «Прикладна механіка», 133 – «Галузеве машинобудування»
(Наказ Міністерства освіти і науки України від від 17 березня 2020 року № 409)

**Журнал представлено у міжнародних наукометричних базах даних,
репозитаріях та пошукових системах**: Index Copernicus International,
Google Scholar, Фахові видання України,
Національна бібліотека України імені В. І. Вернадського,
AGRIS, BASE, Academic Resource Index ResearchBib

Адреса редакції:
Національний університет біоресурсів і природокористування України
вул. Героїв Оборони, 15, м. Київ, 03041, Україна
E-mail: info@technicalscience.com.ua
www: https://technicalscience.com.ua/uk

MACHINERY & ENERGETICS

Founders:
National University of Life and Environmental Sciences of Ukraine

Year of foundation: 2010

Recommended for printing and distribution
via the Internet by the Academic Council
of National University of Life and Environmental Sciences of Ukraine
(Minutes No. 7 of February 23, 2022)

Certificate of state registration
of the print media
Series KV No. 25126-15066 PR

The journal is included in the list of Professional Scientific Publications of Ukraine
Category "B". Branch of sciences – Technical.
Specialty: 131 – "Applied mechanics", 133 – "Branch mechanical engineering
(Order of the Ministry of Education and Science of Ukraine of March 17, 2020, No. 409)

The journal is presented international scientometric databases, repositories and scientific systems: Index Copernicus International,
Google Scholar, Professional publications of Ukraine,
Vernadsky National Library of Ukraine, AGRIS, BASE,
Academic Resource Index ResearchBib

Editors office address:
National University of Life and Environmental Sciences of Ukraine
03041, 15 Heroiv Oborony, Kyiv, Ukraine
E-mail: info@technicalscience.com.ua
www: https://technicalscience.com.ua/en

Machinery & Energetics
Vol. 13, No. 1. 2022

Journal homepage:
https://technicalscience.com.ua/en

UDC 621.87
DOI: 10.31548/machenergy.13(1).2022.5-10

**Vitaly Lysenko[1*], Ihor Bolbot[1], Oleksiy Martynenko[2],
Taras Lendel[1], Kateryna Nakonechna[1]**

[1]National University of Life and Environmental Sciences of Ukraine
03041, 15 Heroiv Oborony, Kyiv, Ukraine

[2]Dalhousie University, Canada
B3H 4R2, 6299 South Str., Halifax, Canada

Software of a mobile robot for phytomonitoring

Abstract. Currently, the world is intensively expanding the areas of research and use of mobile robots – mechatronic systems based on the latest achievements in mechanics, microprocessor technology, control and measurement systems, computer science, and control theory. To successfully complete a wide range of tasks, robots must have both mobility and the ability to interpret, plan, and automatically perform the resulting task using an on-board computing system. Their special feature is the ability to achieve a given goal in an uncertain external environment, avoiding collisions with stationary obstacles and moving objects. Now the confident functioning of mobile robots can be ensured in relatively familiar and well-structured workspaces. Methods of controlling robots based on well-formulated models and algorithms are developed. When working in an unfamiliar or changing environment, the mobile robot must be able to adapt to changes in the environment, respond to unforeseen situations, and act based on previous experience. Thus, the robot needs a control system with elements of artificial intelligence. As a control object, the robot is a multi-channel nonlinear dynamic system. Despite the fact that a number of studies have been conducted in the field of mobile robot management to date, universal approaches to the synthesis of automatic robot control systems have not been sufficiently developed. The purpose of the study is to substantiate the software of a mobile robot for phytomonitoring. The methodology is an algorithm implemented by this programme, which provides for reading and storing information about the state of plants and the value of technological parameters of the environment in the greenhouse. The paper substantiates a flowchart of the mobile robot control algorithm for phytomonitoring in industrial greenhouses. Given the significant area of an industrial greenhouse and, accordingly, a significant number of plants in it, it is necessary to calculate the distance to which a mobile robot for phytomonitoring can transmit a digital signal. The authors prove that the total power of the channel is equal to the sum of all the powers of the transmitter, receiver, and antenna of the transmitter, the sensitivity of the system, and the loss difference of the transmission system

Keywords: mobile robot, phytomonitoring, control system, closed greenhouse, control algorithm

Article's History: Received: 22.10.2021; Revised: 18.01.2022; Accepted: 23.02.2022

INTRODUCTION

Information about the parameters of the atmosphere and the state of plants (phytostate) in industrial greenhouses is essential and necessary to ensure guaranteed yield [1-3]. Growing plant products in industrial greenhouse plants is accompanied by quite large energy costs (up to 70% of the cost of production).

In addition, the output of products should be provided in the maximum quantity with the appropriate quality. The main factors that affect the profit of a modern indoor enterprise that specialises in growing plant products are considered in [4].

Reduce energy costs for the production of technologically justified volumes of products and ensure their appropriate quality by developing the necessary strategies for managing the production of plant products using the results of monitoring the phytostate and atmospheric parameters by an intelligent mobile robot, which would allow getting the maximum profit of production.

Suggested Citation:
Lysenko, V., Bolbot, I., Martynenko, O., Lendel, T., & Nakonechna, K. (2022). Software of a mobile robot for phytomonitoring, *Machinery & Energetics,* 13(1), 5-10.

*Corresponding author

Analysis of Recent Studies in Ukraine, the production of the range of equipment used to assess the parameters of the atmosphere and plant conditions (phytostate) in closed greenhouses is extremely insufficient. The use of phytomonitoring [5; 6] as the main method of monitoring the technological parameters of plant development in greenhouses is considered in the studies by Guido Fagliaa, Camilla Barattoa, Matteo Pardoa, Massimo Maffeic, Marco Vezzolia, Luca Boarinob, Giorgio Sberveglieria, Simone Bossic [7]. The basis of such developments are sensors for monitoring plant development, and their main disadvantage is their "binding" to one plant [8-10]. The paper by Chr. Lamnatou, D. Chemisana [11] primarily analyses the effect of solar radiation on the plant. Technical means accompanying the maintenance of microclimate parameters in a closed-ground structure were not described.

The purpose of the study is to create software for controlling the mobile phytomonitoring robot, which significantly complements the existing automation systems for vegetable production in industrial greenhouses.

RESULTS AND DISCUSSION

Based on the study results, the structure of the plant production management system in an industrial greenhouse is proposed, which, in addition to conventional components, includes a mobile robot for phytomonitoring, which, moving around the greenhouse area with technological guides, monitors the parameters of the atmosphere and plant phytostate with reference to the location, transmits the information obtained to the existing system for the formation of strategies for managing the production of plant products (Fig. 1).

The structure of the mobile robot for phytomonitoring is shown in (Fig. 1) and it is as follows: the control unit 1 determines the location for measuring phytometric parameters and sends control commands through the digital-to-analogue converter 2 to the actuators 3 of the mobile platform, to move the mobile platform 4 of the device to a given location along the guides that serve to move between the rows of plantings and are both greenhouse heating pipes and a platform for moving the ladder trolley. After reaching the specified location, the device stops and the control unit controls the actuators of the tower, which drive the horizontal sliding mechanisms 5 and ensure the rotation of the tower 6, the operation of the surveillance camera 7 and the movements of the vertical sliding mechanisms 8, equipped with a group of phytoclimatic and phytometric sensors 9 for conducting phytoclimatic, phytometric measurements and plant examination for diseases and pests. The measured values are sent via an analogue-to-digital converter 10 to the control unit, which then sends them to the data transmission unit 11 [12]. After the measurement, the process is repeated in reverse order and the mobile phytomonitoring robot moves to the next measurement point. After making measurements at all the necessary points, the mobile robot for phytomonitoring returns to the starting point or to the charging point of the power supply 12 of the entire device.

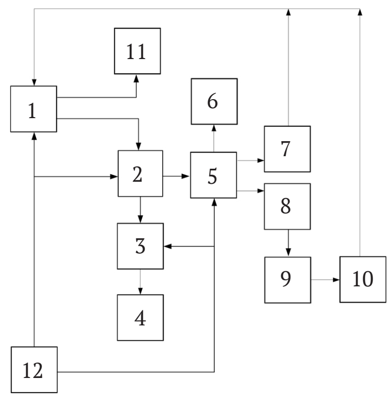

Figure 1. Diagram of links of mobile robot components

A mobile robot for phytomonitoring allows assessing the condition of plants over the entire area of an industrial greenhouse, processing information, and transfering it to the existing system to form a control action to ensure an appropriate microclimate. All this is implemented for the corresponding technological series, since phytometric parameters are measured in an ordinary way, which means that the assessment of plant development is carried out in an ordinary way. The mobile robot for phytomonitoring is equipped with a complex of phytometric sensors for measuring the phytometric parameters of a plant, which are sent through the data transmission unit to the data analysis unit of an industrial computer. A general algorithm for controlling a mobile robot for phytomonitoring in greenhouses was developed (Fig. 2), and for the hardware component of a mobile robot for phytomonitoring, a number of software products were developed that ensure its functioning [13; 14].

All software products run in the software environment of the Raspberry operating system – an analogue of Linux. The operating system was used to create software links between individual software products, which, in turn, manage the hardware components of the mobile robot for phytomonitoring. This operating system is widely used in software and computer engineering. In this case, its functionality allows creating an environment for managing the components of a mobile robot for phytomonitoring.

The Node-RED software environment is used to programme individual components of the mobile robot system for phytomonitoring (Arduino Mega controller), which has an open license, and its interface is shown in Figure 3. This software environment allows developing not only complex production software products in the form of flowcharts, which speeds up their development time for communication with Arduino devices, but also for developing a WEB interface for the purpose of working correctly with them.

The difficulty of developing the proposed software was the use of several programming languages. One of them is JavaScript (the main one for working in Node-Red). The NPM package management system was used for this purpose. This software product is installed on the basis of the Node-Red software environment to extend the functionality of the mobile robot for phytomonitoring. A flowchart for content management is shown in Figure 4.

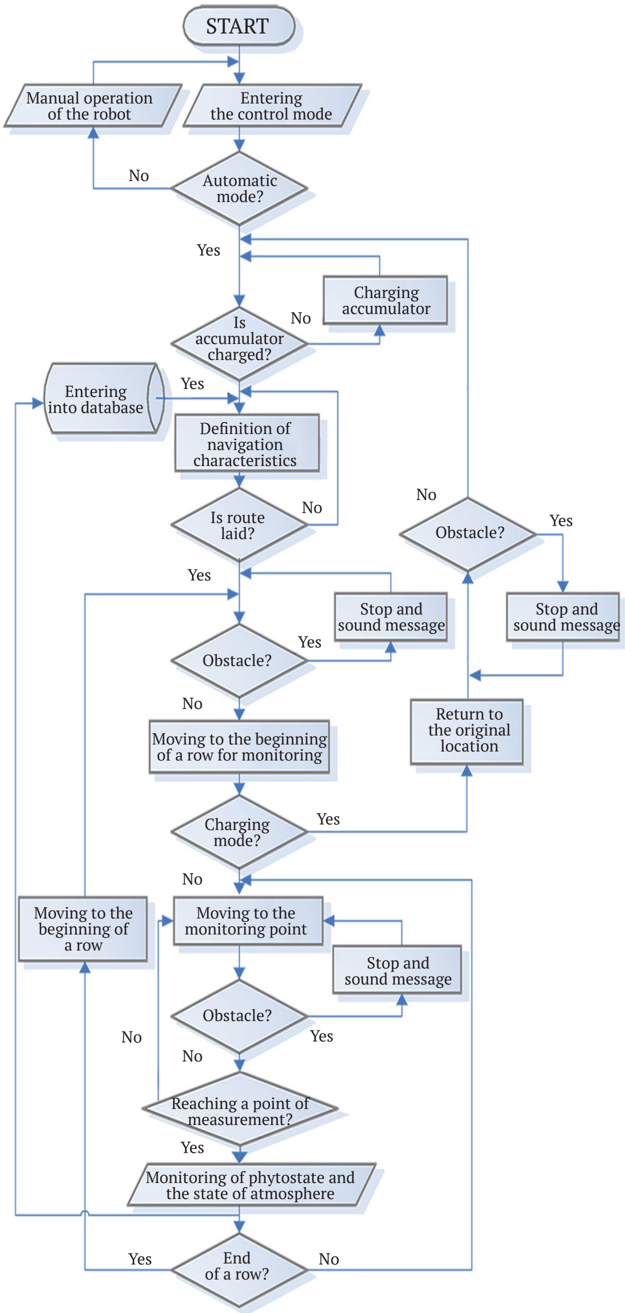

Figure 2. Flowchart of the mobile robot control algorithm for phytomonitoring in industrial greenhouses

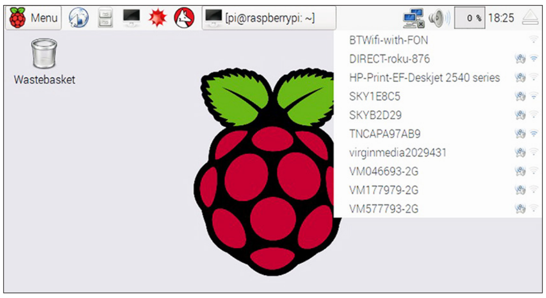

Figure 3. Programming interface for individual components of the mobile robot system for phytomonitoring of the Node-RED software environment

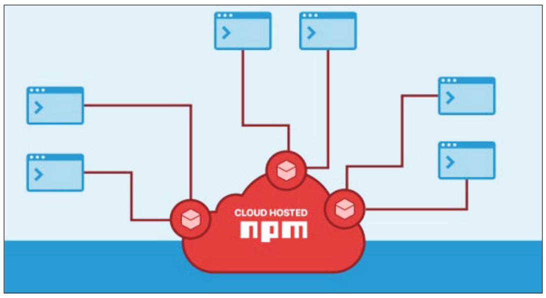

Figure 4. Content management flowchart

Notably, the blocks shown in Figure 3 are already ready-made programme code in JavaScript, where adjustments are made to ensure the performance of the programme as a whole.

In the developed software, the Arduino Mega connects to the Raspberry controller via a USB port and technically provides data transfer. For the correct operation of the entire system, the Arduino controller was initially programmed separately, and appropriate adjustments were made to its programme code. This action was performed to connect the Arduino Mega controller to the Raspberry controller using a specific protocol, the program code is made in the C++ programming language.m At the final stage, the output of information was performed by splitting the data flow, after which it is displayed on a specially designed WEB interface and saved to a file for further use in calculations. The WEB interface of the mobile robot control system for phytomonitoring in an industrial greenhouse is shown in Figure 5.

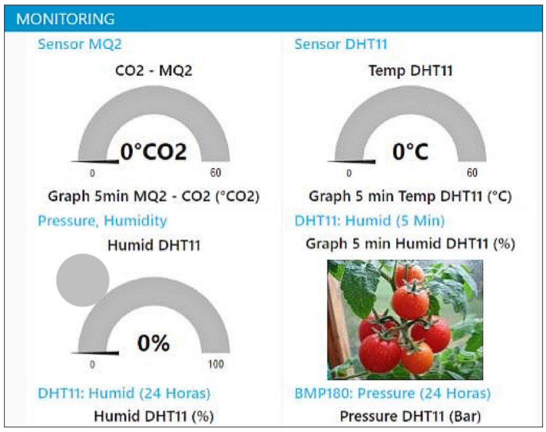

Figure 5. Interface of the mobile robot control system for phytomonitoring

This system also provides for the output of phytometric data. This information is obtained in a contactless way as an image of plants by a camera installed on a mobile robot for phytomonitoring. Analysis and processing of the corresponding phytometric data takes place by using wavelet transformations, when each photo image is decomposed into wavelet wave functions [2; 15].

To manage and gain access to the mobile robot for phytomonitoring, a graphical interface of the operator has been developed as part of: interface of the robot control system (Fig. 6); interface of phytometric and phytoclimatic parameters of plants (Fig. 7); robot settings interface (Fig. 8).

Wi-Fi technology is used to transmit the received data by a mobile robot for phytomonitoring, since this technology provides a high data transfer rate, and has a fairly long range, transmitting a large amount of data within a short period of time, and a high level of security [16-19]. The use of this technology is possible for most modern software environments.

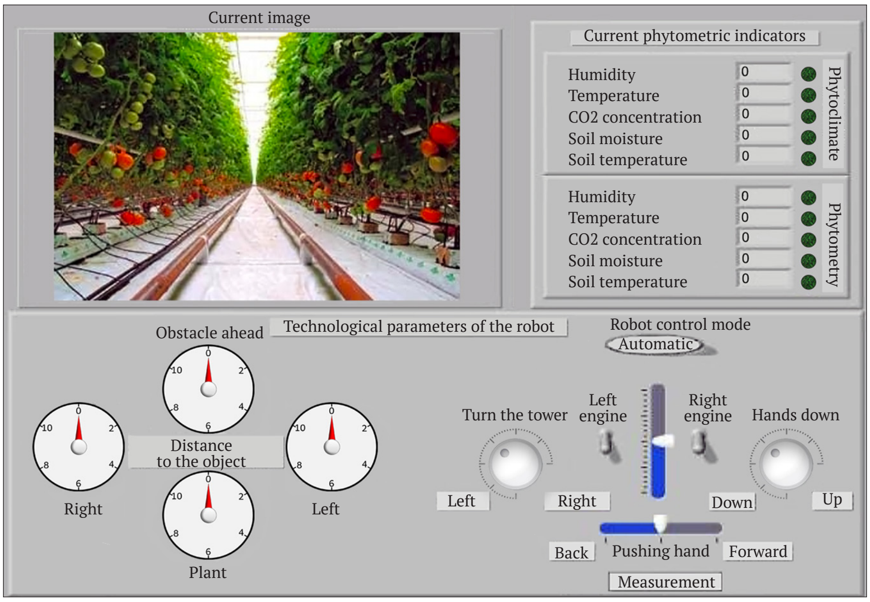

Figure 6. Interface of the mobile robot control system for phytomonitoring

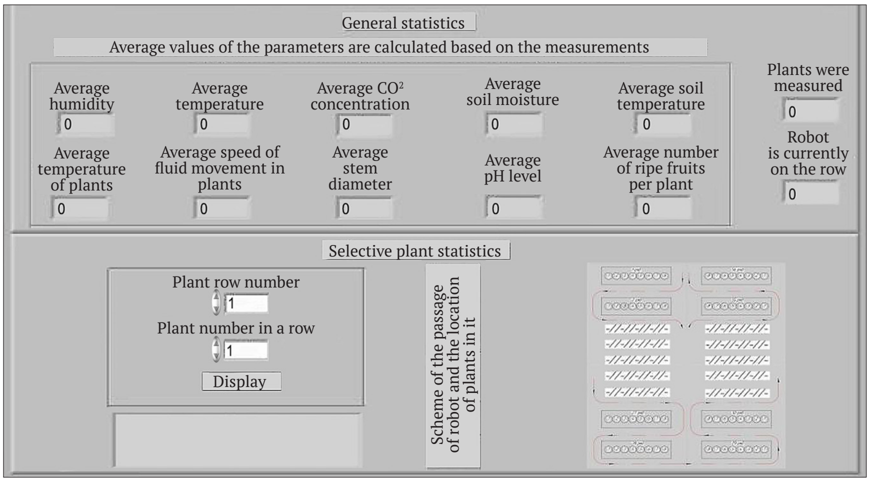

Figure 7. Interface of phytometric and phytoclimatic parameters of plants

The wireless local area network standard is used to transmit the received data from the mobile phytomonitoring robot to the control system. Considering the significant area of an industrial greenhouse and, accordingly, a significant number of plants in it, it is necessary to calculate the distance to which a mobile robot for phytomonitoring can transmit a digital signal:

$$D = 10^{\left(\frac{FSL}{20} - \frac{33}{20} logF\right)} \quad (1)$$

where: F – transmission channel frequency, MHz; FSL (Free Space Loss) – losses in the digital signal space, dB.

Losses in the digital signal space are defined as

$$FSL = Y - S \quad (2)$$

where: S – channel gain margin, dB; Y – total channel power, dB.

To perform the necessary calculations, it is assumed that the channel gain margin is 20 dB.

The total power of the channel is equal to the sum of all the powers of the transmitter, receiver, and antenna of the transmitter, the sensitivity of the system and the loss difference of the transmission system used

$$Y = Pt - Pmin + Gt + Gr - Lt - Lr \quad (3)$$

where: Pt – transmitter power, dB; Gr – receiving antenna gain, dB; Gt – transmission antenna gain, dB; $Pmin$ – receiver sensitivity at the specified transmission rate, dB; Lr – signal losses in the coaxial cable and reception clock connectors, dB; Lt – signal losses in the connectors of the transmission path and coaxial cable, dB.

To calculate the wireless network, input data was used: the router's operating frequency is 2,474 MHz, the transmission rate is 6 Mbit/s, its sensitivity is 88 dB. Hence, the total power of the transmission channel is determined:

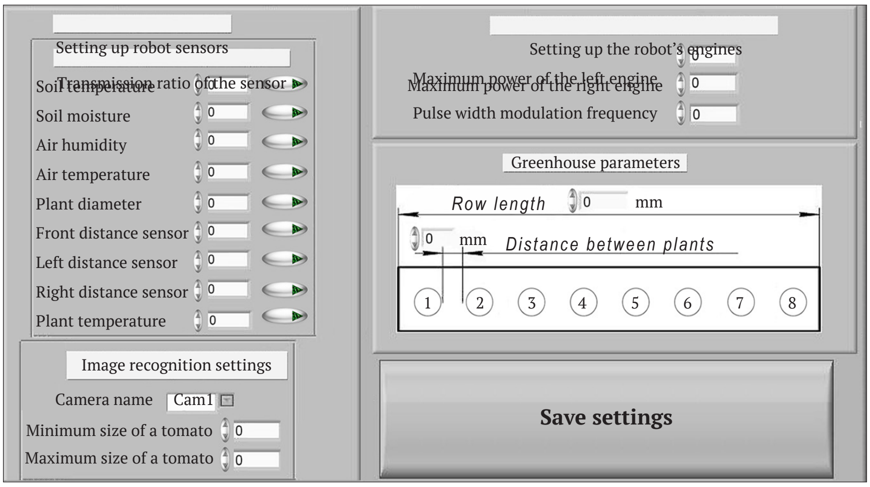

Figure 8. Robot settings interface

Y=18+88+5+5-3-3=110 (dB).

Accordingly, the losses in space will amount to:

FSL=110-20=90 (dB).

Then the distance to which information can be transmitted will be equal to:

$$D = 10^{\left(\frac{90}{20}-\frac{33}{20}-lg2472\right)} = 0.282\ (km).$$

The calculated digital signal transmission distance for the developed mobile robot for phytomonitoring ensures reliable information acquisition, considering the design dimensions of an industrial greenhouse.

The mobile robot for phytomonitoring in an industrial greenhouse is used in conjunction with an intelligent control system for energy flows of the greenhouse, which allows the existing control system to form appropriate control strategies for electrical complexes to consider the spatial distribution of phytometric parameters, and to qualitatively control and perform a number of additional functions necessary for production: to control the parameters of the microclimate and conduct plant phytomonitoring, collect and process the received information of technological parameters in an industrial greenhouse; to create data archives for further use; to function in automatic, manual, and remote control modes of the mobile robot.

CONCLUSIONS

1. The structure of the plant production management system in an industrial greenhouse has been developed, which, in addition to traditional components, includes a mobile robot for phytomonitoring.

2. A general control algorithm and software for using a mobile robot for phytomonitoring in industrial greenhouses based on the use of Node-RED and Processing/Wiring software environments have been developed.

3. It is recommended for hardware and software interactions of heterogeneous technical tools that are components of a mobile robot for phytomonitoring, using a flexible ROS platform; this creates conditions for ensuring the client-server architecture of a mobile robot and evenly distributing computing power.

4. The maximum distance of reliable digital signal transmission for a measuring complex in an industrial greenhouse is calculated – up to 282 metres.

REFERENCES

[1] Fonteijn, H., Afonso, M., Lensink, D., Mooij, M., Faber, N., Vroegop, A., Polder, G., & Wehrens, R. (2021). Automatic phenotyping of tomatoes in production greenhouses using robotics and computer vision: From theory to practice. *Agronomy*, 11(8), article number 1599.

[2] Burud, I., Lange, G., Lillemo, M., Bleken, E., Grimstad, L., & From, P. (2017). Exploring robots and UAV's as phenotyping tools in plantbreeding. *IFAC – PapersOnLine*, 50(1), 11479-11484.

[3] Mao, S., Li, Y., Ma, Y., Zhang, B., Zhou, J., & Wang, K. (2020). Automatic cucumber recognition algorithm for harvesting robots in the natural environment using deep learning and multi-feature fusion. *Computers and Electronics in Agriculture*, 170, article number 105254.

[4] Walter, M.S.J. (2019). Dimensional and geometrical tolerances in mechanical engineering – a historical review. *Machine Design*, 3, 67-74.

[5] Ouammi, A., Achour, Y., Zejli, D., & Dagdougui, H. (2020). Supervisory model predictive control for optimal energy management of networked smart greenhouses integrated microgrid. *Automation Science and Engineering IEEE Transactions*, 17(1), 117-128.

[6] Bodrov, V., Bodrov, M., & Kuzin, V. (2017). Ensuring the parameters of microclimate of hothouses during a warm season. *ARPN Journal of Engineering and Applied Sciences*, 12(6), 1864-1869.

[7] Revathi, S., Radhakrishnan, T.K., Sivakumaran, N. (2017). Climate control in greenhouse using intelligent control algorithms. In *Proceedings of the American control conference* (pp. 887-892). Seattle: Seattle University.

[8] Nazarenko, I., Mishchuk, Y., Mishchuk, D., Ruchynskyi, M., Rogovskii, I., Mikhailova, L., Titova, L., Berezovyi, M., & Shatrov, R. (2021). Determiantion of energy characteristics of material destruction in the crushing chamber of the vibration crusher. *Eastern-European Journal of Enterprise Technologies*, 4(7(112), 41-49.

[9] Vovna, O., Laktionov, I., Sukach, S., Kabanets, M., & Cherevko, E. (2018). Method of adaptive control of effective energy lighting of greenhouses in the visible optical range. *Bulgarian Journal of Agricultural Science*, 24(2), 335-340.
[10] Ouammi, A., Achour, Y., Dagdougui, H., & Zejli, D. (2020). Optimal operation scheduling for a smart greenhouse integrated microgrid. *Energy for Sustainable Development*, 58, 129-137.
[11] Baratto, C., Faglia, G., Pardo, M., Vezzoli, M., Boarino, L., Maffei, M., Bossi, S., & Sberveglieri, G. (2005). Monitoring plants health in greenhouse for space missions. *Sensors and Actuators B: Chemical*, 108(1-2), 278-284.
[12] Lysenko, V.P., Zhyltsov, A.V., Bolbot, I.M., Lendiel, T.I., & Nalyvaiko, V.A. (2020). Phytomonitoring in the phytometrics of the plants. *E3S Web of Conferences*, 154, article number 07012.
[13] Mu, Y., Chen, T.S., Ninomiya, S., & Guo, W. (2020). Intact detection of highly occluded immature tomatoes on plants using deep learning techniques. *Sensors*, 20(10), article number 2984.
[14] Rogovskii, I.L., Titova, L.L., Gumenyuk, Yu.O., & Nadtochiy O.V. (2021). Technological effectiveness of formation of planting furrow by working body of passive type of orchard planting machine. *IOP Conference Series: Earth and Environmental Science*, 839, article number 052055.
[15] Lamnatou, Chr., & Chemisana, D. (2013). Solar radiation manipulations and their role in greenhouse claddings: Fresnel lenses, NIR- and UV-blocking materials. *Renewable and Sustainable Energy Reviews*, 18, 271-287.
[16] Tang, Y.C., Wang, C., Luo, L., Li, J., Lian, G., & Zou, X. (2020). Recognition and localization methods for vision-based fruit picking robots: A review. *Frontiers in Plant Science*, 11, article number 510.
[17] Bac, C.W., Hemming, J., van Tuijl, B., Barth, R., Wais, E., & van Henten, E.J. (2017). Performance evaluation of a harvesting robot for sweet pepper. *Journal of Field Robot*, 34, 1123-1139.
[18] Mráz, M., Urbanovičová, O., & Findura, P. (2019). Use of information systems to support decision making according to analysis machines. *Agricultural Machinery*, 2, 89-93.
[19] Lysenko, V., Bolbot, I., Lendiel, T., Nurseitova, K., & Amirgaliyev, Y. (2021). Mobile robot with optical sensors for remote assessment of plant conditions and atmospheric parameters in an industrial greenhouse. *Photonics Applications in Astronomy, Communications, Industry, and High Energy Physics Experiments*, 12040, 80-89.

Віталій Пилипович Лисенко[1], Ігор Михайлович Болбот[1], Олексій Іванович Мартиненко[2], Тарас Іванович Лендєл[1], Катерина Віталіївна Наконечна[1]

[1]Національний університет біоресурсів і природокористування України
03041, вул. Героїв Оборони, 15, м. Київ, Україна

[2]Університет Далхоусі, Канада
B3H 4R2, вул. 6299 South Str., Галіфакс, Канада

Програмне забезпечення мобільного робота для фітомоніторингу

Анотація. Нині у світі інтенсивно розширюються галузі досліджень та використання мобільних роботів – мехатронних систем, що базуються на останніх досягненнях механіки, мікропроцесорної техніки, контрольно-вимірювальних систем, інформатики та теорії управління. Для успішного виконання великого кола завдань роботи повинні мати як мобільність, так і здатність інтерпретувати, планувати і автоматично виконувати отримане завдання, використовуючи бортову обчислювальну систему. Їх особливість – можливість досягнення заданої мети в невизначеному зовнішньому середовищі, уникаючи зіткнень зі стаціонарними перешкодами та рухомими об'єктами. Зараз впевнене функціонування мобільних роботів може бути забезпечене щодо знайомих і добре структурованих робочих просторах. Розвинуто методи управління роботами на основі добре сформульованих моделей та алгоритмів. При роботі в незнайомому або змінному оточенні мобільний робот повинен мати здатність адаптуватися до змін у навколишньому середовищі, реагувати на непередбачені ситуації та діяти на підставі попереднього досвіду. Таким чином, робот потребує системи управління з елементами штучного інтелекту. Як об'єкт керування робот є багатоканальною нелінійною динамічною системою. Незважаючи на те, що до теперішнього часу проведено цілу низку досліджень у галузі управління мобільними роботами, універсальні підходи до синтезу систем автоматичного управління роботами розроблені недостатньо. Мета дослідження полягає в обґрунтуванні програмного забезпечення мобільного робота для фітомоніторингу. Методологія є алгоритмом, що реалізується зазначеною програмою, передбачає зчитування та зберігання інформації про стани рослин та значення технологічних параметрів навколишнього середовища в теплиці. В статті обґрунтовано блок-схему алгоритму керування мобільним роботом для фітомоніторингу у промислових теплицях. Враховуючи, значну площу промислової теплиці і відповідно значну кількість рослин у ній, потрібно розрахувати відстань, на яку мобільний робот для фітомоніторингу може передати цифровий сигнал. Авторами доведено, що сумарна потужність каналу дорівнює сумі всіх потужностей передавача, приймача і антени передавача, чутливості системи та різниці втрат системи передачі

Ключові слова: мобільний робот, фітомоніторинг, система керування, споруда закритого ґрунту, алгоритм керування

Machinery & Energetics
Vol. 13, No. 1. 2022

Journal homepage:
https://technicalscience.com.ua/en

UDC 621.87
DOI: 10.31548/machenergy.13(1).2022.11-17

Vyacheslav Loveykin[1*], Yuriy Romasevych[1], Tadeus Złoto[2], Anastasia Lyashko[1], Oleg Diachenko[1]

[1]National University of Life and Environmental Sciences of Ukraine
03041, 15 Heroiv Oborony, Kyiv, Ukraine

[2]Polytechnic of Czestochowa
42201, 69 Jan Henryk Dombrowski Str., Częstochowa, Republic of Poland

Optimisation of start-up power mode of rotation mechanism of manipulator crane with a cylindrical articulated load suspension

Abstract. The study deals with the problem of improving the efficiency of the manipulator crane by selecting the driving modes of the rotary mechanism drive during the start-up process. When manipulator cranes operate in areas of transients, significant dynamic loads occur, which lead to swinging of the load on the articulated suspension. This leads to a decrease in the productivity and reliability of the crane manipulator and an increase in the energy consumption of the rotary mechanism drive. It is proposed to reduce dynamic loads during the operation of the turning mechanism in the areas of transients (starting, braking) of the manipulator crane by optimising the driving mode of the drive mechanism. In this case, the manipulator crane is presented in the form of a two-mass dynamic model, where the first mass is the rotary part of the manipulator crane with a drive mechanism, and the second mass is a load on a cylindrical hinge suspension. The purpose of the study is to improve the efficiency of the crane manipulator by optimising the starting mode of the turning mechanism. The methodology is optimal driving modes of crane mechanisms, which minimise the effect of dynamic loads, and provide for optimisation criteria based on the RMS values of the driving forces of the drives. The developed dynamic model allowed constructing a mathematical model described by a system of nonlinear differential equations. Optimisation of the movement mode of the crane manipulator rotation mechanism is carried out by minimising the integral dynamic criterion, which is the RMS value of the driving torque of the drive during the transition process. As a result of the optimisation carried out, the starting mode of the crane manipulator rotation mechanism is found, which minimises power loads and load fluctuations on the articulated suspension in the radial direction. The resulting optimal starting mode of the turning mechanism allowed increasing the productivity and reliability of the manipulator crane, and reducing the energy costs of the drive

Keywords: tower crane, turning mechanism, optimal control, cylindrical hinge suspension, load oscillation

Article's History: Received: 28.10.2021; Revised: 24.01.2022; Accepted: 23.02.2022

INTRODUCTION

During the operation of the manipulator crane rotation mechanism, dynamic loads occur in the drive elements, which lead to the rocking of the load on the hinge suspension and, as a result, reduce the productivity and reliability of the manipulator, and increase energy costs. These loads are especially dangerous during the transition processes of starting and braking the turning mechanism, when the driving or braking forces rarely increase or decrease. At this time, both high-frequency vibrations of the drive elements and low-frequency vibrations of the load on the articulated suspension are generated.

It is possible to reduce dynamic loads in the drive elements and the manipulator structure by selecting a favourable mode of movement of the drive rotation mechanism during transients. The most effective method for choosing a favourable mode of movement of the crane manipulator rotation mechanism is methods for optimising driving modes and, in particular, variational methods. Therefore, it is advisable to optimise the rotation mode of the manipulator crane according to the selected criterion. Since power loads are the most dangerous for a manipulator crane, the optimisation criterion should reflect these

Suggested Citation:
Loveykin V., Romasevych Yu., Złoto T., Lyashko A., & Diachenko O. (2022). Optimisation of start-up power mode of rotation mechanism of manipulator crane with a cylindrical articulated load suspension, *Machinery & Energetics,* 13(1), 11-17.

*Corresponding author

loads. This criterion can be the RMS value of the driving torque of the turning mechanism during start-up or braking. Minimising the selected criterion would reveal the mode of movement of the manipulator crane rotation mechanism in the start-up and braking areas, which reduces the power loads on the elements of the manipulator crane.

The efficiency of using manipulator cranes is determined by their performance, reliability, and safety of operation. The main factor determining these characteristics of the manipulator crane is the dynamic loads that occur in its links and drive mechanisms [1]. These loads become especially dangerous during transients (start-up, braking) [2; 3]. Dynamic loads largely depend on the control system of the drive mechanisms of the manipulator crane [4; 5]. Dynamic loads significantly increase when combining the working movements of the manipulator crane mechanisms [6; 7]. Especially dangerous is the combination of movements of the rotation mechanism and the movement of the boom system links in the process of changing the departure, where loads increase by two or more times [8]. In [9], it was found that a slight decrease in dynamic loads during the passage of transients significantly improves the reliability indicators of manipulator cranes. In addition, dynamic loads have a significant impact on the accuracy of load positioning [10]. Dynamic loads can be reduced by using the fundamental principles of mechanics, based on which methods for optimising manipulators are built [11]. To find the optimal laws of motion of crane mechanisms, mathematical methods were used, where extreme values of control criteria were found [10; 12]. Optimal driving modes of crane mechanisms, which minimise the effect of dynamic loads, are given in [12; 13], where the RMS values of the driving forces of the drives were selected as optimisation criteria. An example of optimising the modes of joint movement of crane mechanisms is found in study [14], which considers the movement of the departure and turn movement mechanism. When solving problems of optimising the mode of movement of the rotation mechanism, deviations from the vertical suspension of the load in the radial direction (plane of departure change) occur, which are ignored in the studies [14; 15]. At the same time, these suspension deviations have a certain impact on the dynamics of turning the manipulator crane and they must be considered when optimising the power mode of turning. Optimal modes of movement of crane mechanisms should be adapted to the operating conditions of cranes [16; 17].

Increase the efficiency of the crane manipulator by optimising the start mode of the rotation mechanism. To achieve this goal, it is necessary to develop a mathematical model of the dynamics of the rotation mechanism of the manipulator crane, choose a criterion for optimising the dynamics of the rotation mechanism, optimise the start mode, and analyse the optimisation results obtained.

RESULTS AND DISCUSSION

To optimise the movement mode of the manipulator crane rotation mechanism, a dynamic model has been developed, which is shown in Figure 1. In this figure, the following designations are used: 1 – rotary part of the manipulator with a drive mechanism; 2 – articulated boom system; 3 – cylindrical hinged cargo suspension; 4 – load. When the boom system of the manipulator is rotated, all links rotate around the fixed axis of the rotary part, and the suspension 3 and load 4 additionally deviate from the vertical in the plane of change of departure (radial direction). Based on the design of the cylindrical hinge A of the load suspension, the latter can deviate from the vertical only in the radial direction when turning the manipulator crane. There are no deviations from the vertical of suspension 3 and load 4 in the plane of rotation of manipulator, since they are blocked by hinge *A*. When constructing a dynamic model, it is assumed that all the links of the crane manipulator are absolutely solid bodies, and there are no gaps in kinematic pairs. Rotation of the manipulator crane is carried out by a drive mechanism with a driving torque *M*.

Based on the above, it can be stated that the presented dynamic model of the crane manipulator has two

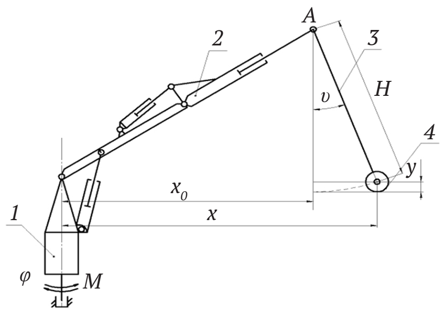

Figure 1. Dynamic model of turning a manipulator crane with cylindrical articulated load suspension

degrees of freedom: rotation of the entire system around a fixed vertical axis and deviation from the vertical of the hinge suspension with a load in the radial direction (plane of change in the departure of the load). The angular coordinate φ of the rotation mechanism and the linear horizontal coordinate of the centre of mass of the load in the radial direction X are selected as the generalised coordinates of the dynamic model when turning the manipulator crane.

To construct a mathematical model of the dynamics of rotation of a manipulator crane with a dynamic model (Fig. 1), the Lagrange equation of the second kind is used:

$$\begin{cases} \dfrac{d}{dt}\dfrac{\partial T}{\partial \varphi} - \dfrac{\partial T}{\partial \varphi} = M - \dfrac{\partial \Pi}{\partial \varphi}; \\ \dfrac{d}{dt}\dfrac{\partial T}{\partial x} - \dfrac{\partial T}{\partial x} = -\dfrac{\partial \Pi}{\partial x}; \end{cases} \tag{1}$$

where: t – time; T, P – kinetic and potential energy of the system, respectively; M – driving moment of the rotation mechanism drive reduced to the axis of the rotary part of the manipulator.

The expression of the kinetic energy of the system, ignoring the weight of the load suspension, has the following form:

$$T = \frac{1}{2} I_o \varphi^2 + \frac{1}{2} m(x^2 + \varphi^2 x^2), \tag{2}$$

where: I_0 – moment of inertia of the rotary part of the manipulator relative to its own axis of rotation; m – weight of the load with the gripper.

The required derivatives of expression (2) are used for the system of equations (1):

$$\frac{\partial T}{\partial \varphi}=0;\ \frac{\partial T}{\partial \varphi}=m\dot{\varphi}^2x;$$
$$\frac{\partial T}{\partial \varphi}=(I_0+mx^2)\varphi;\ \frac{\partial T}{\partial x}=mx; \quad (3)$$
$$\frac{d}{dt}\frac{\partial T}{\partial \varphi}=(I_0+mx^2)\varphi+2mxx\varphi;\ \frac{d}{dt}\frac{\partial T}{\partial x}=mx. \quad (4)$$

The dependence of the potential energy of the system is found

$$\Pi=mgy=mgH(1\text{-}\cos\vartheta), \quad (5)$$

where: g – acceleration of gravity; H – height of the position of the centre of mass of the load relative to the boom joint; Y –angular coordinate of the suspension deviation from the vertical in the plane of departure change, determined by the following dependence:

$$\vartheta=(x\text{-}x_0)/H. \quad (6)$$

where: x_0 – initial coordinate of the position of the centre of mass of the load.

The partial derivatives of expression (5) is taken from the generalised coordinates φ and X, considering that y⩽12° and assuming that sinυ ≈ U, and cosυ ≈ 1, as a result:

$$\frac{\partial \Pi}{\partial \varphi}=0;\frac{\partial \Pi}{\partial x}=mgH\frac{\partial \vartheta}{\partial x}sin\vartheta\approx mgh\vartheta\approx\frac{mg}{H}(x-x_o). \quad (7)$$

Substituting dependencies (3), (4), and (7) in system (1), a mathematical model of the dynamics of rotation of a crane manipulator with a load is obtained, which has the following form:

$$\begin{cases}(I_0+mx^2)\varphi+2m\ddot{x}x\dot{\varphi}=M;\\ mx-m\ddot{x}\dot{\varphi}^2=\dfrac{mg}{H}(x-x_0).\end{cases} \quad (8)$$

A system of two second-order differential equations (8) is reduced to one fourth-order differential equation. To do this, from the second equation of system (8), the angular velocity of the rotating part of the manipulator is expressed in terms of the horizontal coordinates of the load and its time derivatives:

$$\dot{\varphi}=\sqrt{\frac{g}{H}+\frac{1}{x}\left(\ddot{x}-\frac{gh_0}{H}\right)} \quad (9)$$

Taking the time derivative of expression (9), the angular acceleration of the rotary part of the manipulator is found

$$\ddot{\varphi}=\frac{1}{2}\frac{\dot{x}\ddot{x}-\dot{x}(\dot{x}-gh_0/H)}{x^2\dot{\varphi}} \quad (10)$$

Substituting expressions (9) and (10) into the first equation of system (8), the dependence of the driving moment of the rotation mechanism drive on the coordinate of the centre of mass of the load and its time derivatives are obtained

$$M=\frac{1}{2}(I_0+mx^2)\frac{\dot{x}\ddot{x}-\dot{x}\left(\ddot{x}-\frac{g}{H}x_0\right)}{x^2\sqrt{\frac{g}{H}+\frac{1}{x}\left(\ddot{x}-\frac{g}{H}x_o\right)}}+$$
$$+2mx\dot{x}\sqrt{\frac{g}{H}+\frac{1}{x}\left(\ddot{x}-\frac{g}{H}x_0\right)} \quad (11)$$

To optimise the driving mode during the start-up of the turning mechanism, the RMS value of the driving moment is chosen as a criterion, which is presented in the form of intelligent functionality

$$M_{\text{ск}}=\left[\frac{1}{t_1}\int_0^{t_1}M^2dt\right]^{1/2} \quad (12)$$

which must be minimised when ensuring the following boundary traffic conditions:

$$\begin{cases}t=0: x=x_0, \dot{x}=0, \dot{\varphi}=0, \ddot{\varphi}=0;\\ t=t_1: \dot{x}=0, \ddot{x}=0, \dot{\varphi}=\omega, \ddot{\varphi}=0.\end{cases} \quad (13)$$

where: t_1 – duration of the process of starting the rotation mechanism of the crane manipulator; ω – steady-state angular velocity of the rotation mechanism.

Using dependencies (9) and (10), the boundary conditions (13) is reduced to the coordinate of the mass centre of the cargo X and its time derivatives. After that:

$$\left[\begin{array}{l}t=0: x=x_0, \dot{x}=0, \ddot{x}=0, \dddot{x}=0;\\ t=t_1: x=\dfrac{x_0}{\left(1-\frac{\omega^2H}{g}\right)}, \dot{x}=0, \ddot{x}=0, \dddot{x}=0.\end{array}\right. \quad (14)$$

The obtained optimisation problem (12) and (14) cannot be solved analytically, since the integrative expression of the functional (12) is a nonlinear function of the coordinate, velocity, acceleration, and jerk of the load movement in the plane of departure change. Therefore, an approximate method can be used for solving the optimisation problem of determining the power mode of starting the rotation mechanism of the manipulator crane.

The essence of this method [18] is that the solution of the optimisation problem is sought on a class of multiparametric functions that satisfy the given boundary conditions and provide a minimum of the criterion represented as an integral functional. In this form, the solution of the optimisation problem is represented as the solution of the following boundary value problem

$$\begin{cases}L(x)=0\\ \begin{cases}t=0: x=x_0, \dot{x}=0, \ddot{x}=0, \dddot{x}=0;\\ t=t_1/2: x=x(t_1/2), \dot{x}=\dot{x}(t_1/2);\\ t=t_1: x=\frac{x_0}{(1-\omega^2H/g)}, \dot{x}=0, \ddot{x}=0, \dddot{x}=0.\end{cases}\end{cases} \quad (15)$$

Where $L(x)$ – operator that depends on the function $x(t)$. The solution of the above problem (15) has two unknown parameters $x(t_1/2)$ and $\dot{x}(t_1/2)$. In the given boundary value problem, the operator $L(x)$ can be represented by a differential equation of different orders. The operator is used as an ordinary tenth-order differential equation $L(x)$.

As a result of solving the boundary value problem (15), an expression of criterion (12) is developed in the form of a functional that does not depend linearly on the parameters $x(t_1/2)$ and $\dot{x}(t_1/2)$ and it seems to be such a functional dependency:

$$C_r=Cr(xt_1/2), \dot{x}(t_1/2, t_1) \quad (16)$$

Values of parameters $x(t_1/2)$ and $\dot{x}(t_1/2)$ are found, for which criterion (12) takes the smallest value when providing the boundary conditions (14). To solve this problem, a modified metaheuristic method for swarming ME-PSO particles was used [19]. This method does not require continuity and differentiation of the functions on which criterion (12) depends, and also does not impose additional conditions on the optimisation problem. After constructing the functional dependency (16), the Me-PSO method can be used to find the optimal values of unknown parameters $x(t_1/2)$ and $\dot{x}(t_1/2)$. When solving this problem, the following parameters of the ME-PSO method are accepted: the permissible rate of reduction of the AR=0.005 criterion; the swarm population – 50; the number of iterations – 40 (Fig. 2). The given parameters of the method allowed effectively using computational resources to obtain a solution to the optimisation problem.

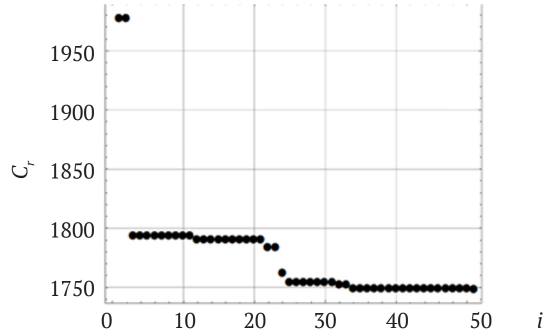

Figure 2. Graph of changes in the C_r criterion during the optimisation procedure (depending on the i-th iteration number)

Calculations were made for the rotation mechanism of the manipulator crane with the following parameters: m=500 kg; I_0=3,200 kg·m^2; x_0=5.5 m; H=1.5 m; g=9.81 m/s^2; t_1=2.0 s; ω=0.42deg/s.

Figure 3-Figure 9 show the graphical dependences of the kinematic, power, and energy characteristics of the optimal power mode of rotation of the manipulator crane.

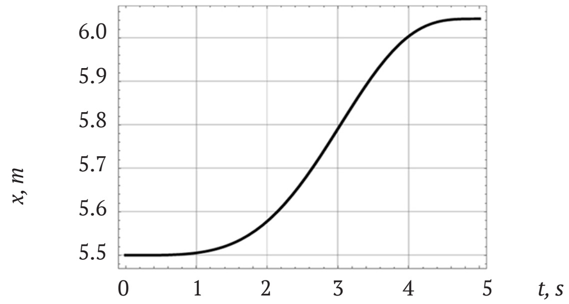

Figure 3. Graph of movement of the centre of mass of the load in the radial direction

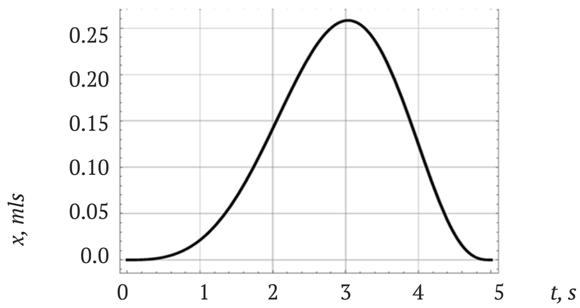

Figure 4. Graph of the velocity of the centre of mass of the load in the radial direction

Figure 3-Figure 5 show graphs of the kinematic characteristics of the movement of the centre of mass of the load in the radial direction. The movement of the centre of mass of the load (Fig. 3) has a smooth change character without fluctuations, which is close to the S-shaped law of motion. At the same time, at the beginning of the movement for one second, the movement of the centre of mass of the load in the radial direction was practically absent, and then it began to grow smoothly. The greatest increase in movement is observed in the section from two to four seconds, and then it begins to gradually decrease and at the end of the movement for 0.5 seconds remains almost unchanged.

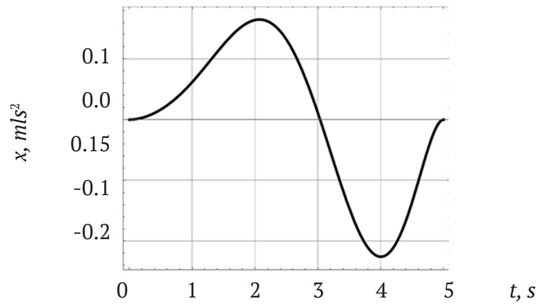

Figure 5. Graph of acceleration of the centre of mass of the load in the radial direction

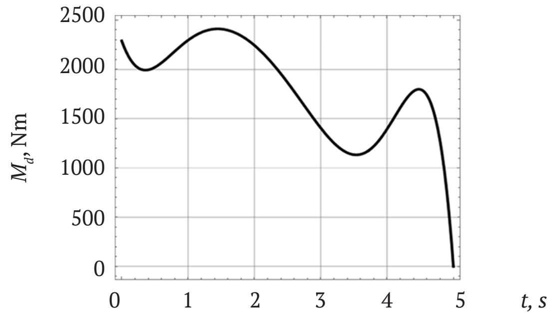

Figure 6. Graph of acceleration of the centre of mass of the load in the radial direction

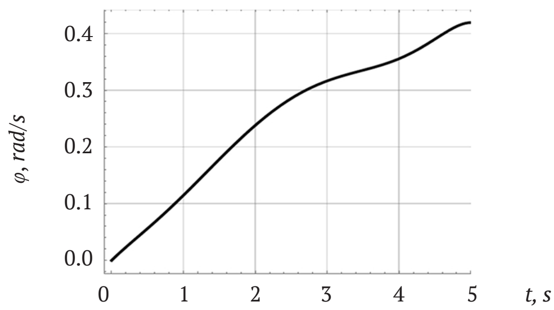

Figure 7. Graph of the angular velocity of the rotary part of the manipulator crane

This mode of moving the load in the radial direction is the most appropriate, since when entering the steady-state mode of movement, there will be no fluctuations of the load in the radial direction.

The change in the load velocity in the radial direction (Fig. 4) also has a smooth change character without fluctuations. Here, the speed of movement of the load gradually increases to the maximum value, which is provided at the third second of movement, and then gradually decreases to zero. The presence at the end of the start-up of a stable value of cargo movement and zero speed confirms the absence of fluctuations in the load in the radial direction during the steady-state mode of rotation of the manipulator crane. The acceleration of the load in the radial direction (Fig. 5) also changes smoothly, increasing from zero to the maximum, and then decreasing to the minimum negative value and gradually increasing from it to zero.

The dynamic component of the driving torque of the manipulator rotation mechanism (Fig. 6) changes from the initial, almost maximum, to the final zero value in the presence of vibrations in the middle of the start-up section. This mode of changing the dynamic component of the driving torque indicates the presence of variable dynamic loads in the drive of the turning mechanism during start-up. The graph of angular acceleration of the crane manipulator rotation mechanism (Fig. 7) is practically a copy of the graph of changes in the dynamic component of the driving torque of the drive. This is conditioned by the fact that the dynamic component of the driving moment is the product of a slightly variable moment of inertia of the rotary part of the manipulator crane and its angular acceleration. The graph of the angular velocity of the rotary part of the manipulator crane (Fig. 8) increases from zero in the first half of the start-up almost according to a linear law, and in the second part of the start-up, this increase slows down with a slight fluctuation in the turn speed.

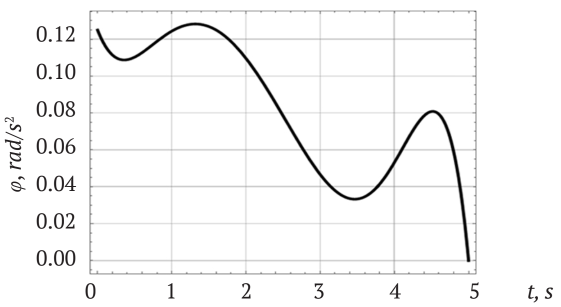

Figure 8. Graph of the angular velocity of the rotary part of the manipulator crane

The dynamic component of the drive power of the manipulator crane rotation mechanism (Fig. 9) increases from zero to the maximum value in the presence of power fluctuations, and then sharply decreases to zero within 0.5 seconds. Fluctuations in the dynamic component of the drive power of the turning mechanism are caused by the nature of changes in the driving torque, which also has an oscillatory character.

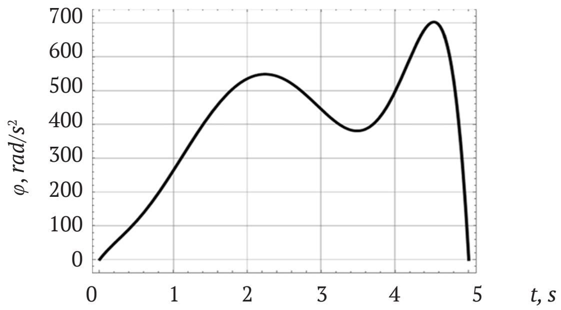

Figure 9. Graph of the dynamic power component of the drive mechanism of the manipulator crane rotation

The obtained optimal modes of movement of crane manipulator mechanisms should be used in real drive designs [20]. For this purpose, control systems are used [21]. It is possible to estimate the influence of optimal driving modes on the strength characteristics of structures by performing calculations for strength and reliability [22]. To assess the impact of optimal movement modes of mechanisms on the efficiency of manipulator cranes, it is necessary to monitor them.

CONCLUSIONS

1. A dynamic model of the rotation mechanism of the manipulator crane is constructed, which considers the main movement of the rotation mechanism and the oscillatory movement of the load on a cylindrical hinge suspension in the radial direction (the plane of change in the departure of the load).

2. Based on the dynamic model, a mathematical model of the dynamics of the movement of the crane-manipulator rotation mechanism is compiled, which is described by a system of nonlinear second-order differential equations.

3. For such a mathematical model, an optimisation problem is set and solved to determine the rotation mode of the manipulator crane, which provides the minimum RMS value of the driving torque of the drive mechanism when the boundary conditions of movement are met. The boundary driving conditions are selected from the condition for eliminating load vibrations in the radial direction when entering the steady-state mode of rotation of the manipulator crane.

4. As a result of solving the optimisation problem, the law of motion of the turning mechanism is determined, which minimises the optimisation criterion and provides the necessary boundary conditions for movement. At the same time, there are some fluctuations in the kinematic characteristics of the turning mechanism with a fairly smooth mode of cargo movement in the radial direction. There are also fluctuations in the driving torque and dynamic power component of the drive mechanism of the manipulator crane rotation.

5. To eliminate these shortcomings of the obtained optimal driving mode, it is necessary to use complex optimisation criteria, which would include other individual criteria that allow eliminating fluctuations in the kinematic, power, and energy characteristics of the crane rotation mechanism.

REFERENCES

[1] Fang, Y., Wang, P., Sun, N., & Zhang, Y. (2014). Dynamics analysis and nonlinear control of an offshore boom crane. *IEEE Transactions on Industrial Electronics*, 61(1), 414-427.

[2] Carmona, I.G., & Colado, J. (2016). Control of a two wired hammerhead tower crane. *Nonlinear Dynamics*, 84(4), 2137-2148.

[3] Kostikov, A.A., Perig, A.V., Larichkin, O.V., Stadnik, A.N., & Gribkov, E.P. (2019). Research into payload swaying reduction through cable length manipulation during boom crane motion. *FME Transactions*, 47(3), 464-476.

[4] Wu, T.S., Karkoub, M., Yu, W.S., Chen, C.T., Her, M.G., & Wu, K.W. (2016). Anti-sway tracking control of tower cranes with delayed uncertainty using a robust adaptive fuzzy control. *Fuzzy Sets and Systems*, 290, 118-137.

[5] Capkova, R., Kozakova, A., & Bucz, S. (2019). Experimental modelling and control of a tower crane. In *International Conference on Process Control* (pp. 97-101). Strbske Pleso: IEEE.

[6] Reutov, A.A., Kobishchanov, V.V., Sakalo, V.I. (2016). Dynamic modeling of lift hoisting mechanism block pulley. *Procedia Engineering*, 150, 1303-1310.

[7] Le, T.A., Dang, V.H., Ko, D.H., An, T.N., & Lee, S.G. (2013). Nonlinear controls of a rotating tower crane in conjunction with trolley motion. *Journal of Systems and Control Engineering*, 227(5), 451-460.

[8] Schlott, P., Rauscher, F., & Sawodny, O. (2016). Modelling the structural dynamics of a tower crane. In *International Conference on Advanced Intelligent Mechatronics* (pp. 763-768). Banff: IEEE.

[9] Michna, M., Kutt, F., Sienkiewicz, L., Ryndzionek, R., Kostro, G., Karkosinski, D., & Grochowski B. (2020). Mechanical-level hardware-in-the-loop and simulation in validation testing of prototype tower crane drives. *Energies*, 13(21), article number 5727.

[10] Chwastek, S. (2021). Finding the globally optimal correlation of cranes drive mechanisms. *Mechanics Based Design of Structures and Machines*, 5, 1-12.

[11] Chwastek, S. (2020). Optimization of crane mechanisms to reduce vibration. *Automation in Construction*, 119, article number 103335.

[12] Nazarenko, I., Mishchuk, Y., Mishchuk, D., Ruchynskyi, M., Rogovskii, I., Mikhailova, L., Titova, L., Berezovyi, M., & Shatrov, R. (2021). Determiantion of energy characteristics of material destruction in the crushing chamber of the vibration crusher. *Eastern-European Journal of Enterprise Technologies*, 4(7(112), 41-49.

[13] Loveikin, V., Romasevych, Y., Kadykalo, I., & Liashko, A. (2019). Optimization of the swinging mode of the boom crane upon a complex integral criterion. *Journal of Theoretical and Applied Mechanics*, 49, 285-296.

[14] Grigorov, O., Druzhynin, E., Strizhak, V., Strizhak, M., & Anishchenko, G. (2018). Numerical simulation of the dynamics of the system "trolley – load – carrying rope" in a cable crane. *Eastern-European Journal of Enterprise Technologies*, 3(7(93), 6-12.

[15] Loveikin, V., Romasevych, Y., Shymko, L., Mushtin, D., & Loveikin, Y. (2021). The optimization of luffing and slewing regimes of a tower crane. *Journal of Theoretical and Applied Mechanics*, 51, 421-436.

[16] Romasevych, Y., & Loveikin, V. (2018). A novel multi-epoch particle swarm optimization technique. *Cybernetics and Information Technologies*, 18(3), 62-74.

[17] Kozakova, A., Capkova, R., & Bucz, S. (2019). Tuning methods to attenuate oscillatory load-disturbance response: A comparative study. In *Proceedings of the 6th international conference on advanced control circuits and systems (ACCS) & 2019 5th international conference on new paradigms in electronics & information technology (PEIT)* (pp. 197-202). Hurgada: IEEE.

[18] Qian, Y., Fang, Y., & Lu, B. (2017). Adaptive repetitive learning control for an offshore boom crane. *Automatica*, 82(8), 21-28.

[19] Qian, Y., & Fang, Y. (2018). Switching logic-based nonlinear feedback control of offshore ship-mounted tower cranes: A disturbance observer-based approach. *IEEE Transactions on Automation Science and Engineering*, 16(3), 1125-1136.

[20] Sanfilippo, F., Hatledal, L.I., Styve, A., Pettersen, K.Y., & Zhang, H. (2016). Integrated flexible maritime crane architecture for the offshore simulation centre AS (OSC): A flexible framework for alternative maritime crane control algorithms. *IEEE Journal Oceanic Engineering*, 41(2), 450-461.

[21] Fidrovska, N., Slepuzhnikov, E., Varchenko, I., Harbuz, S., Shevchenko, S., & Chyrkina, M. (2021). Determining stresses in the metallic structure of an overhead crane when using running wheels of the new design. *Eastern-European Journal of Enterprise Technologies*, 1, 22-31.

[22] Yaping, T., Haibo, W., & Hailong, L. (2015). The wireless monitoring system of tower cranes based on MCP2515/CAN bus. In *Proceedings of the 2015 international conference on intelligent systems research and mechatronics engineering. Series: Advances in intelligent systems research* (pp. 1635-1639). Zhengzhou: Zhengzhou University.

В'ячеслав Сергійович Ловейкін[1], Юрій Олександрович Ромасевич[1], Тадеус Злото[2], Анастасія Петрівна Ляшко[1], Олег Дяченко[1]

[1]Національний університет біоресурсів і природокористування України

03041, вул. Героїв Оборони, 15, м. Київ, Україна

[2]Політехніка Честочовська

42201, вул. Яна Генрика Домбровського, 69, м. Ченстохова, Республіка Польща

Оптимізація силового режиму пуску механізму повороту крана-маніпулятора з циліндричним шарнірним підвісом вантажу

Анотація. В статті розглядається проблема підвищення ефективності роботи крана-маніпулятора за рахунок вибору режимів руху приводу механізму повороту під час процесу пуску. При роботі кранів маніпуляторів на ділянках перехідних процесів виникають значні динамічні навантаження, які призводять до розгойдування вантажу на шарнірному підвісі. Це призводить до зменшення продуктивності та надійності крана-маніпулятора, а також підвищення енергетичних витрат приводу механізму повороту. Зменшити динамічні навантаження при роботі механізму повороту на ділянках перехідних процесів (пуск, гальмування) крана-маніпулятора запропоновано шляхом проведення оптимізації режиму руху приводного механізму. При цьому кран-маніпулятор представлено у вигляді двомасової динамічної моделі, де першою масою виступає поворотна частина крана-маніпулятора з приводним механізмом, а другою масою є вантаж на циліндричному шарнірному підвісі. Мета дослідження – підвищення ефективності крана-маніпулятора шляхом оптимізації режиму пуску механізму повороту. Методологією є оптимальні режими руху кранових механізмів, які до мінімуму зводять дію динамічних навантажень, передбачають наявність критеріїв оптимізації за середньоквадратичними значеннями рушійних сил приводів. Розроблена динамічна модель дозволила побудувати математичну модель, що описується системою нелінійних диференціальних рівнянь. Оптимізацію режиму руху механізму повороту крана-маніпулятора здійснено шляхом мінімізації інтегрального динамічного критерію, який представляє собою середньоквадратичне значення рушійного моменту приводу за час проходження перехідного процесу. В результаті проведеної оптимізації знайдено режим пуску механізму повороту крана-маніпулятора, який до мінімуму зводять силові навантаження та коливання вантажу на шарнірному підвісі в радіальному напрямку. Отриманий оптимальний режим пуску механізму повороту дозволив підвищити продуктивність та надійність роботи крана-маніпулятора, а також зменшити енергетичні витрати приводу

Ключові слова: баштовий кран, механізм повороту, оптимальне керування, циліндричний шарнірний підвіс, коливання вантажу

Machinery & Energetics
Vol. 13, No. 1. 2022

Journal homepage:
https://technicalscience.com.ua/en

UDC 621.87
DOI: 10.31548/machenergy.13(1).2022.18-25

Inna Yakymenko[1*], Vitaly Lysenko[1], Kamil Witaszek[2]

[1]National University of Life and Environmental Sciences of Ukraine
03041, 15 Heroiv Oborony, Kyiv, Ukraine

[2]Poznan University of Life Sciences
60637, 28 Wiyska Polskogo Str., Poznan, Republic of Poland

Methodology of development of an intelligent energy-efficient system of control of temperature and humidity regime in industrial greenhouse

Abstract. The cost of energy carriers affects the cost of products that are grown in industrial greenhouses. The purpose of the study is to develop a methodology for creating an intelligent system for energy-efficient microclimate management in industrial greenhouses operating under conditions of uncertainty, based on a combination of methods for predicting energy consumption and minimising them through the use of artificial neural networks. Methodology – the input parameters of the neural network prediction model are: the value of external and internal greenhouse air temperatures, the value of relative humidity, solar radiation absorbed by the greenhouse, and the level of carbon dioxide in the greenhouse. The outputs of the forecasting model are the values of natural gas and electricity costs. Based on the use of fuzzy logic methods and a genetic algorithm, models for finding and using optimal parameters of PI controller settings adapted to changes in the operating conditions of the automation system are developed and investigated. Methods of improving the quality of regulation of technological parameters by combining various intelligent control algorithms in one automation system are analysed, which helps to reduce energy costs by 10-13%. It is established that for closed-ground structures, heating and ventilation systems have the highest energy consumption (on average, more than 4,000 m^3 of natural gas and almost 1,000 kWh of electricity are consumed per day for heating and ventilation in an industrial greenhouse. Correlation analysis of the relationships between external disturbances and energy costs that ensure compliance with a given technology for growing plant products, confirmed the hypothesis about the presence of conditions of uncertainty in the functioning of an industrial greenhouse formed by random disturbances, incomplete information about the biological component; while the linear correlation coefficients do not exceed $r<0.35$. This creates conditions for the use of neural networks both for predicting energy costs and for forming energy-efficient management strategies. This provides better regulation in conditions of uncertainty, the adjustment time and overshoot are reduced by two to three times. To create an energy-efficient microclimate management system in industrial greenhouses that operates in conditions of uncertainty, a neural network model for predicting the energy costs of natural gas and electricity has been developed. The authors of the study have improved the structural and functional scheme of the automation system for controlling the temperature and humidity regime in industrial greenhouses by combining intelligent algorithms for stabilising the operation of technological equipment at the lower level of control and optimising energy costs by predicting them at the upper level. The introduction of such a system allows to saving natural gas for heating up to 13% and electricity – up to 10%. The study proved that the development of an intelligent energy-efficient system for automatic control of microclimate parameters in closed-ground structures should be based on a combination of methods for intelligent adjustment of PI controller parameters and forecasting energy consumption

Keywords: energy efficiency indicators, resource efficiency, microclimate parameters, indoor structures, industrial greenhouse, intelligent control system

Article's History: Received: 11/01/2021; Revised: 01/23/2022; Accepted: 02/11/2022

Suggested Citation:
Yakymenko, I., Lysenko, V., & Witaszek, K. (2022). Methodology of development of an intelligent energy-efficient system of control of temperature and humidity regime in industrial greenhouse. *Machinery & Energetics,* 13(1), 18-25.

*Corresponding author

INTRODUCTION

The main problem of modern cultivation of products in industrial greenhouses is the cost of energy carriers, which significantly affects the cost of grown products. Thus, the share of energy in the structure of product prices is 60-90%. Therefore, the task of developing new methods and approaches to minimise energy losses is urgent. It is important to take into consideration that the volume of energy consumption in industrial greenhouses is affected by poorly predicted natural factors, such as cloud cover, wind strength and direction, and other factors that create the main features of the functioning of modern industrial greenhouses: non-stationarity, uncertainty. This is explained by the influence of natural disturbances, which are random in nature and incompleteness of information about the states of the biological component. At the same time, agrotechnical standards require high accuracy of temperature stabilisation (+/-1°C), its timely change depending on the level of photosynthetic active radiation, the phase of plant development and the time of day. This increases the requirements for existing automation systems and their provision by using modern intelligent algorithms for processing information coming from the control object, and applying the results obtained to form appropriate management strategies in order to maximise production profits.

Modern economic conditions require the creation of such a greenhouse for growing vegetable crops, which would allow implementing energy-saving technology for their production by minimising energy costs, while ensuring the appropriate quality of products and their volumes. Well-known strategies include regulating temperature and humidity conditions, supply of CO_2 depending on the plant growth phase and time of day, and dynamic control of additional growth factors based on solar radiation values.

Nowadays, several types of algorithms for controlling microclimate parameters have become widespread, such as: traditional, nonlinear, p-system, based on fuzzy logic and the use of neural networks, and hybrid algorithms [1-5]. Traditional control algorithms include: proportional-integral (PI) and proportional-integral-differential (PID), which are most often used in regulating the microclimate in industrial greenhouses due to their flexibility, simplicity, and good control indicators [6]. M. Azaza [2] used an intelligent system based on fuzzy logic to control the temperature and humidity in the greenhouse, with ventilation and maintenance of plant feeding standards. They achieved 22% and 33% energy and water savings, respectively. M. Vera [7] in their study used a fuzzy model that allows adjusting the internal temperature inside the greenhouse, using a proportional servo valve to activate the heating of the coolant at night, and another drive to control the ventilation rate during the day. K. Li [8] used a multilayer perceptron to predict the temperature in the greenhouse. However, the disadvantage of such a system is the need for a large set of input data to achieve appropriate accuracy in the operation of a fuzzy system. In addition, since the algorithm takes into account the experience of experts in formulating the model, comprehensive knowledge of the functioning of the system is required.

Thus, there is a need to create and use new intelligent control systems based on a combination of modern control methods, which would ensure the implementation of optimal control according to the energy efficiency criterion.

The purpose of the study is to develop a methodology for creating an intelligent system for energy-efficient microclimate management in industrial greenhouses operating under conditions of uncertainty, based on a combination of methods for predicting energy costs and minimising them through the use of artificial neural networks.

RESULTS AND DISCUSSION

The conducted systematic analysis of the process of growing products in industrial greenhouses determined the main features of the greenhouse as a complex control object:

– the object identifies a structural set of subsystems that interact with each other;

– each of the systems can be included as a subsystem in a more complex one;

– complex systems interact with the external environment as a whole;

– management processes are implemented both using feedbacks and on the basis of forming a set of goals, each of which is solved by its own method;

– complex management systems have their own characteristics at each stage (information collection, analysis, development of control actions, implementation) [9].

As already noted, an industrial greenhouse has all the features of a complex system with the possibility of separating separate subsystems. Since each of these subsystems has its own local goals, conflict situations may arise during the functioning of the system as a whole. Thus, there is a need for coordination of control subsystems, the solution of which is to determine the interaction of subsystems, in which control actions that are optimal according to the efficiency criteria for each of the subsystems are also optimal according to the general criterion for the process in general.

The conducted studies in the greenhouse complex confirm the non-linearity and non-stationarity of processes occurring in an industrial greenhouse when growing vegetable products. The hypothesis that there are conditions of uncertainty in the functioning of an industrial greenhouse is confirmed, the linear correlation coefficients between the inputs and outputs of the control object do not exceed $r<0.35$. This creates conditions for the use of neural networks that can function effectively in conditions of uncertainty to predict energy consumption. A graphical representation of the correlations is shown in Figure 1.

The correlation relationship is described by regression equations of the form:

– for gas consumption:

$y_1=-0.2608x+6.5303$,

– for electricity consumption:

$y_2=-0.2904x+1.2493$.

The greenhouse, as a control object, is multidimensional with complex internal connections, which affects the stationarity of dynamic characteristics. This leads to a deterioration in the quality of control, since in typical automation systems it depends on the dynamic properties of the object. In turn, the analysis of the operation of the temperature and humidity control system in a greenhouse with a PI controller, as it is most common in closed-ground structures, showed that in order to maintain the progenitors of regulation at a given level and the quality of the transition process, the parameters of the regulator are variable. Therefore, the problem arises of continuously determining the controller settings that adapt to changes in the dynamic properties of the control object, while ensuring the appropriate quality of transients [10; 11].

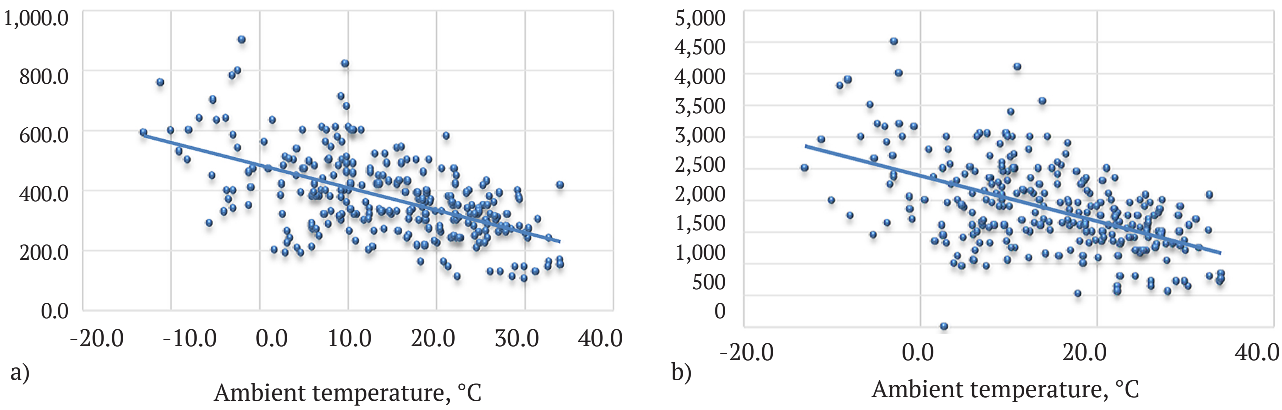

Figure 1. Correlation between gas (a) and electricity (b) consumption and external temperature

The use of various methods for controlling microclimate parameters allows choosing the best algorithm for achieving energy-efficient regulation indicators. Figure 2 shows the use of regulators that implement PI-algorhythm, but the calculation of parameters of their settings is carried out based on the results of using fuzzy logic, a genetic algorithm, and a typical engineering technique (for comparison).

The proposed approach provides the necessary opportunities for practical use of the results for predicting the further behaviour of the object and forming energy-efficient strategies for managing the greenhouse complex in the future [6].

The genetic algorithm method was used to find the optimal PI controller settings [12]. The comparison block constantly compares the coordinates of the object's state with their specified value. If there is a difference between a given signal value and a valid one in the control object $\varepsilon = X_{pv} - x \neq 0$, then the signal is sent to the optimisation unit, the functional purpose of which is to find the optimal settings of the regulator based on the genetic algorithm.

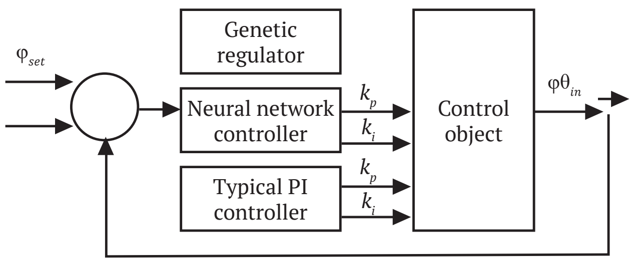

Figure 2. Structural and functional diagram of the automatic control system using various methods for determining the optimal parameters of the PI controller settings for the temperature and humidity regime in the greenhouse: θ_{set}, φ_{set} – set temperature and humidity values, k_p, k_i – transmission coefficient and isodrome time of the PI controller, θ_{in}, φ_{in} – output values of internal temperature and humidity

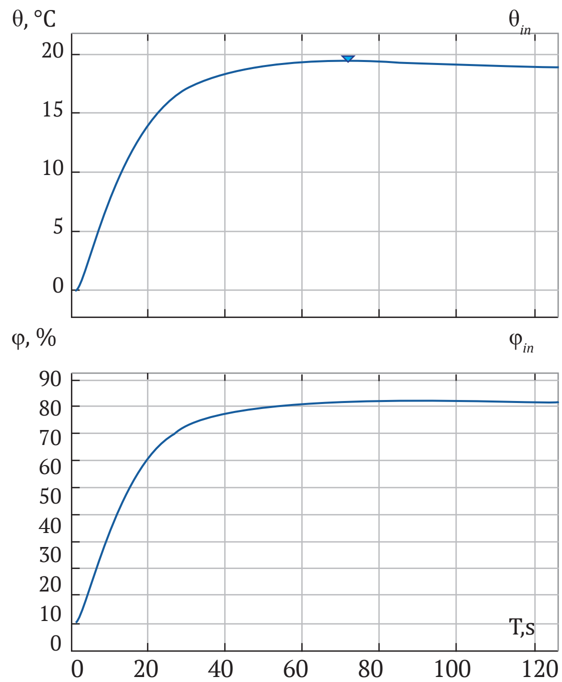

Figure 3. Transient characteristic of the automatic control system for the temperature change channel (θ_{in}) and humidity (φ_{in}) with settings parameters determined based on the use of a genetic algorithm for the PI controller

At the first stage, the training parameters are selected that are set by the optimisation function, which includes the equations of the control object, regulator, and perturbation. Next, the process of obtaining a solution for fixed parameter values and comparing them with the input values takes place based on training, and the optimal parameters of the controller are selected. The use of a genetic algorithm has yielded the following results (Fig. 3): optimal settings for the temperature control channel k_p=74.8 proportional component, k_i=1.8 integral component; for humidity control channel k_p=72.7 proportional component, k_i=2.1 integral component for the specified values of temperature and humidity in the greenhouse: $\theta_{in\ set}$=18°C and $\varphi_{in\ set}$=80%.

A fuzzy expert system was also used to optimise the settings of the local control system with a PI controller. The rules of the fuzzy expert system are based on ensuring a minimum area between the transition process and the time axis (1):

$$I = \int_{t_o}^{t} (x_{\mathrm{pv}} - x)\, dt \rightarrow \underset{k_p, k_i}{min,} \qquad (1)$$

where: x_{pv}, x – respectively, the set value of the parameter and its value at the output of the object; k_p, $k_i \in [k_{max}, k_{min}]$ – transmission coefficient and isodrome time of the PI controller.

Production rules for a fuzzy knowledge base are developed based on the expert knowledge and have the form: if E=vid, $I\int E$=*dod*, then K_p=*zero*, $I\ T_i$=*zero*, where vid – negative values, dod – positive values, ser – average values, vel – large values, and zero – zero values (Fig. 4).

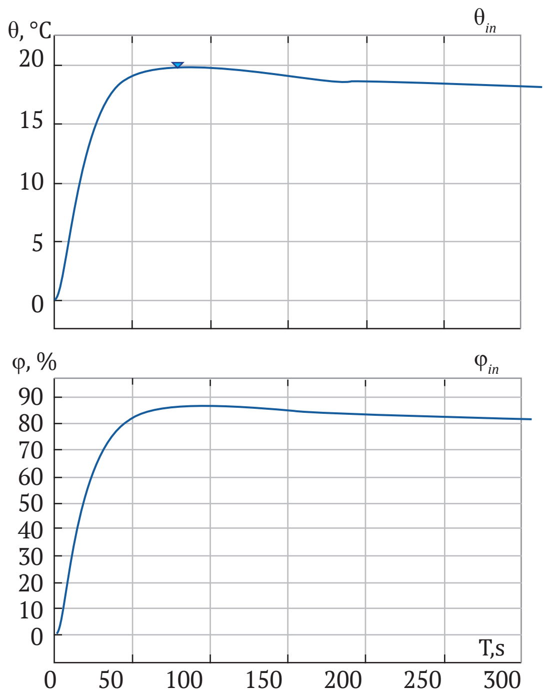

Figure 4. Transient characteristic of the automatic control system for the temperature change channel (θ_{in}) and humidity (φ_{in}) with the parameters of the PI controller settings determined based on the use of a neural network expert system

The algorithm for setting up a neural network controller includes the following steps:

– collection of information about an object's behaviour when it is affected by perturbations;

– development of production rules, considering technological data;

– phasification of input and output parameters;

– development of a neural network structure;

– training of a neural network expert system;

– testing of results based on modelling.

For the specified values of temperature and humidity in the greenhouse: $\theta_{in\ set}$=18°C and $\varphi_{in\ set}$=80% of the PI controller settings for the output temperature control channel of the fuzzy expert system were (Fig. 4): k_p= 73.1 proportional component, k_i=3.3 integral component; for humidity control channel k_p=71.2 proportional component; k_i=3.6 integral component.

As a reference model for comparing the obtained modelling results, the traditional method of searching for the parameters of the PI controller is used.

Using the traditional method of calculating the optimal parameters of regulator settings, namely the Ziegler Nichols method [13], the following values of the parameters of the PI controller settings were obtained under constant initial conditions (Fig. 5): transmission coefficient for the temperature control channel k_p=75.2 proportional component, and isodrome time k_i=3.1 integral component.

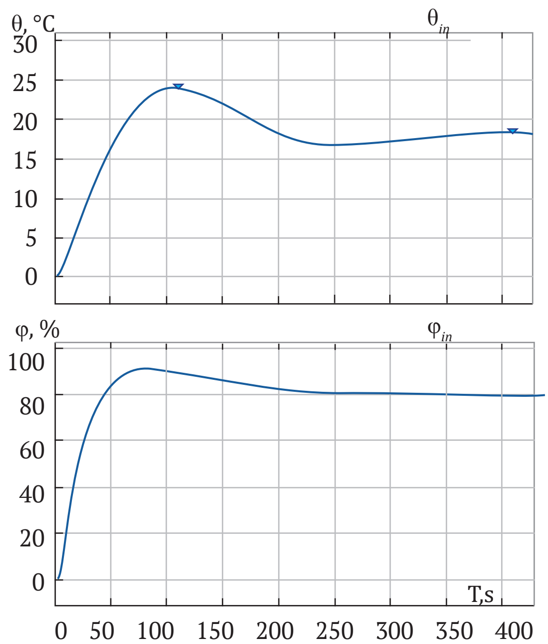

Figure 5. Transient characteristics of an automatic control system with a PI controller, the settings of which are determined according to the standard method, for the temperature change channel (θ_{in}) and air humidity (φ_{in})

To solve the problem of improving the energy efficiency of greenhouse enterprises, it is advisable to apply forecasting of energy costs, namely, gas and electricity, at the upper level of management [14]. This allows developing energy-efficient strategies for managing microclimate parameters in industrial greenhouses. To do this, it is advisable to use artificial neural networks. The structure of such an automation system is shown in Figure 6.

The neural time series software package was used to synthesise and study the corresponding artificial neural networks. Minimisation the relative root-mean-square learning error was chosen as a criterion for stopping learning. The Bayesian linear regression method was chosen for training artificial neural networks, since this results in the smallest root-mean-square error with respect to deviation [15]. The number of hidden layers of artificial neural networks – 50.

The learning process is illustrated by a graph of the dependence of the functioning assessment on the number of the learning cycle (Fig. 7).

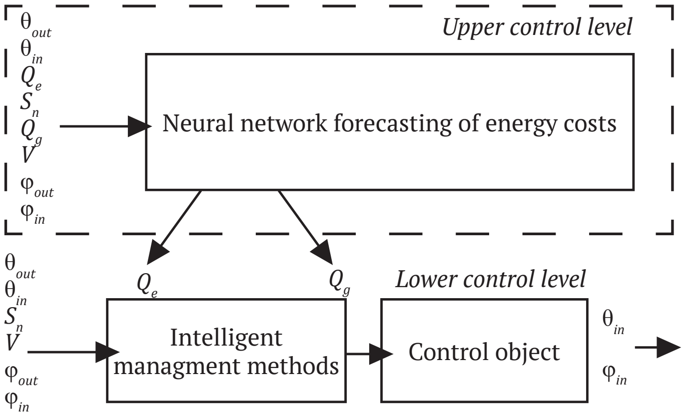

Figure 6. Structural and logical diagram of energy-efficient microclimate management (where θ_{in}, θ_{out} – air temperature inside and outside the greenhouse; S_{abs} – solar radiation absorbed by the greenhouse; Q_e, Q_g – gas and electricity consumption in the greenhouse; υ – power of the ventilation system; φ_{in}, φ_{out} – relative humidity of the air inside and outside the greenhouse)

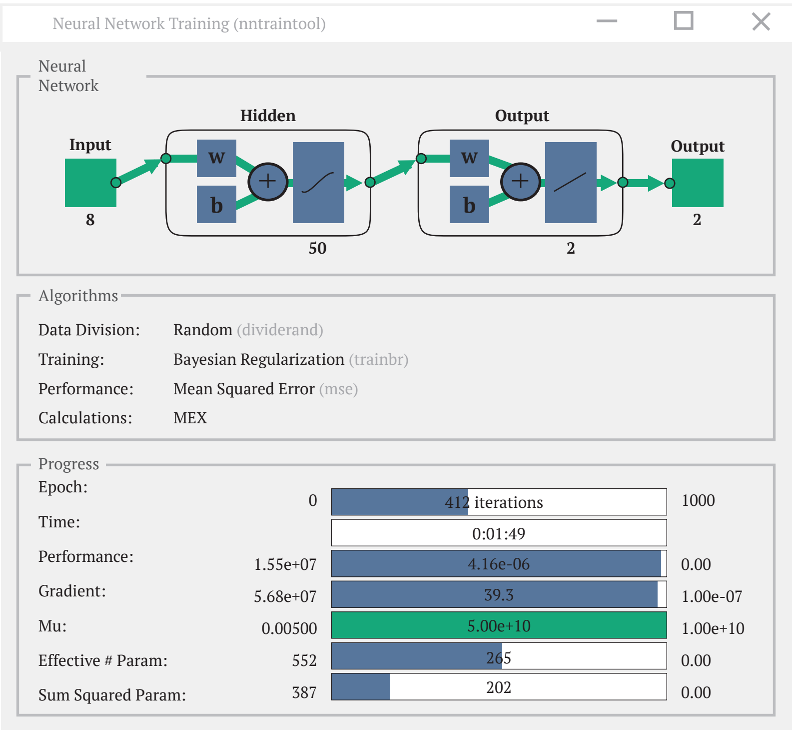

Figure 7. Block diagram of neural network training

A test data array was used to determine the degree of reliability of the results. It was checked whether the pre-dicted values coincided with the actual data of microclimate parameters taken directly at the production site. Regression analysis methods [16-18] obtained by comparing reference val-ues with values at the network output were used to assess the reliability of the results of artificial neural networks. Evaluation of the developed model for forecasting energy costs was carried out based on the following criteria: determination R^2, root-mean-square error σ, Fischer F and Student's t (Table 1).

According to the materials presented in the table, the correlation and determination coefficients are within 90%, which indicates a close relationship between the inputs and outputs of the model. The measurement error is insignificant – 0.0013. The Student's t indicates the significance of correlation coefficients, which signifies the adequacy of the neural network model for predicting energy consumption.

Table 1. Criteria for the adequacy of a mathematical model

Sample	Criteria			
	R^2	σ	F	t
Gas consumption, m^3	0.99	0.0013	9.39	0.98
Electricity consumption. W/h	0.99	0.0013	9.39	0.97

The methodology for developing an intelligent energy-efficient system for automatic control of microclimate parameters in closed-ground structures is based on a combination of methods: intelligent adjustment of PI controller parameters and forecasting of energy consumption.

The practical implementation of the algorithm for developing an energy-efficient control system takes place according to the following sequence.

1. Conducting experimental studies.

2. Creating a database of microclimate parameters inside and outside the greenhouse.

3. Creating a fuzzy expert system for managing groups of greenhouse coolant supply and ventilation equipment.

4. Development of rules by experts based on the requirements for ensuring the quality of grown products.

5. Processing of information on projected energy consumption values.

6. Select an equipment management strategy to minimise energy consumption by adjusting the regulator settings.

7. Determination of PI controller parameters and simulation.

8. Synthesis of an energy-efficient control system for microclimate parameters in a greenhouse.

To assess economic efficiency, the indicators of minimising energy resources and the payback period of the implemented methods were used. In the course of the study, the following was calculated: distribution, capital expenditures, operating costs, profit from system implementation, and payback periods.

Criteria for evaluating economic efficiency:

$$\begin{cases} \text{Natural gas consumption} \rightarrow min \\ \text{Electricity consumption} \rightarrow min \\ \text{Enterprise profit} \rightarrow max \end{cases} \tag{2}$$

The functions of belonging to the input parameters of the automatic temperature and humidity control system, which are used for technical regulation of microclimate parameters in greenhouses, are synthesised. The following terms are used for all input parameters: "minor impact on energy efficiency", "average impact on energy efficiency", and "significant impact on energy efficiency" (Fig. 8).

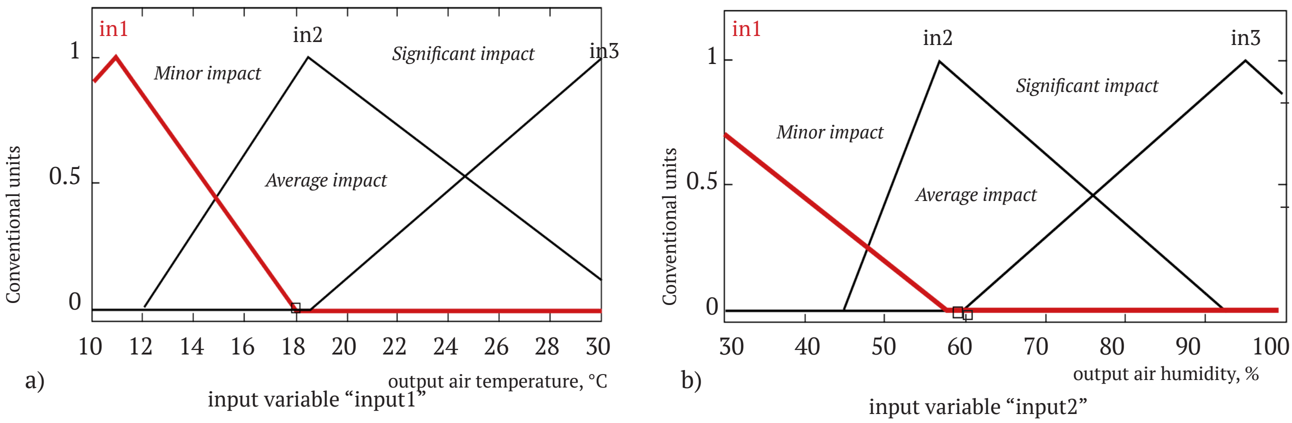

Figure 8. Functions of belonging to energy-efficient parameters of quality control
a) temperature; b) humidity in closed-ground structures

The obtained membership functions allow: predicting the potential effect of the developed methods of controlling technological processes in the greenhouse, taking into account current disturbances, and tracking the qualitative zones of input parameters that affect the energy consumption of the process of growing vegetable products in closed-ground structures

CONCLUSIONS

1. Analysis of the quality of transients as a response to disturbances in automatic systems with a PI controller and an improved model of the object regarding the temperature and humidity regime showed that the parameters of the regulator settings are variable. This proves the relevance of developing methods for finding regulator settings that adapt to changes in the operating conditions of the automation system.

2. Based on the use of fuzzy logic methods and a genetic algorithm, models for finding optimal parameters of the PI controller's settings that adapt to changes in the operating conditions of the automation system are developed and studied. According to the linear integral quality indicator, the best quality of the transition process is demonstrated by a system whose PI controller is configured based on using a genetic algorithm for the following indicators: k_p=74.8, k_i=1.8 to comply with the microclimate parameters: $\theta_{in\ set}$=18°C and $\varphi_{in\ set}$=80%.

3. A system of intelligent automated energy-efficient control of microclimate parameters in protected ground structures and its algorithmic support has been developed, containing: a block of neural network forecasting of energy costs, a block of decision support, where prices for energy resources are considered, a block of optimisation of regulator parameters based on the use of fuzzy logic and genetic algorithms. The introduction of such a system allows saving natural gas for heating and electric energy – up to 10%.

REFERENCES

[1] Achkoski, J., Koceski, S., Bogatinov, D., Temelkovski, B., Stevanovski, G., & Kocev, I. (2017). Remote triage support algorithm based on fuzzy logic. *Journal of the Royal Army Medical Corps*, 163(3), 164-170.

[2] Azaza, M., Tanougast, C., Fabrizio, R., & Mami, A. (2016). Smart greenhouse fuzzy logic-based control system enhanced with wireless data monitoring. *ISA Trans*, 61, 297-307.

[3] Dudnyk, A., Lysenko, V., Zaets, N., Komarchuk, D., Lendel, T., & Yakymenko, I. (2018). Intelligent control system of biotechnological objects with fuzzy controller and information channel filtration unit. In *2018 International scientific-practical conference on problems of infocommunications science and technology* (pp. 586-590). Kharkiv: National University of Radio Electronics.

[4] Dudnyk, A., Hachkovska, M., Zaiets, N., Lendel, T., & Yakymenko, I. (2019). Managing a greenhouse complex using the synergetic approach and neural networks. *Eastern-European Journal of Enterprise Technologies*, 4(2(100), 72-78.

[5] Huang, N. (2015). On Holo-Hilbert spectral analysis: A full informational spectral representation for nonlinear and non-stationary data. *Philosophical Transactions of the Royal Society*, 6, 13-26.

[6] Ladanyuk, A., Kyshenko, V., Shkolna, E., & Sych, M. (2016). Development of the algorithm of determining the state of evaporation station using neural networks. *Eastern-European Journal of Enterprise Technologies*, 5(2(83), 54-62.

[7] Marquez-Vera, M.A., Ramos-Fernandez, J.C., Cerecero-Natale, L.F., Lafont, F., Balmat, J.F., & Esparza-Villanueva, J.I. (2016). Temperature control in a MISO greenhouse by inverting its fuzzy model. *Computers and Electronics in Agriculture*, 124, 168-174.

[8] Li, K., Qi, X., Wei, B., Huang, H., Wang, J., & Zhang, J. (2017). Prediction of transformer top oil temperature based on kernel extreme learning machine error prediction and correction. *High Voltage Engineering*, 43(12), 4045-4053.

[9] Lendiel, T., Lysenko, V., & Nakonechna, K. (2021). Computer-integrated technologies for fitomonitoring in the greenhouse. In *Lecture Notes on Data Engineering and Communications Technologies* (pp. 711-729). Cham: Springer.

[10] Nazarenko, I., Mishchuk, Y., Mishchuk, D., Ruchynskyi, M., Rogovskii, I., Mikhailova, L., Titova, L., Berezovyi, M., & Shatrov, R. (2021). Determiantion of energy characteristics of material destruction in the crushing chamber of the vibration crusher. *Eastern-European Journal of Enterprise Technologies*, 4(7(112), 41-49.

[11] Korobiichuk, I., Shostachuk, A., Shostachuk, D., Shadura, V., Nowicki, M., & Szewczyk, R. (2016). Development of the operation algorithm for an automated system assessing the high-rise building. *Solid State Phenomena*, 251, 230-236.

[12] Rogovskii, I.L., Titova, L.L., Gumenyuk, Yu.O., & Nadtochiy, O.V. (2021). Technological effectiveness of formation of planting furrow by working body of passive type of orchard planting machine. *Earth and Environmental Science*, 839, article number 052055.

[13] Yadav, A., Malik, H., & Chandel, S. (2014). Selection of most relevant input parameters using WEKA for artificial neural network based solar radiation prediction models. *Renewable and Sustainable Energy Reviews*, 31, 509-519.

[14] Zhang, X., Shahidehpour, M., Alabdulwahab, A.S., & Abusorrah, A. (2017). Reliability based optimal planning of electricity and natural gas interconnections for multiple energy hubs. *IEEE Transactions on Smart Grid*, 8(4), 1658-1667.

[15] Shah, B., Iqbal, F., Abbas, A., & Kim, K.I. (2015). Fuzzy logic-based guaranteed lifetime protocol for real-time wireless sensor networks. *Sensors (Basel)*, 15(8), 20373-20391.

[16] Prokopenko, T., Ladaniuk, A., & Reshetiuk, V. (2017). Mathematical model of operational management technological complex continuous type. *Agriculture*, 69, 107-112.

[17] Malinin, A. Molnar, K. & Malinina, A. (2021). Parameters of Gas-Discharge Plasma of Barrier Discharge on Mixtures of Vapours of Diiodide, Dibromide and Mercury Dichloride with Helium. *Scientific Herald of Uzhhorod University. Series "Physics"*, (50), 9-14.

[18] Molodetska, T. (2021). Investigation of the Stress-Strain State of the Bending Process of Coated Materials. *Scientific Herald of Uzhhorod University. Series "Physics"*, (50), 15-24.

Інна Юріївна Якименко[1], Віталій Пилипович Лисенко[1], Каміл Віташек[2]

[1]Національний університет біоресурсів і природокористування України
03041, вул. Героїв Оборони, 15, м. Київ, Україна

[2]Познанський університет наук про життя
60637, вул. Wiyska Polskogo, 28, м. Познань, Республіка Польща

Методологія розроблення інтелектуальної енергоефективної системи керування температурно-вологістним режимом в промисловій теплиці

Анотація. Вартість енергоносіїв впливає на собівартість продукції, яку вирощують в промислових теплицях. Мета дослідження – формування методології розробленні інтелектуальної системи енергоефективного керування мікрокліматом у промислових теплицях, що функціонують в умовах невизначеності, на основі поєднання методів прогнозування енерговитрат та їх мінімізації через використання штучних нейронних мереж. Методологія – вхідними параметрами нейромережевої моделі прогнозування є: значення зовнішньої та внутрішньої температур повітря теплиці, значення відносної вологості повітря, поглинуте теплицею сонячне випромінювання та рівень вуглекислоти в теплиці. Виходами моделі прогнозування є значення витрат природного газу та електроенергії. На основі використання методів нечіткої логіки та генетичного алгоритму розроблено та досліджено моделі пошуку та використання оптимальних параметрів налаштувань ПІ-регулятора, адаптованих до зміни умов функціонування системи автоматизації. Проаналізовані методи покращення якості регулювання технологічних параметрів шляхом поєднання в одній системі автоматизації різноманітних інтелектуальних алгоритмів керування, що сприяє зменшенню енергетичних витрат на 10–13 %. Встановлено, що для споруд закритого ґрунту системи опалення й вентиляції мають найбільшу енергозатратність (в середньому за добу на обігрів та вентилювання в промисловій теплиці витрачається понад 4000 $м^3$ природного газу та майже 1000 кВт×год електроенергії. Кореляційний аналіз зв'язків між зовнішніми збуреннями та енергетичними витратами, що забезпечують дотримання заданої технології вирощування рослинної продукції, підтвердив гіпотезу щодо наявності умов невизначеності функціонування промислової теплиці формуються випадковими збуреннями, неповною інформацією про біологічну складову; при цьому коефіцієнти лінійної кореляції не перевищують $r<0.35$. Зазначене створює умови для використання нейронних мереж як для прогнозування енергетичних витрат, так і для формування енергоефективних стратегій керування. Зазначене забезпечує більш якісне регулювання в умовах невизначеності час регулювання, перерегулювання зменшуються в два-три рази. Для створення енергоефективної системи керування мікрокліматом в промислових теплицях, що функціонує в умовах невизначеності, розроблено нейромережеву модель прогнозування енергетичних витрат природного газу та електроенергії. В статті автори удосконалили структурно-функціональну схему системи автоматизації керування температуровологісним режимом в промислових теплицях шляхом поєднання інтелектуальних алгоритмів стабілізації роботи технологічного обладнання на нижньому рівні керування та оптимізації енергетичних витрат, шляхом їх прогнозування на верхньому рівні. Упровадження такої системи дозволяє заощадити природний газ на опалення до 13 % та електричну енергію – до 10 %. Авторами доведено, що розроблення інтелектуальної енергоефективної системи автоматичного керування параметрами мікроклімату в спорудах закритого ґрунту має базуватись на поєднанні методів інтелектуального налаштування параметрів ПІ-регулятора та прогнозування енерговитрат

Ключові слова: енергоефективність показників, ресурсоефективність, параметри мікроклімату, споруди закритого ґрунту, промислова теплиця, інтелектуальна система керування

Machinery & Energetics
Vol. 13, No. 1. 2022

Journal homepage:
https://technicalscience.com.ua/en

UDC 621:664: 669.01(075)
DOI: 10.31548/machenergy.13(1).2022.26-33

Yevgen Aftandiliants[1*], Dainis Viesturs[2]

[1]National University of Life and Environmental Sciences of Ukraine
03041, 15 Heroiv Oborony, Kyiv, Ukraine

[2]Latvian University of Life Sciences
LV-3001, 2 Velika Str., Jelgava, Latvia

Oxidation processes of superalloys of the working layer and interfacial surfaces of bimetallic pairs

Abstract. Most superalloy steels, especially those alloyed with chromium, tungsten, cobalt, and molybdenum, are strongly riveted during plastic deformation by drawing. Superalloy steels with a clean, scale-free surface are susceptible to stick-slip with the carbide tool – drag. Therefore, in case of cold deformation, it is necessary to use special lubricants with extreme pressure components and strong lubricating coatings. After cleaning the surface from scale, a lime-salt coating is applied. Recently, a fairly effective sub-coating of the composition (in an aqueous solution) has been used: sodium sulphate Na_2SO_4 – 130...250 g/l; liquid glass Na_2SiO_3 – 20...30 g/l; treatment at a temperature of 80...90°C. In some technological processes, thin metal coatings are used as an oil coating – copper, lead-tin, and oxalate. After deformation, all types of coatings must be completely removed, since heat treatment can lead to processes of interaction of metal with lubricating coatings. This can lead to deterioration of the surface quality and loss of the necessary properties. The purpose of the study is to create a methodological framework for the oxidation processes of superalloys of the working layer and interfacial surfaces of bimetallic pairs. Methodology – thermodynamic calculations of the equilibrium of chemical reactions on the metal – gas phase interface surfaces. The paper presents the results of experimental studies with the established dependence of the isobaric potential on temperature for reactions on the interfacial surface "Me_2 – gas phase". The authors obtained the dependence of the isobaric potential on temperature for gaseous reaction products on the surface of superalloys. The existence of the dependence of the isobaric potential on temperature for reactions of the formation of complex oxides on the surface of superalloys is confirmed. Scientific significance – the adequacy of oxidation processes of superalloys of the working layer and interfacial surfaces of bimetallic pairs has been experimentally confirmed

Keywords: steel, alloys, chemical composition, oxides, interface surfaces, bimetallic castings

Article's History: Received: 11/10/2021; Revised: 14.01.2022; Accepted: 23.02.2022

INTRODUCTION

The production of high-quality bimetallic castings is possible only if a high-quality connection of the working layer with the base is formed [1].

The development of a high-quality technological process for the production of bimetallic castings makes it necessary to conduct a complex of research measures to investigate the features of their development [2]. The main purpose of this stage is to investigate the oxidation processes of steels and alloys of the main and working layers and determine the chemical composition of simple and complex oxides on the base, working layer, and interfacial surfaces [3].

A reliable diffusion bond between alloys belonging to bimetallic pairs can be obtained after studying the oxidation processes of superalloys of the working layer and calculating the composition of complex oxides on interfacial surfaces [4].

Therefore, the problem of investigating the features of oxidation processes of superalloy working layers and calculating the composition of complex oxides on interfacial surfaces is urgent.

Investigations of the oxidation processes of carbon, low-alloy steels and superalloys belonging to bimetallic pairs, and the content of complex oxides, were carried

Suggested Citation:
Aftandiliants, Ye., & Viesturs, D. (2022). Oxidation processes of superalloys of the working layer and interfacial surfaces of bimetallic pairs. *Machinery & Energetics,* 13(1), 26-33.

*Corresponding author

out using the method of thermodynamic calculations of the equilibrium of chemical reactions on the surfaces of the metal-gas phase interface [5]. The main advantage of thermodynamic research methods is the possibility of conducting a theoretical analysis of the oxidation process without its preliminary experimental implementation [6]. A special feature of the method is the preliminary systematisation of not only the temperature functions of the logarithm equation of the equilibrium constant K_r, but also the functions of the enthalpy ΔH, changes in the entropy ΔS, and changes in the thermal coefficients of the heat capacities of all participants in the reaction ΔCp [7]. The values of the logarithms of the reaction equilibrium constant are calculated according to the equation given in [8].

$$IgK_r = \frac{\Delta f(\Delta H)}{T} + \Delta f(\Delta S) + \Delta C_0 \cdot M_0 + +\Delta C_1 \cdot M_1 + \Delta C_2 \cdot M_2 + \Delta C_{-2} \cdot M_{-2} \quad (1)$$

where *T* – temperature, *K; M_0, M_1, M_2, M_{-2}* – temperature functions; ΔC_0, ΔC_1, ΔC_2, ΔC_{-2} – heat capacity coefficients.

To assess the possibility of implementing the studied reactions, the isobaric potential was determined at a given temperature in [9]:

$$\Delta Z_T^0 = -4{,}575 \cdot T \cdot l\ell gK_r \quad (2)$$

The composition of complex oxides on interfacial surfaces was studied by x-ray phase analysis on a DR-2 x-ray diffractometer [10]. Samples of cylindrical alloys with a diameter of 20 mm and a height of 15 mm oxidised at a temperature of 1,000°C with an exposure time of 30 hours were used as the object of research [11]. Diffraction spectra were obtained in monochromatic Cukl – radiation [12]. A single graphite crystal placed on a diffracted beam was used as a monochromator [13].

This shooting geometry allows reducing the fluorescent background and recording the diffraction spectra of iron-based alloys in copper radiation [14]. Diffragrams were obtained by step scanning in the range of angles 2θ from 10 to 90° [15]. The scanning step was 0.05°, and the exposure time was 3-5 seconds. The scanning speed was 0.5°/min. Data processing of the diffractometric experiment was performed using a program for full-profile analysis of x-ray spectra from a mixture of polycrystalline phase components powder cell 2.4 [16].

During the calculation process, the periods of elementary cells of phase components [17], the half-width of x-ray profiles [18], the background line [19], and the mass fractions of phases [20] were specified.

The purpose of the study is to create a methodological framework for the oxidation processes of superalloys of the working layer and interfacial surfaces of bimetallic pairs.

RESULTS AND DISCUSSION

To investigate the processes of oxide formation on the surfaces of superalloys of the working layer of bimetallic castings, thermodynamic calculations of possible oxidation reactions at the interfacial boundaries "Me_2 – gas phase" in the temperature range of 1,100-1,700 K were performed.

On the surface of superalloys 240x16 (12% Cr – ASTM A532 Class II Type A), 300x12g5 (300 Cr12Mn5 – marking of Ukraine) and 260x28 (25% Cr-ASTM A532 Class III Type A), oxidation of iron, carbon, silicon, manganese, chromium, sulphur, and phosphorus is possible. Reactions of interaction of iron and manganese with sulphur with the generation of iron and manganese sulphides are also possible. Oxidation of iron, silicon, manganese, and chromium is carried out by reactions (3)-(9).

$$Fe+½O_2 \rightarrow FeO, \quad (3)$$
$$4Fe+3O_2 \rightarrow Fe_2O_3, \quad (4)$$
$$3Fe+2O_2 \rightarrow Fe_3\,O_4, \quad (5)$$
$$[Si]_{0.36}+O_2 \rightarrow SiO_2, \quad (6)$$
$$[Mn]_{0,65}+O_2 \rightarrow MnO, \quad (7)$$
$$3[Mn]_{0,65}+2O_2 \rightarrow Mn_3O_4, \quad (8)$$
$$4[Cr]_{0,3}+3O_2 \rightarrow 2Cr_2O_3. \quad (9)$$

The formation of sulphides corresponds to reactions (10) and (11).

$$Fe+[S] \rightarrow FeS, \quad (10)$$
$$[Mn]+[S] \rightarrow MnS. \quad (11)$$

On the surface of superalloys, the formation of a complex oxide $MnSiO_3$ is possible by reaction:

$$[Mn] + [Si] + \frac{3}{2O_2} \rightarrow MnSiO_3, \quad (12)$$

superalloys 300X12M (GJN-HV600 (XCR11 – EN – JN3019), 300X12G3M (300Cr12Mp3Mo – marking of Ukraine), 300X12G5M (300Cr12Mp5Mo – marking of Ukraine), 300X20M2 (GJN-HV600 (XCr18) –EN-JN3039) are oxidised and form oxides of iron, silicon, manganese, and chromium on the surface by reactions (3)-(9), and iron and manganese sulphides can be formed by reactions (10) and (11). The reaction (13) of Mo oxidation to MoO_3 is added to the above:

$$2[Mo]+3[O_2\,] \rightarrow MoO_3. \quad (13)$$

Alloy 300x22 (20% Cr-Mo – ASTM A532 Class II Type D) in addition to the main elements such as iron, carbon, silicon, manganese, and chromium contains vanadium and titanium. The following oxidation reactions of these elements were studied:

$$4[V]+3O_2 \rightarrow 2V_2O_3, \quad (14)$$
$$[V]+O_2 \rightarrow VO_2(\beta), \quad (15)$$
$$2[V]+2O_2 \rightarrow V_2O_4(\beta), \quad (16)$$
$$Ti+O_2 \rightarrow TiO_2(\text{rutile}), \quad (17)$$
$$2Ti+3/2O_2 \rightarrow Ti_2O_3. \quad (18)$$

On the surface of the alloy 300X16M2 (GJN-HV600 (XCr14) – EN-JN3029), oxidation of elements by reactions (3)-(12), and oxidation of copper to CuO and Cu_2O oxides is possible:

$$[Cu]+½O_2 \rightarrow Cuo, \quad (19)$$
$$[Cu]+½O_2 \rightarrow Cu_2O. \quad (20)$$

On the surface of a superalloy 350XH2 (GJN-HV550 – EN-JN2029), oxidation by reactions is possible (3)-(9), (12), and the formation of sulphides by reactions (10) and (11). To these reactions, it is necessary to add the nickel oxidation reaction to NiO:

$$NiT+½O_2 \rightarrow NiO, \quad (21)$$

Dependence of the isobaric potential on temperature for reactions on the interfacial surface "Me_2 – gas phase" is shown in Figure 1.

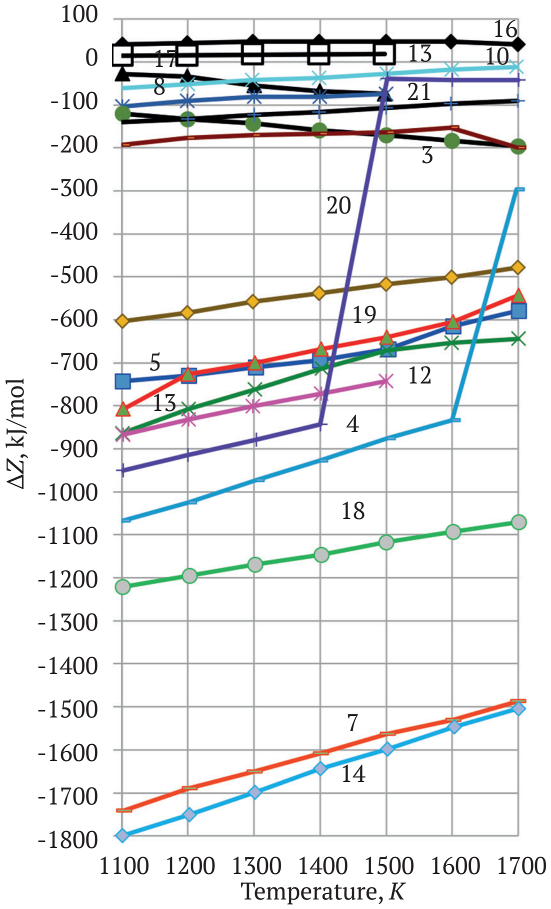

Figure 2. Dependence of the isobaric potential on temperature for reactions on the interfacial surface "Me_2 – gas phase"

The most likely reactions for superalloys are 240x16 (12% Cr – ASTM A532 Class II Type A), 300X12G5 (300 $Cr_{12}Mn_5$ – marking of Ukraine) and 260x28 (25% Cr – ASTM A532 Class III Type A) there are reactions (9) – oxidation of chromium to Cr_2O_3, reaction (4) oxidation of iron to hematite at temperatures below 1,600 K, reaction (8) oxidation of manganese to Mn_3O_4 at temperatures of 1,400 K and below, and reaction (12) – oxidation of manganese and silicon to form a complex oxide $MnSiO_3$ at temperatures below 1,500 K.

At temperatures of 1,500-1,700 K, the reaction (16) is unlikely, and in the range of 1,400-1,500 K, the isobaric potential drops sharply. The reactions (13) and (18) are less likely – oxidation of iron to magnetite and oxidation of silicon to SiO_2 reaction (7) – oxidation of manganese to MPO. The following are unlikely: reaction (3) – oxidation of iron to visstite, reaction (11) – formation of manganese sulphide, and reaction (10) – formation of iron sulphide.

For superalloys 300X12M (GJN-HV600 (XCR11) – EN-JN3019), 300X12G3M (300$Cr_{12}Mn_3$Mo – marking of Ukraine), 300 $Sg_{12}Mn_5$Mo – marking of Ukraine) and 300X20M2 (GJN-HV600 (XCr18) – EN-JN3039) to the reactions discussed above, the reaction (13) – oxidation of molybdenum to MoO_3 is added, which is most likely, and the isobaric potential decreases in this temperature range with $\Delta Z_{1,700}$=-577 kJ mol to $\Delta Z_{1,100}$=-863 kJ/mol.

On the surface of a superalloy 300X22 (20% Cr-Mo-ASTM A532 Class II Type D) to reactions (3)-(9), (10) and (11) the reactions (14)-(16) – vanadium oxidation and reactions (17), (18) – titanium oxidation are added.

Thermodynamic calculation of reactions (14)-(16) vanadium oxidation revealed that reaction (14) – vanadium oxidation to V_2O_3, is the most likely: $\Delta Z_{1,700}$=-1,491 kJ/mol, $\Delta Z_{1,100}$=-1,801 kJ/mol. Reactions (15) and (16) are impossible, since their isobaric potential is a positive value. Reactions (17) and (18) – oxidation of titanium to TiO_2 and Ti_2O_3, accordingly, they are the most likely and with a decrease in temperature the potential decreases: $\Delta Z_{1,700}$=-1,066 kJ/mol, $\Delta Z_{1,100}$=-1,218 kJ/mol of reaction (16), a $\Delta Z_{1,700}$=-642 kJ/mol and $\Delta Z_{1,100}$=-746 kJ/mol – for reaction (17).

On the surface of a superalloy 300X16M2 (GJN – HV600 (XCr14) - EN-JN3029), reactions (3)-(12) are added to reactions (19) and (20) – oxidation of copper to CuO and Cu_2O. Both of these reactions are the least likely: ΔZ≈-12÷-98 kJ/mol.

On the surface of a superalloy 350XH2 (GJN-HV550 – (EN-JN2029) to reactions (3)-(9), (10)-(12) added reaction (21) – oxidation of nickel to NiO_t oxide. Based on the value of the isobaric potential, it can be assumed that it is unlikely, ΔZ≈-90÷-142 kJ/mol.

When superalloys are oxidised, gaseous reaction products are also formed: CO_2, CS_2, COS, SO, SO_2, SiO, and PO. Figure 2 shows the dependence of the isobaric potential in the range of 1,100-1,700 K reactions (22)-(28) – the formation of gaseous products.

$$[C]O_2 \rightarrow C2\uparrow, \qquad (22)$$

$$[C]+2[S] \rightarrow CS_2\uparrow, \qquad (23)$$

$$[C]+ [S]+½O_2 \rightarrow COS\uparrow, \qquad (24)$$

$$[S]+½O_2 \rightarrow SO\uparrow, \qquad (25)$$

$$[S]+O_2 \rightarrow SO_2\uparrow, \qquad (26)$$

$$[Si]+½O_2 \rightarrow SiO\uparrow, \qquad (27)$$

$$[P]+½O_2 \rightarrow PO\uparrow. \qquad (28)$$

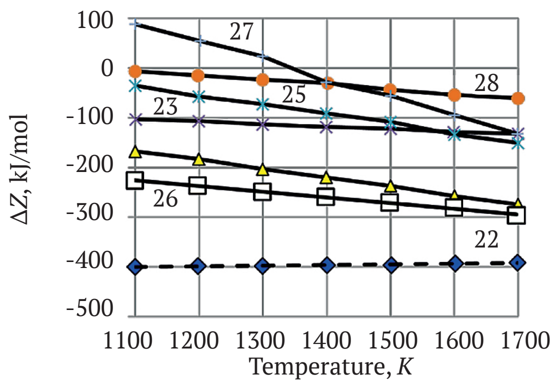

Figure 2. Dependence of the isobaric potential on temperature for gaseous reaction products on the surface of superalloys

The most likely reaction is (22) – carbon oxidation to $CO_2\uparrow$. Reactions (26) and (24) – formation of SO2 and COS are less likely. Reactions (25), (27), and (28) – formation of SO, SiO, and PO, respectively, are less likely. Reaction (21) – formation of CS_2 in the range of 1,350-1,700 K is less likely, and at temperatures below 1,350 K it is impossible.

The superalloys listed above have their own number of most likely oxidation reactions. Figure 3 shows a histogram for superalloys.

For superalloys 240X16 (12% Cr – ASTM A532 Class II Type A), 300x12g5 (300 Cr12Mn5 – marking of Ukraine), 260x28 (25% Cr-ASTM A532 Class III Type A), a number of reaction probabilities are presented in Table 1.

For superalloys 300X12M (GJNHV600 (XCr11) – EN-JN3019), 300X12G3M (300Cr12Mn3Mo – marking of Ukraine), 300X12G5M (300Cr12Mn5Mo – marking of Ukraine) and 300X20M2 (GJN – HV600 (XCr18) – EN-JN3039) a number of probabilities are shown in Table 2.

a)

b)

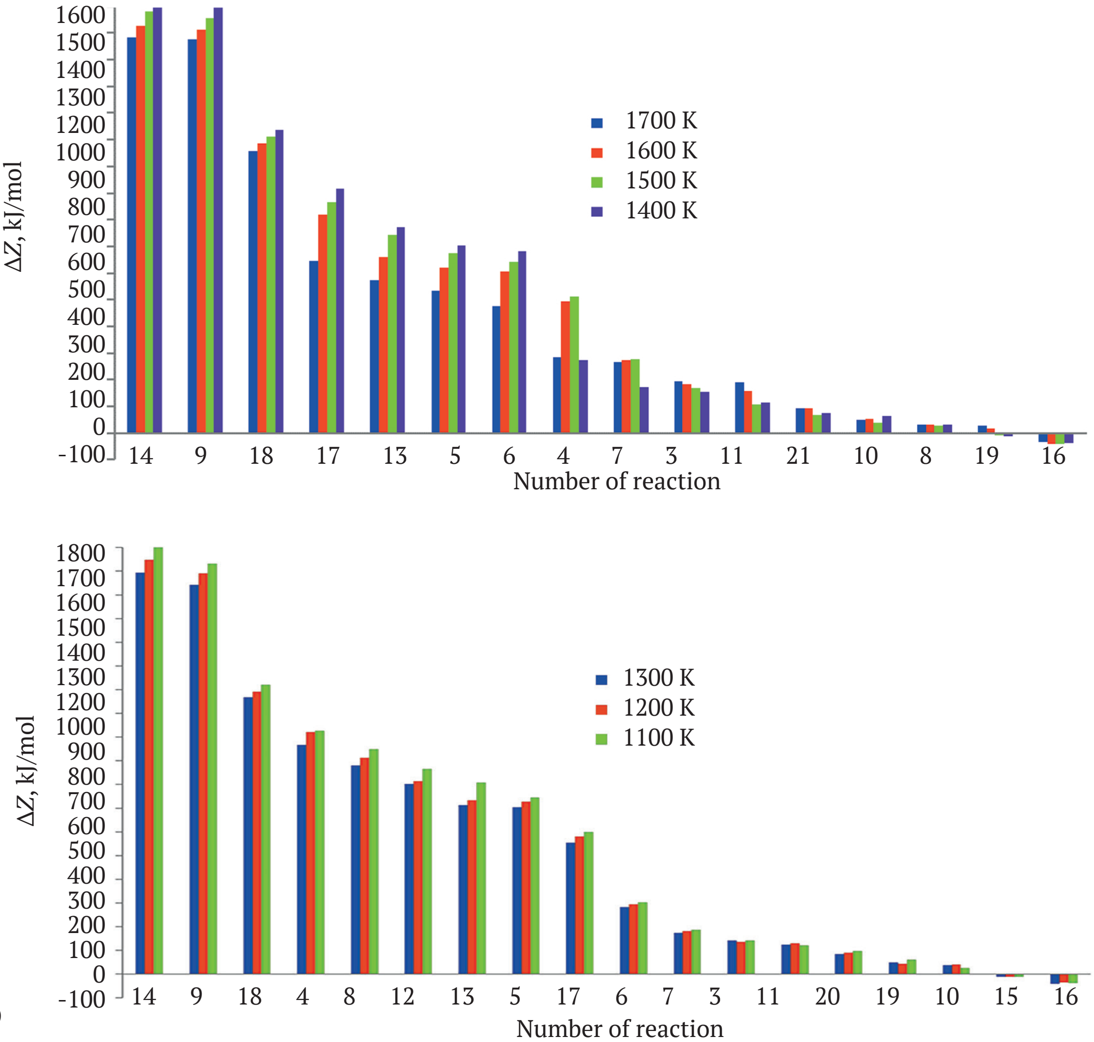

Figure 3. Dependence of the isobaric potential on temperature for solid-phase products on superalloys: a) temperature range from 1,400 to 1,700 K; b) 1,100 to 1,300 K

Table 1. A number of probabilities of oxidation reactions and formation of iron and manganese sulphides on superalloys 240X16 (12% Cr – ASTM A532 Class II Type A), 300x12g5 (300 Cr12Mn5 – marking of Ukraine), 260x28 (25% Cr-ASTM A532 Class III Type A)

T, K	Number of reaction probabilities									
1.700	9	5	6	4	7	3	11	10	8	–
1.600	9	4	5	6	7	11	3	10	8	–
1.500	9	4	12	5	6	7	11	3	10	8
1.400	9	4	8	12	5	6	7	3	11	10
1.300	9	4	8	12	5	6	7	3	11	10
1.200	9	4	8	12	5	6	7	3	11	10
1.100	9	4	8	12	5	6	7	3	11	10

Table 2. A number of probabilities of oxidation reactions and formation of iron and manganese sulphides on superalloys 300X12M (GJN – HV600 (XCr11) – EN-JN3019), 300X12G3M (300Cr12Mn3Mo – marking of Ukraine), 300X12G5M (300Cr12Mn5Mo – marking of Ukraine) and 300X20M2 (GJN – HV600 (XCr18) – EN-JN3039)

Temperature, K						
1.100	1.200	1.300	1.400	1.500	1.600	1.700
Number of reaction probabilities						
9	9	9	9	9	9	9
4	4	4	4	4	4	13
8	8	8	8	12	13	5
12	12	12	12	13	5	6
13	13	13	13	5	6	4
5	5	5	5	6	7	7
6	6	6	6	7	11	3
7	7	7	7	11	3	11
3	3	3	3	3	10	10
11	11	11	11	10	8	8
10	10	10	10	8	–	–

A number of probabilities for a superalloy 300x22 (20% Cr-Mo – ASTM A532 Class II Type D) are presented in Table 3.

Table 3. A number of probabilities of oxidation reactions and formation of iron and manganese sulphides on a superalloy 300x22 (20% Cr-Mo – ASTM A532 Class II Type D)

Temperature, K						
1,100	1,200	1,300	1,400	1,500	1,600	1,700
Number of reaction probabilities						
14	14	14	14	14	14	14
9	9	9	9	9	9	9
18	18	18	18	18	18	18
4	4	4	4	4	4	17
8	8	8	8	12	17	5
12	12	12	12	17	5	6
5	5	17	17	5	6	4
17	17	5	5	6	7	7
6	6	6	6	7	11	3
7	7	7	7	11	3	11
3	3	3	3	3	10	10
11	11	11	11	10	8	8
10	10	10	10	8	14	16
14	14	14	14	14	16	–
16	16	16	16	16	–	–

For a superalloy 300X16M2 (GJNHV600 (XCr14) – EN-JN3029), a number of probabilities are presented in Table 4.

Table 4. A number of probabilities of oxidation reactions and formation of iron and manganese sulphides on a superalloy 300X16M2 (GJN-HV600 (XCr14) – EN-JN3029)

Temperature, K						
1.100	1.200	1.300	1.400	1.500	1.600	1.700
Number of reaction probabilities						
9	9	9	9	9	9	9
4	4	4	4	4	4	13
8	8	8	8	12	13	5
12	12	12	12	13	5	6
13	13	13	13	5	6	4
5	5	5	5	6	7	7
6	6	6	6	7	11	3
7	7	7	7	11	3	11
3	3	3	3	3	10	10
11	11	11	11	20	8	8
20	20	20	20	10	15	19
19	19	10	10	19	16	16
10	10	19	19	8	-	-
15	15	15	15	15	-	-
16	16	16	16	16	-	-

A number of probabilities on a superalloy 350XH2 alloy (GJN-HV550 – EN-JN2029) are presented in Table 5.

Table 5. A number of probabilities of oxidation reactions and formation of iron and manganese sulfides on a superalloy 350XH2 (GJNHV550 – EN-JN2029)

Temperature, K						
1,100	**1,200**	**1,300**	**1,400**	**1,500**	**1,600**	**1,700**
Number of reaction probabilities						
9	9	9	9	9	9	9
4	4	4	4	4	4	5
8	8	8	8	12	5	6
5	5	5	5	6	7	7
12	12	12	12	5	6	4
5	5	5	5	6	7	7
6	6	6	6	7	11	3
7	7	7	7	11	3	11
3	3	3	3	3	21	21
21	21	11	11	21	10	10
11	11	21	21	10	8	8
10	10	10	10	8	-	-

Figure 2 shows a histogram of gaseous reaction products on the surface of superalloys.

A number of probabilities of possible gaseous reaction products are shown in Table 6.

Table 6. A number of probabilities of gaseous products of oxidation reactions at the interfacial boundary “Me_2 – gas phase”

T, K	Number of reaction probabilities						
1,700	22	26	24	25	27	23	28
1,600	22	26	24	25	27	23	28
1,500	22	26	24	27	25	23	28
1,400	22	26	24	27	25	28	23
1,300	22	26	23	27	25	28	23
1,200	22	26	24	27	25	28	23
1,100	22	26	24	27	25	28	22

Oxides formed on the surface of superalloys can interact with each other to form complex oxides by reactions:

$$FeO+ Cr_2O_3 \rightarrow FeO{\cdot}Cr_2O3, \quad (29)$$

$$MnO+SiO_2 \rightarrow MnSiO_3, \quad (30)$$

$$FeO+SiO_2 \rightarrow FeO{\cdot}SiO_2. \quad (31)$$

To determine the possibility formation of complex oxides on the surfaces of alloys 300X12M (GJN-HV600 (XCr11) – EN-JN3019), 300X12G3M (300Cr12Mn3Mo – marking of Ukraine), 300X12G5 (300 Cr12Mn5 – marking of Ukraine), 300X16M2 (GJN-HV600 (XCr14) – EN-JN3029), 300X20M2 (GJNHV600 (XCr18) – EN-JN3039) thermodynamic calculation of the isobaric potential of these reactions of complex oxide formation in the range of 1,100-1,800 K is performed.

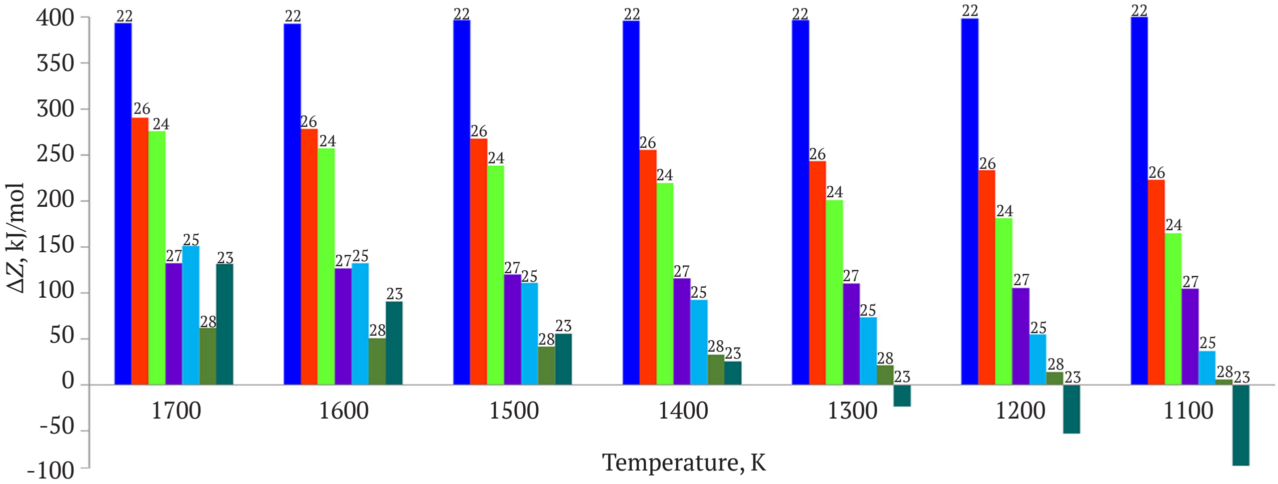

Figure 3. Dependence of the isobaric potential on superalloys

The dependence of the isobaric potential on temperature for complex oxide formation reactions is shown in Figure 5.

Calculations show that the following complex oxides can form on the surface of superalloys: $FeO{\cdot}Cr_2O_3$, $MnO{\cdot}SiO_2$ and $2FeO{\cdot}SiO_2$. The most likely reaction is (29) – the formation of a complex oxide $FeO{\cdot}Cr_2O_3$. Reactions (30) and (31) – formation of complex oxides $MnO{\cdot}Sio_2$ and $2FeO{\cdot}SiO_2$ – accordingly, they are unlikely due to their small size ΔZ. Reaction (31) at temperatures of 1,700-1,800 K is not possible.

In order to study the phase composition of complex oxides, an x-ray phase analysis of oxide films formed on the surface of superalloys was performed.

The results of x-ray phase analysis are presented in Table 7.

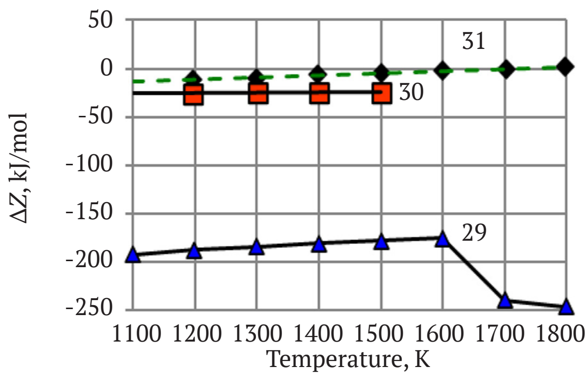

Figure 5. Dependence of the isobaric potential on temperature for reactions of formation of complex oxides on the surface of superalloys

Table 7. Results of studying the phase composition of oxide films on superalloys

Object of research	Phase composition
300X12M GJN-HV600 (XCr11) (EN-JN3019)	Fe_2O_3 (rhombohedral lattice); Fe_2O_3 (cube); Cr_2O_3; $Fe_2O_3{\cdot}Mn_2O_3$; $Cr_2O_3{\cdot}Fe_2O_3$
300X12G3M 300Cr12Mn3Mo	Fe_2O_3 (rhombohedron); Fe_2O_3 (cube); $Cr_2O_3{\cdot}FeO$; $Cr_2O_3{\cdot}Fe_2O_3$; $Fe_2O_3{\cdot}Mn_2O_3$; $Cr_2O_3{\cdot}3Fe_2O_3$
300X12G5 300Cr12Mn5	γ- Fe; α- Fe; Fe_2O_3 (rhombohedron); Fe_2O_3 (cube); $Fe_2O_3{\cdot}Cr_2O_3$; $Fe_2O_3{\cdot}Mn_2O_3$
300X16M2 GJN-HV600 (XCr14) (EN-JN3029)	α- Fe; γ- Fe; Fe_2O_3 (rhombohedron); Fe_2O_3 (cube); Fe_3O_4; $Fe_2O_3{\cdot}Mn_2O_3$; $Cr_2O_3{\cdot}3Fe_2O_3$
300X20M2 GJN-HV600 (XCr18) (EN-JN3039)	α- Fe; γ- Fe; Fe_2O_3 (rhombohedron); Fe_2O_3 (cube); Fe_3O_4; $Mn_2O_3{\cdot}Fe_2O_3$; $Cr_2O_3{\cdot}Fe_2O_3$

The results of the x-ray phase study showed that complex oxides are formed on all superalloys. The largest amount of complex oxides is formed on the alloy 300x12G3M ($300Cr_{12}Mn_3Mo$ – marking of Ukraine): $Cr_2O_3{\cdot}FeO$; $Cr_2O_3{\cdot}Fe_2O_3$; $Fe_2O_3{\cdot}Mn_2O_3$; $Cr_2O_3{\cdot}3Fe_2O_3$. Superalloys 300X12M (GJN-HV600 (XCr_{11}) – EN-JN3019), 300X12G5 (300 $Cr_{12}Mn_5$ – marking of Ukraine) and 300X20M2 (GJN-HV600 (XCr_{18}) – EN-JN3039) form two complex oxides Fe_2O_3 each. Mn_2O_3 and Cr_2O_3 Fe_2O_3. Complex oxides Fe_2O_3 are formed on the 300x16M2 alloy. Mn_2O_3 and $Cr_2O_3{\cdot}3Fe_2O_3$. Presence of complex oxide $Cr_2O_3{\cdot}FeO$ and lack of MnO·SiO2 and $2FeO{\cdot}SiO_2$ in oxide films confirm the results of the performed thermodynamic calculations.

CONCLUSIONS

1. It is established that on the surfaces of superalloys of the working layer in the temperature range of 1,700-1,100 K as a result of oxidation reactions, the following solid-phase oxides are formed: FeO, Fe_2O_3, Fe_3O_4, SiO_2, MnO, Mn_3O_4, $MnSiO_3$, Cr_2O_3, MoO_3, V_2O_3, TiO_2 (rutile), Ti_2O_3, Sio, Cu_2O, NiO. As gaseous products of reactions, Co_2, SS_2, COS, SO, SO_2, SiO, PO are formed.

2. It is established that complex oxides are formed on the surfaces of superalloys due to oxidation reactions: $Cr_2O_3{\cdot}FeO$, $Cr_2O_3{\cdot}3Fe_2O_3$, $3Cr_2O_3{\cdot}2Fe_2O_3$, $Cr_2O_3{\cdot}Fe_2O_3$, $Fe_2O_3{\cdot}Mn_2O_3$.

REFERENCES

[1] Wróbel, T. (2014). Characterization of bimetallic castings with an austenitic working surface layer and an unalloyed cast steel base. *Journal of Materials Engineering and Performance*, 23(5), 1711-1717.

[2] Eivani, A.R., & Karimi Taheri, A. (2007). A new method for producing bimetallic rods. *Materials Letters*, 61(19-20), 4110-4113.

[3] Kizu, T., Nagataki, Y., Inazumi, T., & Hosoya, Y. (2001). Effects of chemical composition and oxidation temperature on the adhesion of scale in plain carbon steels. *ISIJ International*, 41(12), 1494-1501.

[4] Lavrishchev, A.V., Prokopev, S.V., & Tynchenko, V.S. (2021). Investigation of the solid-phase joint of VT-14 titanium alloy with 12KH18N10T stainless steel obtained by diffusion welding through intermediate layers. *Metals*, 11(8), number article 1325.

[5] Zhang, H.L., Huang, P.Z., Sun, J., & Gao, H. (2004). Morphological healing evolution of penny-shaped fatigue microcracks in pure ironat elevated temperatures. *Applied Physics Letters*, 85, 1143-1145.

[6] Göbl, M., Eder, H., Prestl, A., Siller, I., & Schnitzer, R. (2020). Diffusion bonding of high-alloyed tool steels with maraging and precip-itation hardening steels. *Metals*, 10, number article 1622.

[7] Aftandiliants, Y., & Gnyloskurenko, S. (2021). Development of advanced alloy steels for machinery. *Engineering for Rural Development*, 20, 706-711.

[8] Du, J., Wang, H., & Zhao, R. (2013). Size-dependent thermodynamic properties and equilibrium constant of chemical reaction in nanosystem: an experimental study (II). *The Journal of Chemical Thermodynamics*, 65, 29-33.

[9] Rogovskii, I.L., Titova, L.L., Voinash, S.A., Melnyk, V.I., Remshev, E.Yu., Galiyev, G.R., Nuretdinov, D.I., & Vornacheva, I.V. (2021). Design of landing of assembly machine building units with circulating load rolling bearing rings. *Journal of Physics*, 1889, number article 042004.

[10] Yang, L., Haber, J.A. Armstrong, Z., & Yang, S.J. (2021). Discovery of complex oxides via automated experiments and data science. *Proceedings of the National Academy of Sciences*, 118(37), number article e2106042118.

[11] Behrens, B.-A., Brunotte, K., Peddinghaus, J., & Heymann, A. (2022). Influence of dwell time and pressure on SPS process with titanium aluminides. *Metals*, 12(1), number article 83.

[12] Nazarenko, I., Mishchuk, Y., Mishchuk, D., Ruchynskyi, M., Rogovskii, I., Mikhailova, L., Titova, L., Berezovyi, M., & Shatrov, R. (2021). Determiantion of energy characteristics of material destruction in the crushing chamber of the vibration crusher. *Eastern-European Journal of Enterprise Technologies*, 4(7(112), number article 49.

[13] Veklich, A., Tmenova, T., Zazimko, O., Trach, V., Lopatko, K., Titova, L., Boretskij, V., Aftandiliants, Y., Lopatko, S., & Rogovskiy, I. (2020). Regulation of biological processes with complexions of metals produced by underwater spark discharge. *Springer Proceedings in Physics. Nanostructure Surfaces, and Their Applications*, 247, 283-306.

[14] Lutz, J., & Pernicka, E. (2007). Energy dispersive X-ray fluorescence analysis of ancient copper alloys: Empirical values for precision and accuracy. *Archaeometry*, 38(2), 313-323.

[15] Mukhametzyanov, T., Fatkhutdinova, A., & Schick, C. (2022). Step-scan differential calorimetry of protein denaturation: Modeling and experiment. *Thermochimica Acta*, 710, number article 179181.

[16] Rogovskii, I.L., Titova, L.L., Voinash, S.A., Sokolova, V.A., Pushkov, Yu.L., Krivonogova, A.S., & Kokieva, G.E. (2020). Modeling the distribution of internal stresses in surface strengthened layer of steel parts after cementation and hardening. *Journal of Physics: Conference Series*, 1679, number article 042069.

[17] Wang, Y., Zhou, B., Zhao, R., Wang, B., Liu, Q., & Dai, M. (2022). Super-accuracy calculation for the half width of a voigt profile. *Mathematics*, 10, number article 210.

[18] Chausov, M., Brezinova, J., Pylypenko, A., Maruschak, P., Titova, L., & Guzanova. A. (2019). Modification of mechanical properties of high-strength titanium alloys VT23 and VT23m due to impact-oscillatory loading. *Metals*, 9(80), 2-18.

[19] Mahar, A., Wang, P., Ali, A., Awasthi, M.K., Lahori, A.H., & Wang, Q. (2020). Challenges and opportunities in the phytoremediation of heavy metals contaminated soils: A review. *Ecotoxicol Environ Saf*, 126, 111-121.

[20] Abdallah, A., Reichel, E., Heinisch, M., & Jacoby, B. (2021). Symmetric plate resonators for viscosity and density measurement. *Procedia Engineering*, 87, 36-39.

Євген Григорович Афтанділянц[1], Дайніс Віастурс[2]

[1]Національний університет біоресурсів і природокористування України
03041, вул. Героїв Оборони, 15, м. Київ, Україна

[2]Латвійський університет наук про життя
LV-3001, вул. Velika, 2, м. Єлгава, Латвія

Процеси окислення високолегованих сплавів робочого шару і міжфазних поверхонь біметалевих пар

Анотація. Більшість високолегованих сталей, особливо легованих хромом, вольфрамом, кобальтом, молібденом, сильно наклепуються при пластичній деформації волочінням. Високолеговані сталі з чистою поверхнею без окалини схильні до схоплювання-налипання з твердосплавним інструментом – волоками. Тому при холодній деформації необхідно застосовувати спеціальні мастила з протизадирними компонентами та міцні підмастильні покриття. Після очищення поверхні від окалини наносять вапняно-сольове покриття. Останнім часом почали застосовувати досить ефективне підмастильне покриття складу (у водному розчині): сульфат натрію Na_2SO_4 – 130…250 г/л; рідке скло Na_2SiO_3 – 20…30 г/л; обробка при температурі 80…90 °C. В окремих технологічних процесах використовують як підмастильні покриття металеві тонкі покриття – мідні, свинцево-олов'яні, а також оксалатне. Після деформації всі види покриттів повинні бути повністю видалені, так як при термообробці можуть протікати процеси взаємодії металу зі змащувальними покриттями. Це може призвести до погіршення якості поверхні та втрати необхідних властивостей. Мета статті – створення методологічного апарату процесів окислення високолегованих сплавів робочого шару і міжфазних поверхонь біметалевих пар. Методологія – термодинамічні розрахунки рівноваги хімічних реакцій на поверхнях розділу "метал – газова фаза". В статті представлено результати експериментальних досліджень із встановлена залежність ізобарного потенціалу від температури для реакцій на міжфазній поверхні "Ме2 – газова фаза". Авторами отримана залежність ізобарного потенціалу від температури для газоподібних продуктів реакцій на поверхні високолегованих сплавів. Підтверджено існування залежності ізобарного потенціалу від температури для реакцій утворення комплексних оксидів на поверхні високолегованих сплавів. Наукова значимість – експериментальним шляхом підтверджена адекватність процесів окислення високолегованих сплавів робочого шару і міжфазних поверхонь біметалевих пар

Ключові слова: сталь, сплави, хімічний склад, оксиди, поверхні розділу, біметалеві виливки

Machinery & Energetics
Vol. 13, No. 1. 2022

Journal homepage:
https://technicalscience.com.ua/en

UDC 21.87
DOI: 10.31548/machenergy.13(1).2022.34-39

Mykola Kiktev[1*], Pavel Obstawski[2]

[1]National University of Life and Environmental Sciences of Ukraine
03041, 15 Heroiv Oborony, Kyiv, Ukraine

[2]Warsaw University of Natural Sciences
02787, 166 Novoursynovska Str., Warsaw, Republic of Poland

Determination of forecast indicators of electricity quality in the mode of synchronised vector measurements

Abstract. New electrical technologies apply real-time synchronised vector measurement technologies to improve the reliability of power supply systems based on the use of synchrophasors to monitor and analyse the functioning of the network in real time. This was an important milestone in the implementation of the goal of developing the country's energy system through the use of sophisticated innovative control and measuring devices. The new technologies are based on the use of synchronised vector measurement devices (phasor measurement unit – PMU) to collect data from more than 344 installed devices at a frequency of 30 times per second. This significantly distinguishes new technologies from traditional ones, which allow recording measurement data every 4 seconds. This data has GPS timestamps, which allows synchronising measurements at different points and combining the results obtained for a detailed and comprehensive assessment of the state of the system over a wide geographical area. Having such data at your disposal creates more opportunities for detecting, diagnosing, and preventing network disruptions, which means it makes it smarter. The integration of these technologies into a real-time network monitoring system significantly increases our situational awareness of network functioning and contributes to its modernisation. Synchronised vector measurement technologies provide unique data that can significantly improve reliability. Due to these devices, it is possible to expand the possibilities for dynamic monitoring of the state of the power system. The purpose of the study is to summarise research on determining the forecast indicators of electricity quality in the mode of synchronised vector measurements. The authors substantiated the block diagram of the technology for diagnosing the quality of electricity. As a result of analytical approaches, a graphical interpretation of the order of receiving packets through a given communication method at a frame rate of 50 frames/s is reproduced. Conclusion – four programme codes simultaneously generate real-time indicators and are written to the MySQL database, these indicators are used to calculate voltage and frequency deviations. Scientific significance – the adequacy of modelling electricity quality data in synchronised vector measurement mode using the Google Colab service and implementation in Pytpon language is confirmed

Keywords: electricity production, quality, diagnostics, synchronised vector measurement devices, forecasting methods, dynamic database, web application

Article's History: Received: 15.10.2021; Revised: 12.01.2022; Accepted: 23.02.2022

INTRODUCTION

In the last 2 years, due to the covid-19 pandemic, there has been a need to make adjustments to the operation of various technical systems [1]. One of the most important components of providing hospitals, in particular, infectious diseases, is high-quality power supply for the uninterrupted operation of medical equipment, in particular, artificial ventilation devices [2]. There are cases when patients connected to a ventilator died due to an emergency power outage in the hospital [3]. In particular, such a case occurred in the Lviv Oblast of Ukraine [4]. According to the state emergency service of Ukraine, in the city of Enerhodar, Zaporizhzhia Oblast of Ukraine, rescuers on Sunday, June 27, 2021, in the evening provided assistance to the hospital during an

Suggested Citation:
Kiktev, M., & Obstawski, P. (2022). Determination of forecast indicators of electricity quality in the mode of synchronised vector measurements. *Machinery & Energetics,* 13(1), 34-39.

*Corresponding author

emergency power outage [5]. Other similar cases are also known: rescuers helped doctors of the Alchevsk Hospital of the Luhansk Oblast of Ukraine by connecting generators to artificial ventilation devices.

The relevance of scientific research and development, which is devoted to this study, is conditioned by the unresolved problem of creating an automated system for diagnosing the quality of electricity of consumers using renewable energy sources [6]. Currently, some customers of energy companies use devices for generating electricity (solar panels, wind installations, etc.) [7]. And to save costs or generate revenue, they also return energy to the grid [8]. Since an electric power company is legally required to buy electricity produced by consumers [9], it wants to make sure that it does not damage the grid [10]. Now there is a need to measure and control the quality of electricity to make sure that the power supplied to the network from other sources has the same quality and standards that customer equipment expects from it [11].

Many publications are devoted to the study of the quality of electricity. Researchers from the National Technical University of Ukraine "Igor Sikorsky Kyiv Polytechnic Institute" studied the system of monitoring the quality of electric energy in decentralised power supply systems [12]. Researchers of the Institute of Electrodynamics of NASU have developed a recording device "Regina-H", which in its technical and functional characteristics is not inferior to the best foreign analogues [9]. The device provides recording of instantaneous values of currents and voltages [13], storage and processing of measurement results [14]; their display in the form most informative for personnel text messages, graphs, tables, waveforms [15], and transmitting information to any level of the control hierarchy with its binding to exact time signals [16]. These devices are an integral part of a transient mode monitoring system integrated into a local area network that combines measurement converters or other lower-level monitoring devices and a 100 Mbit/s TCP/IP Fast Ethernet data acquisition server [17]. A top-level remote computer is installed in the control centre of the united energy system of the National energy company Ukrenergo and the corresponding electrical system to receive information from the switching server [9].

Intelligent electronic devices ENIP-2 manufactured by Energoservice Engineering Centre LLC [10] measure synchronised vectors of synchrophasors of currents and voltages by PMU Phasor Measurement Unit [18]. Synchronised measurements of the parameters of the power system mode by the current and voltage values and by the main harmonic are also performed [19]. Further, parameters are transmitted to automated technological control systems via a digitally galvanically isolated Ethernet interface [20].

These devices are intended for use in monitoring systems of transient modes WAMS and in automated technological control systems of the new generation WACS, in automated process control systems of substations and automated dispatching control systems, in automatic technological control systems of active adaptive networks, mode automation [21]. ENIP-2 devices can transmit data directly when connected to the local network of a substation or power plant, and through data collection and transmission devices for synchronised PDC measurements.

The purpose of the study was to predict quality in a distributed information and control system for diagnosing electricity quality using renewable management sources and web applications.

RESULTS AND DISCUSSION

The process of diagnosing electricity quality by synchronised vector measurements is summarised in the form of a block diagram (Fig. 1).

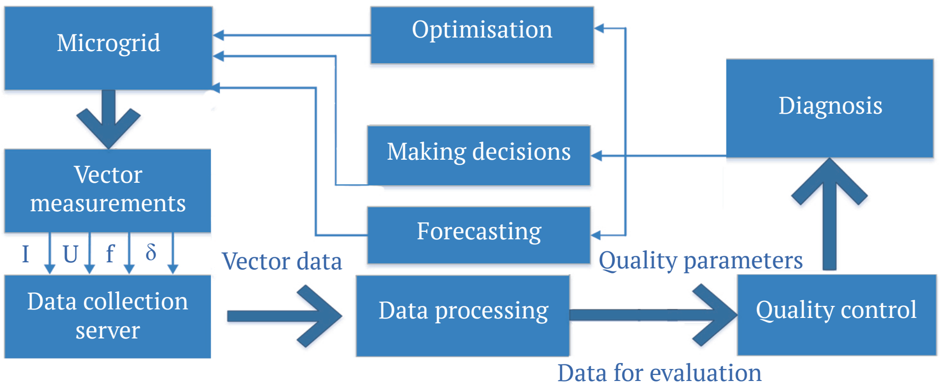

Figure 1. Block diagram of electricity quality diagnostics technology

The standards establish the following indicators of the quality of electric energy [1; 2]:

– voltage deviation δU_y;
– voltage change range δU_t;
– flicker dose P_t;
– sine wave distortion coefficient of the voltage curve K_U;
– coefficient n-th harmonic component of voltage $K_U(n)$
– reverse sequence voltage unbalance coefficient $K2_U$;
– zero-sequence voltage unbalance coefficient $K0_U$;
– frequency deviation Δf;

– voltage failure duration Δt_n;
– pulse voltage U_{imp};
– temporary overvoltage coefficient K_{perU}.

The input information will be an array of measured electrical parameters related to the measurement and values of the vector format of electrical parameters that were extracted from the online system of indicators obtained from the ENIP-2 device (Fig. 2) [22]. This electricity data were collected primarily for scientific purposes. The data relate to the measurement of electricity parameters and were extracted from the online electricity indicator system.

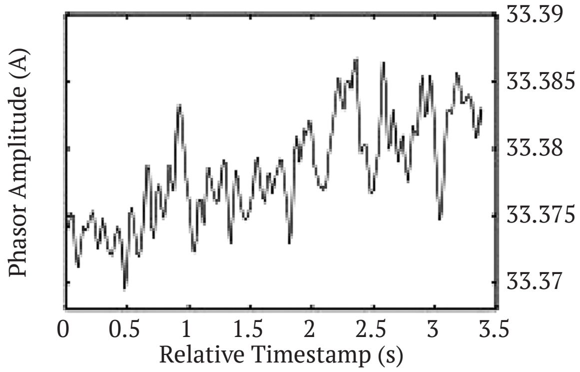

Figure 2. Procedure for receiving packages – preset communication method, frame rate 50 frames/s

1. t, s (countdown, s).
2. f, Hz (frequency per minute).
3. I, A (Current 1, A).
4. U, V (voltage, V).
5. I , A (Current 1, A).

For further statistical processing and forecasting, a dataset will be created containing 100 rows and 6 columns (Table 1).

Table 1. Fragment of the generated data set

No.	f. Hz	I. A.	U. V	I2. A.
1	49.9803	2.0511	230.705	33.374
2	49.9669	2.0512	230.694	33.375
3	49.9942	0.0513	230.661	33.371
4	49.9982	2.0507	230.629	33.374
5	50.0154	2.0506	230.596	33.375
6	49.961	2.0508	230.552	33.373
7	50.0107	2.051	230.535	33.375
8	49.9887	2.0509	230.508	33.3735
9	49.9905	2.0512	230.469	33.3745
10	49.9715	2.0514	230.442	33.3735
11	49.9701	2.0512	230.42	33.369
12	49.9611	2.0514	230.409	33.375
13	49.9822	2.0513	230.381	33.372
14	49.9847	2.0513	230.359	33.3745
15	49.9821	2.0511	230.337	33.379

The calculated statistical indicators for frequency, voltage, and current are shown in Table 2.

Table 2. Statistical characteristics of the measured parameters

Statistical characteristics	Frequency	Voltage	Current
Average values	49.992	33.378	228.884
Median	49.992	33.377	229.318
Maximum value	50.024	33.386	230.705

Columns (1) and (2) will predict the values of column (3) using two methods: KNN and Ridge regression.

The matrix for processing Predict data is shown in Table 3.

Table 3. Matrix for data processing

f. Hz	U. V
50.0228	228.569
49.9793	228.492
50.0041	228.404
50.0248	228.332
50.0233	228.272
49.9803	228.195
49.9734	228.113
49.9666	228.041
50.0249	227.926

Features of the software implementation include:

1. Data reading and primary processing using the Pandas library.
2. Plotting graphs using the Matplotlib and Plotly Express libraries.
3. Building a correlation table using the Seaborn library.
4. Standardisation of data, division of the training set into a training sample and validation sample, and implementation of classification models using the Scikit-Learn library.

Initially, the data was normalised for the highest calculation accuracy. An example of calculation based on normalised data is shown in Figure 3, without normalisation for Ridge regression – in Figure 4.

```
In [208]: from sklearn.linear_model import Ridge
          model = Ridge()
          model.fit(X_train_norm, Y_train)
          model.score(X_train_norm,Y_train)

Out[208]: 0.4774677178673772
```

Figure 3. Programme code snippet and calculation based on normalised data

```
In [209]: model.fit(X_train, Y_train)
          model.score(X_train,Y_train)

Out[209]: 0.45478502803711784
```

Figure 4. Programme code snippet and data calculation without normalisation

Evidently, the accuracy of the model is higher for normalised data.

Columns (1), (2) frequency and voltage, respectively. Predicted column (3) – current. The results of forecasting using the k-nearest neighbour algorithm KNN method and the accuracy of calculating the method are shown in Figure 5, and the predicted model is shown in Figure 6.

```
In [206]: model.score(X_train_norm, Y_train)
Out[206]: 0.6012872304007943
```

Figure 5. Programme code snippet and prediction results using the nearest neighbour method

```
In [207]: model.predict(X_prednorm)
Out[207]: array([33.3764, 33.3723, 33.3761, 33.3794, 33.383 , 33.38  , 33.3798,
           33.3798, 33.3815])
```

Figure 6. Predicted model using the nearest neighbour method

The Ridge regression method and the accuracy of the calculation method are shown in Figure 7: the predicted model is shown in Figure 8.

```
In [208]: from sklearn.linear_model import Ridge
          model = Ridge()
          model.fit(X_train_norm, Y_train)
          model.score(X_train_norm,Y_train)
Out[208]: 0.4774677178673772
```

Figure 7. Code snippet of the ridge regression method and method calculation accuracy

```
In [210]: model.predict(pred)
Out[210]: array([33.38373138, 33.38404514, 33.38446656,
                 33.38480939, 33.38508349, 33.3853977 ,
                 33.38576735, 33.38608706, 33.38666182])
```

Figure 8. Predicted model using the comb regression method

Analysing the resulting forecast graph (Fig. 9), according to the normalised data, the accuracy of the Ridge regression model is higher by 10%-15%.

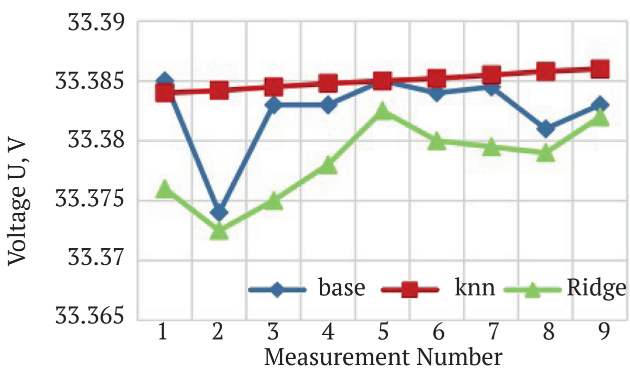

Figure 9. Graphical representation of output and predicted data using KNN and Ridge regression methods

A web-based software application for displaying synchronised vector measurements in the analysed system is described in [13]. Input information is represented by the readings of 4 electricity indicator recorders (PMU devices), which are located in 4 different locations in Ukraine:

– Central PMU, Kyiv Oblast;
– West PMU, Lviv Oblast;
– East PMU, Slovyansk city;
– South PMU, Kherson city.

Data modelling is performed using the Google Colab service and implemented in the Pytpon language. Four programme codes generate real-time metrics in parallel and are written to a MySQL database. These indicators are used to calculate the voltage and frequency deviation. This web interface should provide the ability to view readings from measuring devices connected to the power grid in different locations. These indicators should be presented both in tabular form and in a more user-friendly form – graphically.

The system uses the following tables: Locations, PMUS, Indicators, Quality. Next, an analytical system was constructed for determining the quality of electricity using a mathematical apparatus, which is implemented using the Google Colab service in Python. A fragment of the program results with dynamic data in the Indicators table is shown in Figure 10. The main page of the web interface is shown in Figure 11.

indicator_id	pmu_id	datatime	frequency	voltage	amperage
10 000	1	2020-12-06 13:03:43	50,646	212	18
30 000	3	2020-12-06 13:03:45	49,015	228	22
20 000	2	2020-12-06 13:03:45	51,399	211	21
10 001	1	2020-12-06 13:03:46	49,485	241	21
40 000	4	2020-12-06 13:03:46	51,161	200	24
30 001	3	2020-12-06 13:03:47	48,926	229	22
20 001	2	2020-12-06 13:03:48	49,211	214	17
40 001	4	2020-12-06 13:03:49	49,114	203	16
10 002	1	2020-12-06 13:03:49	50,711	234	25
30 002	3	2020-12-06 13:03:49	51,051	236	19
20 002	2	2020-12-06 13:03:51	50,107	241	18
40 002	4	2020-12-06 13:03:51	50,523	241	18
10 003	1	2020-12-06 13:03:52	51,301	231	22
30 003	3	2020-12-06 13:03:52	48,969	239	19
40 003	4	2020-12-06 13:03:53	50,062	205	24
20 003	2	2020-12-06 13:03:53	48,798	202	15
30 004	3	2020-12-06 13:03:54	50,159	203	22
10 004	1	2020-12-06 13:03:54	50,366	240	11
40 004	4	2020-12-06 13:03:56	50,707	203	10
20 004	2	2020-12-06 13:03:56	50,283	218	26

Figure 10. Dynamic data in the Indicators table

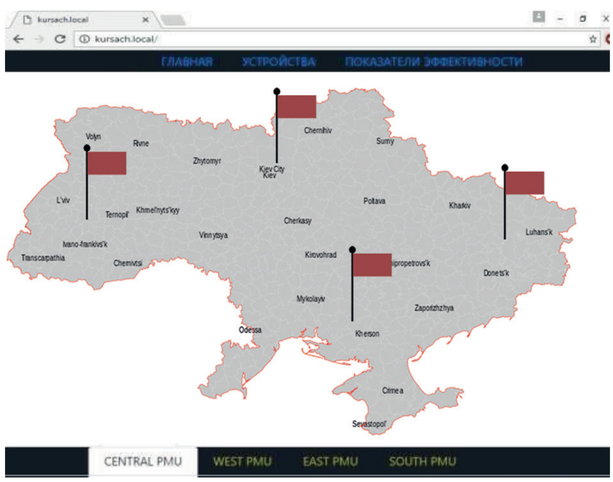

Figure 11. Home page of the web interface

In the future, it is planned to develop this project as follows:

– connecting multiple types of PMU devices, integrating them into the system, and collecting information at various facilities;

– application of optimisation and decision-making methods for managing the quality of electricity at the connection points of renewable generation sources;

– conducting tests in various objects of electricity consumption, in particular, the electrical complex of an industrial greenhouse, described in [23];

– investigation of information security methods and tools for transmitting data from the measurement source to the server.

CONCLUSIONS

1. To determine the quality of electricity, the following parameters are presented: frequency, voltage, and current strength, which are used to diagnose the quality of electricity.

2. A web interface for interactive interaction and visualisation of indicators with tables and graphs was designed and developed. This information is used for further analysis, graphical representation, and output of power quality results.

3. The developed software application allows quickly analysing the quality of electrical energy, and detecting power outages at an early stage.

REFERENCES

[1] Shing, C.K., Yiu, C.Y., & Xiong, C. (2021). Housing market in the time of pandemic: A price gradient analysis from the COVID-19 epicentre in China. *Journal of Risk and Financial Management*, 14, article number 108.

[2] Borghetti, A., Nucci, C.A., & Paolone, M. (2011). Synchronized phasors monitoring during the islanding maneuver of an active distribution network. *IEEE Transactions on Smart Grid*, 2(1), 1-8.

[3] Lixia, M., Benigni, A., Flammini, A., Muscas, C., Ponci, F., Monti, A. (2012). A software-only PTP synchronization for power system state estimation with PMUs. *IEEE Transactions on Instrumentation and Measurement*, 61(5), 1476-1485.

[4] Dileep, G. (2020). A survey on smart grid technologies and applications. *Renewable Energy*, 146, 2589-2625.

[5] Singh, A., & Surjan, B.S. (2014). Microgrid: A review. *International Journal of Research in Engineering and Technology*, 6, 185-198.

[6] Agapova, O., Popovych, N., Shulika, B., & Fylenko, V. (2018). Research of the spatial aspects of using renewable energy sources for sustainable development of the territory. *Technology Audit and Production Reserves*, 6(1(44)), 50-58.

[7] Oliveira, R., Camanho, A., & Zanella, A. (2017). Expanded eco-efficiency assessment of large mining firms. *Journal of Cleaner Production*, 12, 2364-2373.

[8] Volodarskyi, Y.T., & Voloshko, A.V. (2014). System monitoring electrical quality energy in decentralized systems power supply. *Eastern-European Journal of Enterprise Technologies*, 3(8-69), 10-17.

[9] Díaz-Villavicencio, G., Didonet, S., & Dodd, A. (2017). Influencing factors of eco-efficient urban waste management: Evidence from Spanish municipalities. *Journal of Cleaner Production*, 164, 1486-1496.

[10] Huang, X., Wang, X., Chen, L., Ye, C. (2020). Optimal portfolio strategies of purchasing electricity for electricity company based on distributional robust CVaR. *IOP Conference Series Earth and Environmental Science*, 467(1), article number 012200.

[11] Skok, S., Frlan, K., & Ugarković, K. (2017). Detection and protection of distributed generation from island operation by using PMUs. *Energy Procedia*, 141, 438-442.

[12] Hudson, J., Hudson, D., Morini, P., Clarke, H., & Stewart, M.C. (2020). Not one, but many “publics”: Public engagement with global development in France, Germany, Great Britain and the United States. *Development in Practice*, 30(6), 795-808.

[13] Kiktev, N., Osypenko, V., Shkurpela, N., & Balaniuk, A. (2020). Input data clustering for the efficient operation of renewable energy sources in a distributed information system. In *2020 IEEE 15th international conference on computer sciences and information technologies (CSIT)* (pp. 9-12). Tokyo: The University of Tokyo.

[14] Lu, W., Jiang, W., Zhang N., & Xue, F. (2021). A deep learning-based text classification of adverse nursing events. *Journal of Healthcare Engineering*, 2, article number 110.

[15] Rogovskii, I.L., Titova, L.L., Gumenyuk, Yu.O., & Nadtochiy, O.V. (2021). Technological effectiveness of formation of planting furrow by working body of passive type of orchard planting machine. *Earth and Environmental Science*, 839, article number 052055.

[16] Usman, M.U., Faruque, M.O. (2019). Applications of synchro phasor technologies in power systems. *Journal of Modern Power Systems and Clean Energy*, 7, 211-226.

[17] Al Hadi, A., & Sinha, U. (2019). Internet of things (IOT) – enabled solar micro inverter using blockchain technology. In *IEEE industry applications society annual meeting* (pp. 128-138). Baltimore: IEEE.

[18] Rogoskii, I., Mushtruk, M., Titova, L., Snezhko, O., Rogach, S., Blesnyuk, O., Rosamaha, Yu., Zubok, T., Yeremenko, O., & Nadtochiy, O. (2020). Engineering management of starter cultures in study of temperature of fermentation of sour-milk drink with apiproducts. *Potravinarstvo Slovak Journal of Food Sciences*, 14, 1047-1054.

[19] Soetens, N., Famaey, J., Verstappen, M., & Latr'e, S. (2015). SDN-based management of heterogeneous home networks. In *11th international conference on network and service management* (CNSM) (pp. 402-405). Barcelona: IEEE Computer Society.

[20] Anisha, N.P., Prasanna, V., & Suyampulingam, A. (2015). Soft phasor measurement unit. *Procedia Technology*, 21, 533-539.

[21] Venkatesh, T., & Trapti, J. (2017). Placement of synchronized measurements for power system observability during cascaded outages. *International Journal of Emerging Electric Power Systems*, 18(6), article number 1021.

[22] Leibovich, P., Issouribehere, F., & Barbero, J. (2019). Synchrophasor communication over internet: Performance analysis of different methods based on real experiences. In *IEEE power & energy society general meeting* (PESGM), (pp. 78-89). Atlanta: Georgia State University.

[23] Lysenko, V., Bolbot, I., Lendel, T. (2019). Energy efficient system of electrotechnological complex control in industrial greenhouse. *Technical Electrodynamics*, 2, 78-81.

Микола Олександрович Кіктєв[1], Павел Обставські[2]

[1]Національний університет біоресурсів і природокористування України
03041, вул. Героїв Оборони, 15, м. Київ, Україна

[2]Варшавський університет природничих наук
02787, вул. Новоурсиновська, 166, м. Варшава, Республіка Польща

Визначення прогнозних показників якості електроенергії у режимі синхронізованих векторних вимірювань

Анотація. Нові електротехнології застосовують технології синхронізованих векторних вимірювань у режимі реального часу для підвищення надійності енергосистем, засновану на використанні синхрофазорів, для моніторингу та аналізу функціонування мережі в режимі реального часу. Це стало важливою віхою на шляху реалізації мети щодо розвитку енергосистеми країни за допомогою застосування складних інноваційних контрольно-вимірювальних пристроїв. Нові технології базуються на використанні пристроїв синхронізованих векторних вимірювань (phasor measurement unit — PMU) для збору даних від більш ніж 344 встановлених пристроїв із частотою 30 разів на секунду. Це значно відрізняє нові технології від традиційних, що дозволяють реєструвати дані вимірювань кожні 4 секунди. Ці дані мають тимчасові мітки GPS, що дозволяє синхронізувати вимірювання на різних точках та комбінувати отримані результати для детальної та всебічної оцінки стану системи на широкій географічній території. Маючи в своєму розпорядженні такі дані, виникає більше можливостей для виявлення, діагностики та запобігання порушенням у функціонуванні мережі, а значить, робить її розумнішою. Інтеграція цих технологій у систему моніторингу мережі в режимі реального часу значно підвищує нашу ситуаційну поінформованість про функціонування мережі та сприяє її модернізації. Технології синхронізованих векторних вимірювань надають унікальні дані, що дозволяють суттєво покращити надійність. Завдяки цим пристроям існує можливість розширили можливості щодо динамічного моніторингу стану енергосистеми. Мета статті – узагальнити дослідження з визначення прогнозних показників якості електроенергії у режимі синхронізованих векторних вимірювань. В статті автори обґрунтували структурну схему технології діагностики якості електроенергії. В результаті аналітичних підходів відтворено графічну інтерпретацію порядку прийому пакетів через заданий метод зв'язку в частоті кадрів 50 кадрів/с. Висновок – чотири програмні коди паралельно генерують показники в реальному часі і записуються в базу даних MySQL, за цими показниками розраховується відхилення напруги та частоти. Наукова значимість – підтверджена адекватність моделювання даних якості електроенергії у режимі синхронізованих векторних вимірювань за допомогою сервісу Google Colab та реалізацією мовою Phyton

Ключові слова: електроенергії, якість, діагностика, пристрої синхронізованих векторних вимірювань, методи прогнозу, динамічна база даних, веб-додаток

Machinery & Energetics
Vol. 13, No. 1. 2022

Journal homepage:
https://technicalscience.com.ua/en

UDC 631.1.004
DOI: 10.31548/machenergy.13(1).2022.40-48

Liudmyla Titova[1*], Henryk Sobczuk[2]

[1]National University of Life and Environmental Sciences of Ukraine
03041, 15 Heroiv Oborony, Kyiv, Ukraine

[2]Polish Academy of Sciences
00-901, 1 Defilad Sq., Warsaw, Republic of Poland

Typology of means of technical control of physiological and ergonomic indicators of machines for forestry works

Abstract. Nowadays, during logging and timber transportation operations, most of the equipment that is used was put into mass production at the beginning of the millennium. Due to the lack of own funds at the enterprises of the forest complex in recent years, there is no renewal of machines for forestry works, and the worn-out equipment is re-introduced into the same devices as replaceable parts and other fragile elements. In the structure of the existing machinery fleet, 80% is occupied by fully amortised equipment that needs to be upgraded or written off, and the disposal rate is 10 times higher than the renewal rate. The existing repair policy was developed in pre-market conditions with appropriate ratios of prices for raw materials and machinery. At that time, the concept of technical control of machines for forestry operations, which is still in force today, was created: admissions, regulations, standards, etc. In the current economic conditions, new approaches to the development of a methodology for technical control and repair of machinery for forestry operations are needed. Technical support for the operation of machines for forestry operations can be considered as a tool for managing the stock of their potential capabilities laid down during manufacturing and restored during technical control and repair. Determining the time to carry out work to restore the technical condition of the machine depends on various factors, which often contradict each other. The goal is to perform analytical and experimental studies to confirm the existence of typological means of technical control of physiological and ergonomic indicators of machines for forestry operations by modelling the processes of their functioning. Methodology – to test the means of a systematic approach and a systematic analysis of the typology of technical control tools for physiological and ergonomic indicators of machines for forestry operations. The paper presents the generated result in the form of a recording algorithm of the module for technical control of machines for forestry operations. Based on the results of experimental studies, the authors present a graphical interpretation of Integral noise levels at the workplace of a forward driver in a loaded state, in an empty state. Conclusion – the conducted research allows suggesting the optimal placement of elements on the vehicle's instrument panel in terms of information perception and reading time. Scientific significance – it is confirmed that when analysing the impact of the frequency of performing technical control operations of forestry equipment on the listed indicators, it is advisable to use a pair correlation analysis, which consists in determining the relationship between the frequency of performing technical control operations and the amount of total unit costs, reliability indicators, and functional properties indicators

Keywords: ergonomics of timber road trains, typology of technical control tools, reliability indicator, forestry equipment, technical control and repair

Article's History: Received: 26.10.2021; Revised: 28.12.2021; Accepted: 23.02.2022

INTRODUCTION

The issue of improving the use of the suitability of machines for forestry operations is multifaceted [1]. This multiplicity is a direct consequence of the close connection of the advantages and disadvantages of machines as objects of managing their technical condition and reliability with the economic processes of using them for their intended purpose [2].

The content of the scientific foundations of the organisation, technology of technical control and repair

Suggested Citation:
Titova, L., & Sobczuk, H. (2022). Typology of means of technical control of physiological and ergonomic indicators of machines for forestry works. *Machinery & Energetics,* 13(1), 40-48.

*Corresponding author

of machines for forestry works is mainly aimed at studying the dynamics and identifying the causes of changes in their condition [3], assessing and predicting further changes in the technical condition of parts, components, and the machine as a whole to develop optimal methods [4] and ways to manage the technical condition of machines [5].

In accordance with this, the main research areas were formulated, dictated by the need to improve the organisation, technology of maintenance and repair of machines for forestry operations.

Adjustment of technical control modes of machines for forestry operations consists in clarifying the list of maintenance operations [6] and the frequency of their implementation to achieve modes that are optimal for these operating conditions of machines for forestry operations [7].

In this regard, when adjusting the modes, both specific costs for technical control and repair of machinery for forestry operations, and reliability indicators were considered [8]. Thus, the task under consideration is to determine the numerical values of the list of technical control operations and the frequency of their maintenance [9], which ensure not only the necessary reliability of the forestry equipment in operation [10], but also the minimum costs for maintenance and repair of the forestry equipment [11], which fall on a unit of mileage or transport work [12].

MATERIALS AND METHODS

For each group and homogeneous elements, the task of adjusting the frequency of technical control of the forestry equipment to find l_{oi} – the optimal frequency of technical control operations of one group of elements [13] is formulated in the form of an objective function as follows:

$$C_{un_i}=f(l_{oi})\rightarrow min,$$

provided that:

$$P_{i_1}=\varphi_1(l_{oi})=\overline{P_{i_1}}, Z_{i_1}=\psi_1(l_{oi})=\overline{Z_{i_1}},$$
$$P_{i_m}=\varphi_m(l_{oi})=\overline{P_{i_m}}, Z_{i_k}=\psi_k(l_{oi})=\overline{Z_{i_k}}, \quad (1)$$

where: l_{oi} – optimal frequency of technical control operations of one group of forestry equipment elements, years [14]; C_{un_i} – total specific reduced costs for technical control of a homogeneous group of forestry equipment elements, UAH/1,000 km [15]; $P_{i_1},\dots,P_{i_m}$ – indicators of reliability of forestry equipment elements, to be taken into account when determining the frequency [16]; $\overline{P_{i_1}},\dots,\overline{P_{i_m}}$ – standard values of reliability indicators of forestry equipment elements to be taken into account [17]; $Z_{i_1},\dots,Z_{i_k}$ – indicators of functional properties of forestry equipment elements forestry equipment, which must be taken into account when determining the frequency [18]; $\overline{Z_{i_1}},\dots,\overline{Z_{i_k}}$ – normative values of indicators of functional properties of forestry equipment elements [19]; $\varphi_1(l_{oi}),\dots,\varphi_m(l_{oi})$ – dependence of reliability indicators of forestry equipment elements on the frequency of technical control [20]; $\psi_1(l_{oi}),\dots,\psi_m(l_{oi})$ – dependence of indicators of functional properties of forestry equipment on the frequency of technical control [21].

A second-degree polynomial was used to approximate these dependencies (1) [14]. Therefore, the considered dependency models have a form:

$$P_i=a_o+a_1l+a_2l^2, |Z_i=b_o+b_1l+b_2l^2. \quad (2)$$

where: a_o, a_1, a_2, b_o, b_1, b_2 – coefficients of the polynomial.

Then the objective function:

$$C_{un}=C_o+C_1l+C_2l^2\rightarrow min, P_l=a_{01}+a_{11}l+a_{21}l^2=\overline{P_l}; \quad (3)$$
$$P_2=a_{0m}+a_{lm}l+a_2ml^2=\overline{P_m};$$
$$Z_1=b_{01}+b_{11}l+b_{21}l^2=\overline{Z_1};$$
$$Z_K=b_{0K}+b_{1K}l+b_{2K}l^2=\overline{Z_K}. \quad (4)$$

To obtain sufficiently objective data when adjusting the technical control modes, the number of controlled vehicles for forestry operations was 15...20, and the duration of follow-up was 3...6 months [22].

When analysing the influence of the frequency of performing technical control operations of forestry equipment on the listed indicators, a pair correlation analysis was used, which consists in determining the relationship between the frequency of performing technical control operations (X) of the amount of total unit costs, reliability indicators, and indicators of functional properties (Y) [23].

The correlation ratio is used as an indicator of the tightness of the connection:

$$\rho=\sqrt{\frac{S_x^2(Y)}{S_n^2(Y)}}, \quad (5)$$

where:

$$S_x^2(Y)=\frac{1}{N-1}\Sigma_1^N(y_c-\overline{y})^2, \quad (6)$$

$$S_n^2(Y)=\frac{1}{N-1}\Sigma_1^N(y_j-\overline{y})^2, \quad (7)$$

where: $S_x^2(y)$ – variance of the regression line deviation from the overall average; $S_n^2(y)$ – total variance of the dependent variable specific costs, reliability indicator, functional indicator; N – scope of observation.

Variable costs are the cost of paying staff C_{rs}, for spare parts and materials C_{sp}:

$$C_{ver}=C_{rs}+C_{sp}+E_NK_o \quad (8)$$

Determining the cost of spare parts and materials:

$$C_{sp}=\Sigma_{j=1}^{k}P_i, \quad (9)$$

where: P_i – cost of j-th detail or materials, UAH; j – the number of materials and parts that are replaced at the considered mileage interval of forestry equipment.

Staff labour costs are determined by:

$$C_{rs}=C_{tar}\Sigma t, \quad (10)$$

where: C_{tar} – average staff rate, UAH.; Σt – total labour intensity of maintenance and repair of forestry equipment at the mileage interval, person-hour.

Determination of capital investments for technical control and repair of forestry equipment:

$$K=mN, \quad (11)$$

where: N – rate of capital investment per production worker, UAH; m – the number of workers required for technical control and repair of the controlled forestry equipment at the mileage interval.

Value m is calculated using the equation:

$$m=\frac{\sum t_i}{T_F}, \quad (12)$$

where: $\sum t_i$ – total labour intensity of technical control and repair in a given mileage interval, person-hour; T_F – time fund of repair workers for this period, h.

To get unit costs, the resulting value C_{ver} is divided by the mileage interval of forestry equipment [24].

After determining the values of functional indicators [25], reliability indicators, and unit costs for each controlled unit of forestry equipment, the information obtained can be provided in the form of a matrix:

$$\begin{vmatrix} x_1, P_{11}, P_{21}, \ldots, P_{m1}, & Z_{11}, Z_{21}, \ldots, Z_{k1} \\ \ldots \quad \ldots & \ldots \quad \ldots \\ x_n, P_{1n}, P_{2n}, \ldots, P_{mn}, & Z_{1n}, Z_{2n}, \ldots, Z_{kn} \end{vmatrix} \tag{13}$$

where: $x_1, x_2, \ldots, x_n$ – the value of periodicity in controlled forestry equipment, h; $P_{i1}, P_{i2}, \ldots, P_{in}$ – values of reliability indicators of controlled forestry equipment; $Z_{j1}, Z_{j2}, \ldots, Z_{jn}$ – the value of functional indicators of controlled forestry equipment.

The output data matrix (13) is used to find the regression coefficients of models included in the objective function (4). The task is to determine the regression coefficients of the equation:

$$y = b_o + b_1 x + b_2 x^2. \tag{14}$$

In this case, the task of b_i evaluation is to find a curved regression using the least squares method. Using Chebyshev system of orthogonal polynomials, equation (14) can be represented as follows:

$$y = c_0 + c_1 \varphi(x) + c_2 \varphi_2(x). \tag{15}$$

For this equation, the formulas for calculating Chebyshev polynomials will have the form:

$$\varphi_1(x) = x - \frac{1}{N}\sum_{j=1}^{N} x_j,$$

$$\varphi_2(x) = x^2 - \frac{\sum x^3 - \frac{1}{N}\sum x^2 \sum x}{\sum x^2 - \frac{1}{N}\left(\sum x^2\right)}\left(x - \frac{1}{N}\sum x\right) - \frac{\sum x^2}{N} \tag{16}$$

The values of the coefficients included in equation (15) are determined by:

$$C_o = \frac{1}{N}\sum_{j=1}^{S} m_j \overline{y_j}, \tag{17}$$

$$C_o = \frac{\sum_{j=1}^{S} \varphi_1(\overline{x_j}) m_j \overline{y_j}}{\sum_{j=1}^{S} \varphi_1^2(\overline{x_j}) m_j}, \tag{18}$$

$$C_1 = \frac{\sum_{j=1}^{S} \varphi_2(\overline{x_j}) m_j \overline{y_j}}{\sum_{j=1}^{S} \varphi_2^2(\overline{x_j}) m_j}, \tag{19}$$

where: S – the number of intervals for changing the frequency of performing operations of technical control of forestry equipment; $\overline{xj}, \overline{yj}$ – average value of values x and y in j interval; m_j - the number of machines for forestry operations, in which the frequency is in the j interval.

Checking the adequacy of the constructed equation is performed using the F-criterion:

$$F = \frac{S_f^2(y)}{S_{res}^2(y)} > F_\alpha(f_m, f_{res}) \tag{20}$$

where: $S^2_{res}(y)$ – residual variance, which characterises the scattering of experimental points relative to the regression line; $S^2_f(y)$ – total variance, which characterises the scattering of points near the general average.

The adequacy hypothesis is accepted.

Value $S^2_{res}(y)$ (y) is final and $S^2_f(y)$ is determined by the equations:

$$S_{res}^2(y) = \frac{1}{N-k-1}\sum_{j=1}^{N}(y_i - y_c)^2, \tag{21}$$

$$S_f^2(y = S_p^2(y) + S_{res}^2(y) = \frac{1}{f_p}\sum_{j=1}^{N}(y_j - \overline{y}) + S_{res}^2(y) \tag{22}$$

where: k – the number of parameters of machines for forestry operations when y; f_p – number of degrees of freedom, $f_p=k-1$.

Value f_f and f_{res} are calculated using the formula $f_f=N-1$, $f_{res}=N-k-1$. If the equations are adequate, the constructed objective function is used to calculate the optimal frequency of technical control of forestry equipment [26-28]. If the adequacy condition is not met, then additional terms are introduced into the polynomials, after which regres-sion coefficients are calculated again and the adequacy of the refined model is determined. This process is repeated sequentially until models that satisfy the adequacy condition are obtained.

When adjusting the list of technical control operations for mechanisms that ensure traffic safety, the condition for including the operation in the corresponding type of technical control is determined at the value of the repeatability coefficient that satisfies the following ratios:

a) for TC-1 – $1 \geqslant k_1 \geqslant 0.26$;

b) for TC-2 – $0.26 \geqslant k_2 \geqslant 0.12$.

The operation remains under current repair if $k<0.12$.

For other mechanisms, the condition for including troubleshooting operations of forestry equipment during a particular period of technical control is determined from the ratio:

a) for TC-1 – $1 \geqslant k_1 \geqslant 0.30$;

b) for TC-2 – $0.30 \geqslant k_2 \geqslant 0.13$.

The operation remains in the current process of technical control of forestry equipment if $k<0.13$.

The purpose of the study is to perform analytical and experimental investigation to confirm the existence of typological means of technical control of physiological and ergonomic indicators of forestry equipment by modelling the processes of their functioning.

RESULTS AND DISCUSSION

The study presents a methodology for assessing the reliability of drivers of forestry equipment vehicles of the forwarder type.

To assess the driver's level of reliability, it is suggested to use the reliability criterion:

$$K = K_S \cdot K_Q \cdot K_E \cdot K_{EC} \cdot K_{BM}, \tag{23}$$

where: K_S – criterion of safety for performing forestry operations by machine; K_Q – criterion of productivity of timber transportation by car; K_E – criterion of cost-effectiveness of performing forestry operations by machine; K_{EC} – criterion of extreme conditions for performing forestry operations by machine; K_{BM} – criterion of knowledge of the basic mechanics by the driver of forestry equipment.

It is proposed to determine the safety criterion for performing forestry operations by a machine:

$$K_S = \frac{K_{DB} + K_{un.m X} + K_{un.m Y}}{3}, \tag{24}$$

where: K_{DB} – criteria for evaluating driver behaviour,

$$K_{DB} = \frac{3}{\left(1+\frac{H_{er(o.b)}}{S}\right)\frac{H_{er(o.b)}}{T^2_{er(o.b)} \cdot j_{adm(o.b)}}+\left(1+\frac{H_{er(M)}}{S}\right)} \cdot$$
$$\cdot \frac{3}{\frac{H_{er(M)}}{T^2_{er(M)} \cdot j_{adm(M)}}+\left(1+\frac{H_{er}}{S}\right)\frac{H_{er}}{T_{er} \cdot v_{razr}}},$$

where: $H_{er(o.b)}$ – number of errors during acceleration and braking; $H_{er(M)}$ – number of errors when performing transverse manoeuvres; $T_{er(o.b)}$ – time of movement of the forwarder with longitudinal acceleration, s; $j_{adm(o.b)}$ – permissible value of longitudinal accelerations, m/s^2; $K_{un.mX}$, $K_{un.mY}$ – criteria for the degree of uniformity of movement along the longitudinal and transverse axes of forestry equipment.

Transportation productivity criterion:

$$K_Q = \frac{v_{av}}{v_{av_b}} \tag{25}$$

where: v_{av} – average movement speed by the test driver, km/h; v_{av_b} – the basic speed of forestry equipment, km/h.

Cost-effectiveness criterion:

$$K_E = \frac{\frac{L_{Qb}}{L_Q}+1-\frac{\left|N_{En}-N_{En_b}\right|}{N_{En_b}}+\frac{Q_F}{Q}}{3}, \tag{26}$$

where: E_{n_b} – standard value of the number of rotations of the engine crankshaft; Q_F – standard value of fuel consumption, cm^3; Q – actual fuel consumption when traveling along the route, cm^3.

Indicators that characterise the assessment of driver behaviour in extreme conditions K_{EC} and the driver's knowledge of basic mechanics K_{BM}, were determined using the simulator programme.

On-board recording equipment (Figure 1) was equipped with: fuel consumption sensor, motion sensor, transverse acceleration sensor, crankshaft speed sensor, driving speed sensor, longitudinal acceleration and deceleration sensor.

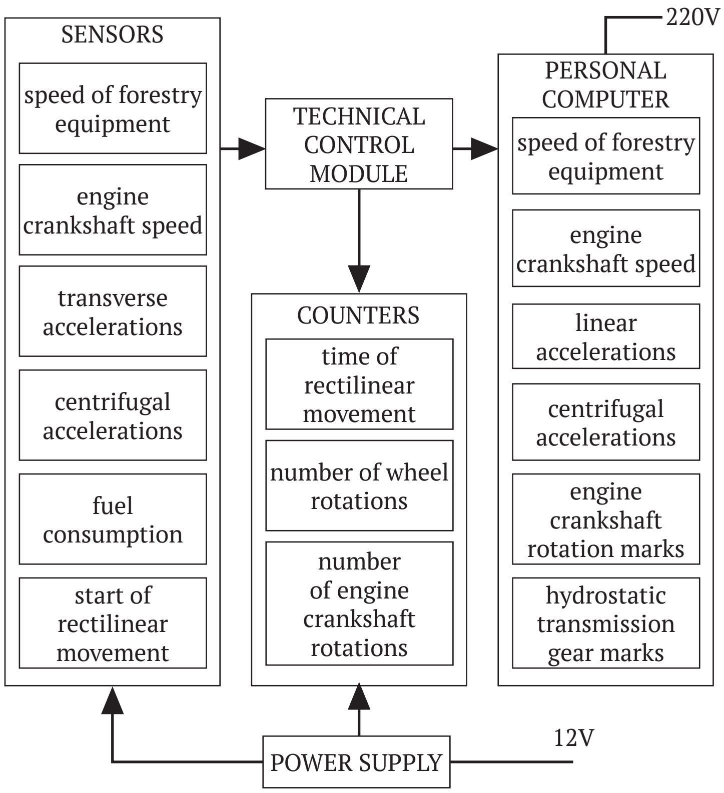

Figure 1. Correlation between gas (a) and electricity (b) consumption and external temperature

Test algorithm:

1. Checking the serviceability and technical condition of indicators and control and measuring devices of forestry equipment.

2. Determination of the test route with a length of one hour drive at a speed of 40...80 km/h.

3. Synchronisation of data acquisition, calibration of channels of measuring and recording equipment.

4. Determination of standard speed values v_{av_b}, fuel consumption on the route Q_b, the weighted average value of the gearbox gear ratio i'_{tr}.

5. Performing 39 runs by 20 test drivers along a given route on forestry equipment machines, equipped with a complex of the module of technical control of forestry equipment with measurement of the duration of movement of forestry equipment D_M, the number of rotations of the crankshaft N_{En_b}.

6. Processing of results and conclusion about the level of reliability of the driver of a timber road train.

Based on the criteria K_Q, K_E, K_S, K_{EC}, and K_{BM} an integral driver reliability criterion is defined K. Moreover, if the driver's reliability is high, then K_Q, K_E, K_S, K_{EC}, K_{BM}, $K_{ECc} \geqslant 1.0$. If the driver's skill is not sufficient, the values of the indicators K_Q, K_E, K_S, K_{EC}, K_{BM}, and $K_{EC} < 1.0$. The developed technique improves the handling of forestry equipment. The position of the model of the oscillating system of a forestry machine with two controlled axles and independent wheel suspension is determined by generalised coordinates: the angle of rotation of the wheels of the first axle around the pivot axis – Q_1, deg.; the angle of rotation of the wheels of the second axle around the pin axis – Q_2, deg.; the angle of rotation of the wheels (body) in the transverse vertical plane Ψ, deg.

Equation of motion by coordinates q_k=Q_1, Q_2, Ψ is compiled in the form of the second order Lagrange equations:

$$L(q_k, \dot{q}_k, t)\frac{d}{dt}\cdot\frac{\partial E_k}{\partial \dot{q}_k}-\frac{\partial E_k}{\partial q_k}+\frac{\partial E_p}{\partial q_k}, \quad (28)$$

where: E_k – kinetic energy of the system, J; E_p – potential energy of the system, J; R_k – generalised reactions of elastic wheel connections with the road.

After the transformations, the equation of motion of the two-bridge model is obtained. When solving the system of equations (27) on a PC, the physical parameters were represented by their electrical counterpart –voltage. Physical differential equations were transformed into machine equations. Where: Q_t – real-time variable; Q_τ – variable in machine time τ and M_t=5:

$$\theta_t = \theta_\tau;\ \frac{d\theta_t}{dt} = 5\frac{d\theta}{d\tau};\ \frac{d^2\theta_t}{dt^2} = 25\frac{d^2\theta_t}{d^2\tau}. \quad (29)$$

Value of scale coefficients: M_Θ=1,000 r/rad; M_φ=1,000 r/rad; M_Ψ=1,000 r/rad; M_λ=2,000 r/rad. Physical variables expressed in terms of machine and time scales:

$$X_t = \frac{1}{M_X}X_\tau;\ \frac{dX_t}{dt} = \frac{M_t}{M_X}\cdot\frac{dX_\tau}{d\tau};\ \frac{d^2X_t}{dt^2} = \frac{M_t^2}{M_x}\cdot\frac{d^2X_\tau}{d\tau^2}, \quad (30)$$

where: t – index of physical quantities; τ – index of machine variables.

Then a system of machine equations is obtained describing the motion of a two-bridge model with three basic degrees of freedom (Q_1, Q_2, Ψ). For testing, a machine for forestry operations was allocated, which has a factory setting of the parameters of steerable wheels. The technical condition of forestry equipment met the requirements of the factory instructions. Recording and measurement of oscillation parameters was carried out using a measuring complex, which was developed considering the specifics of the experiment and the conditions of its conduct.

Operational tests of the timber road train were carried out to determine reliability, operability, compliance with safety and ergonomics requirements in the general technological cycle in two shifts in LLC "European timber processing group" of Zhytomyr Oblast. Export of forest products was carried out on three types of haul roads: forest tracks, roadways, highways in the amount of 20 thous. km of mileage. The actual load ranged from ±10% of the rated load. Timekeeping observations were carried out during 15 control runs in each season (winter and off-road).

Studies to determine the effect of wheel convergence on self-oscillation have shown little effect. In general, there is a tendency to slightly decrease the intensity of self-oscillations with a change in convergence towards negative values. At small values of the angle γ, the effect of convergence is greater than at large positive values.

Self-oscillations for forestry equipment exist when γ<-1.9°, that is, the stability of movement of the steered wheels is ensured when setting the angle γ within the range of -1,5° to -9°. At angles γ less than -9° aperiodic instability occurs. Stability of the steered wheels is also possible at other values of angle γ – with large positive results. The movement will be stable even when γ>13°. The greatest intensity of fluctuations is observed at γ=3°...5° and v=45 km/h.

If there are no gaps in the power steering mounting hinges (δ=0) the movement of the steered wheels is stable when setting the angle of the longitudinal pin γ<-1.5°. Considering the operational gaps, the pins must be installed with a slope of γ=2°...3°. If there are gaps in the system of the order δ⩾6 mm, the movement of the steered wheels becomes unstable at any negative angle values γ. The intensity of vibrations is the lowest at γ=-4°, that is, the lowest required damping energy of reservations at γ=-4°.

When considering the working conditions of drivers, the study used a noise-vibration measuring equipment, a luxmeter, and a thermometer. The external noise spectra are shown in Figure 2.

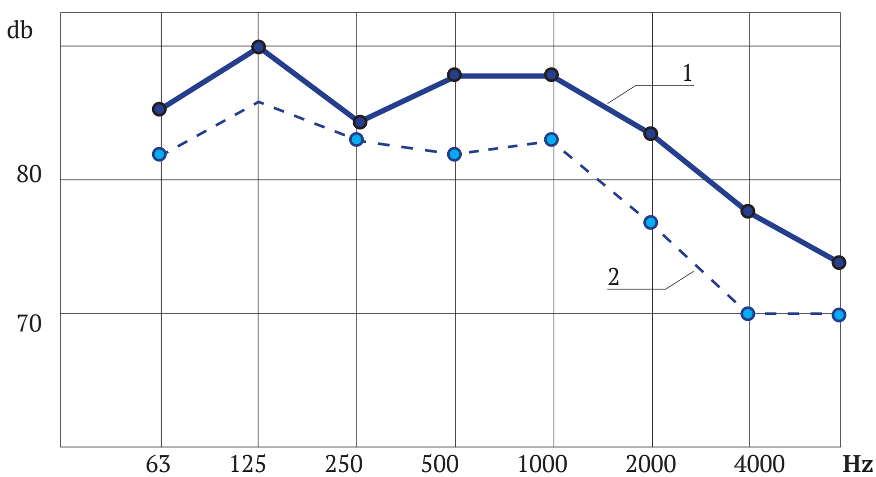

Figure 2. External noise spectra of the forwarder: 1 – on the left; 2 – on the right

The noise spectrum in the cabin is shown in Figure 3. The forwarder does not meet the ISO requirements for external noise, and it meets the ISO requirements for noise at the driver's workplace.

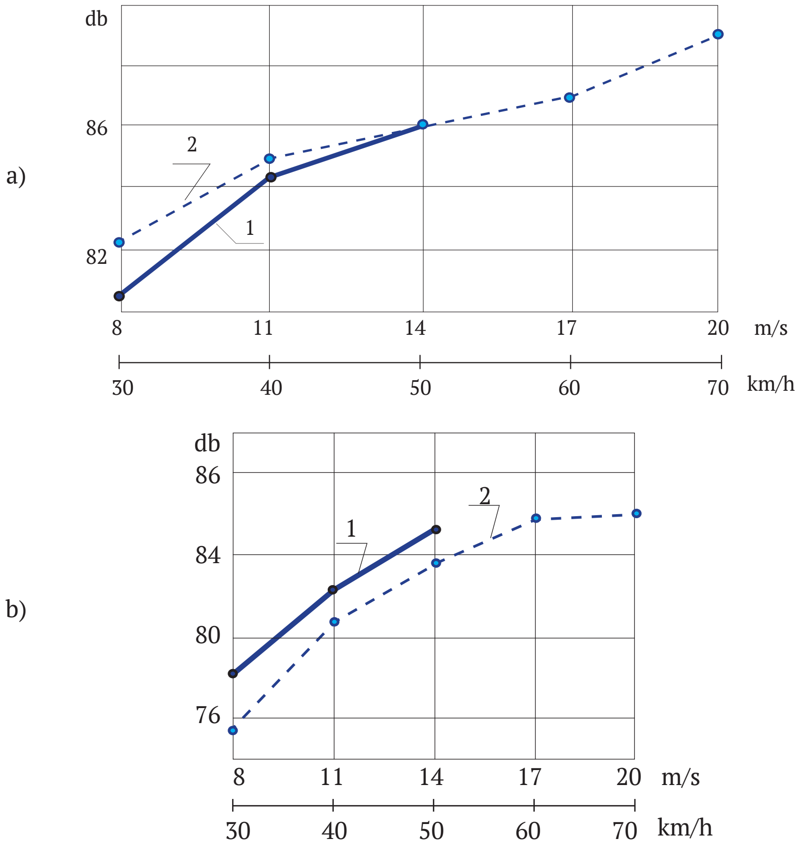

Figure 3. Integral noise levels at the forwarder driver's workplace: a) in the loaded state; b) in the empty state. 1, 2 – speed in 7-th gear

The average operating fuel consumption per shift was carried out by refilling the fuel tank during daily refuelling. The regular load of each road train was checked by control weighing using a dynamometer. Identification of the reliability and operability of the road train during operational tests was carried out by registering failures. At the same time, the average time to failure separately for the tractor and semi-trailer and the complexity of eliminating failures were determined. Tests were carried out to determine the speed characteristics (Fig. 4).

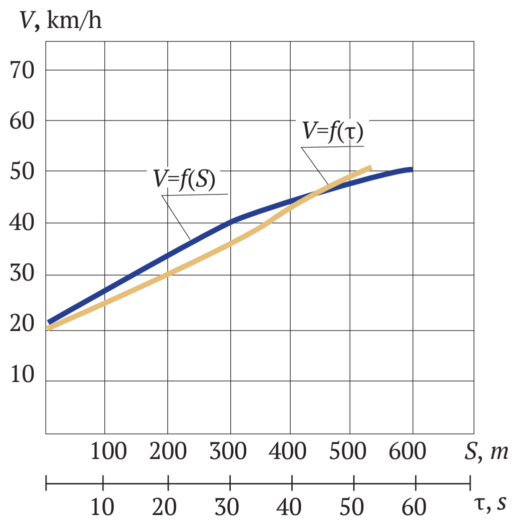

Figure 4. Speed characteristic of acceleration in direct transmission

To improve the ergonomics of timber road trains, a different layout of display elements on the instrument panel is offered. The best layout option was determined based on consideration of the load of the driver's visual analyser. There are 4 options for placing indicators, from which the best option was selected. When modelling the information display elements of the instrument panel of a timber road train, indicators of various car brands were used.

When processing the findings, an assessment scale of psychophysiological indicators of drivers was used. The conducted research offers the optimal placement of elements on the vehicle instrument panel from the standpoint of information perception and reading time: place the speed sensor in the centre of the driver's field of view; place the water temperature and oil pressure indicator to the left of the speedometer; place the fuel level sensor and ammeter vertically to the right of the speedometer; place the tachometer to the left of the temperature indicator; place the indicator system at the top of the field.

A set of measures has been developed to improve the organisation and technology of maintenance of machinery for forestry operations, which reduces downtime in routine repairs and improves the quality of maintenance. Savings from the implementation of the proposed measures amount to 523,572 UAH/year in December 2021 prices.

CONCLUSIONS

1. A methodology for assessing the reliability of drivers and operators has been developed, which allows determining measures to improve traffic safety on forest roads. The effectiveness of implementing measures is determined by reducing traffic violations, reducing physical and psychological injuries from road accidents, reducing the degree of danger to the driver's profession, and improving the reliability of timber removal. Reduction of accidents occurs by increasing the professional skills of drivers and reducing fuel consumption.

2. The developed analytical dependencies allow calculating an integral criterion that characterises the reliability of the driver of forestry equipment based on the data of recording equipment.

3. The developed method of improving the handling of forestry equipment allows determining the permissible value of wheel imbalance for any model of forestry equipment. Self-oscillations for forestry equipment exist when γ<-1,9°, that is, the stability of movement of the steered wheels is ensured when setting the angle γ within the range of -1,5° to -9°. At angles γ less than -9° aperiodic instability occurs. The movement will be stable even when γ>13°. The greatest intensity of fluctuations is observed at γ=3°...5° and v = 45 km/h.

4. Different placement of control and measuring sensors on the instrument panel of a forestry machine affects the speed and accuracy of information perception. The compact pairwise-symmetrical vertical arrangement of control and measuring sensors on the instrument panel reduces the time of reading information and the number of errors.

REFERENCES

[1] Beier, G., Ullrich, A., Niehoff, S., Reibig, M., & Habich, M. (2020). Industry 4.0: How it is defined from a sociotechnical perspective and how much sustainability it includes – A literature review. *Journal of Cleaner Production*, 259, article number 120856.

[2] Ackerman, S.A., Talbot, B., & Astrup, R (2022). The effect of tree and harvester size on productivity and harvester investment decisions. *International Journal of Forest Engineering*, 33(1), 22-32.

[3] Hartsch, F., Kemmerer, J., Labelle, E.R., Jaeger, R., & Wagner, T. (2021). Integration of harvester production data in German wood supply chains: Legal, social and economic requirements. *Forests*, 12(4), article number 460.

[4] Klein, D., Wolf, C., Schulz, C., & Weber-Blaschke, G. (2015). 20 years of life cycle assessment (LCA) in the forestry sector: State of the art and a methodical proposal for the LCA of forest production. *The International Journal of Life Cycle Assessment*, 20, 556-575.

[5] Brewer, J., Talbot, B., Belbo, H., Ackerman, P., & Ackerman, S. (2018). A comparison of two methods of data collection for modelling productivity of harvesters: Manual time study and follow-up study using on-board-computer stem records. *Annals of Forest Research*, 61(1), 109-124.

[6] Eker, M., & Kurt, Y. (2019). Development of a time measurement and recording tool for forestry works. *Turkisj Journal of Forestry*, 20(3), 157-167.

[7] Cantú, R.P., LeBel, L., & Gautam, S. (2017). A context specific machine replacement model: A case study of forest harvesting equipment. *International Journal of Forest Engineering*, 28(3), 124-133.

[8] Kemmerer, J., & Labelle, E.R. (2020). Using harvester data from on-board computers: A review of key findings, opportunities and challenges. *European Journal of Forest Research*, 140, 1-17.

[9] Harrill, H., & Visser, R. (2019). A survey of NZ ground-based harvesting systems. *Forest Growers Research Harvesting*, 12(4), 1-7.

[10] Kiktev, N., Osypenko, V., Shkurpela, N., & Balaniuk, A. (2020). Input data clustering for the efficient operation of renewable energy sources in a distributed information system. *2020 IEEE 15th international conference on computer sciences and information technologies* (pp. 9-12). Zbarazh: Lviv Polytechnic National University.

[11] Rogovskii, I.L., Titova, L.L., Gumenyuk, Yu.O., & Nadtochiy, O.V. (2021). Technological effectiveness of formation of planting furrow by working body of passive type of orchard planting machine. *Earth and Environmental Science*, 839, article number 052055.

[12] Berg, S., Yoshida, M., Sakurai, R., & Sakai, H. (2017). Comparison of productivity and cost depending on slope when forwarding short length logs with small Japanese forwarders. *International Journal of Forest Engineering*, 28(3), 176-185.

[13] Nurminen, T., Korpunen, H., & Uusitalo, J. (2006). Time consumption analysis of the mechanized cut-to-length harvesting system. *Silva Fennica*, 40(2), 335-363.

[14] Marchi, E., Chung, W., Visser, R., Abbas, D., Nordfjell, T., Mederski, P.S., McEwan, A., Brink, M., & Laschi, A. (2018). Sustainable forest operation: A new paradigm in a changing world and climate. *Science of the Total Environment*, 634, 1385-1397.

[15] Proto, A.R., Bacenetti, J., Macrì, G., & Zimbalatti, G. (2017). Roundwood and bioenergy production from forestry: Environmental impact assessment considering different logging systems. *Journal of Cleaner Production*, 165, 1485-1498.

[16] Nazarenko, I., Mishchuk, Y., Mishchuk, D., Ruchynskyi, M., Rogovskii, I., Mikhailova, L., Titova, L., Berezovyi, M., & Shatrov, R. (2021). Determiantion of energy characteristics of material destruction in the crushing chamber of the vibration crusher. *Eastern-European Journal of Enterprise Technologies*, 4(7(112), 41-49.

[17] Rogovskii, I.L., Titova, L.L., Voinash, S.A., Sokolova, V.A., Pushkov, Yu.L., Krivonogova, A.S., & Kokieva, G.E. (2020). Modeling the distribution of internal stresses in surface strengthened layer of steel parts after cementation and hardening. *Journal of Physics: Conference Series*, 1679, article number 042069.

[18] Schweier, J., Magagnotti, N., Labelle, E.R., & Athanassiadis, D. (2019). Sustainability impact assessment of forest operations: A review. *Current Forestry Reports*, 5(3), 101-113.

[19] Rogovskii, I.L., Titova, L.L., Voinash, S.A., Maksimovich, K.Yu., Galimov, R.R., Sokolova, V.A., Parfenopulo, G.K., & Taraban, M.S. (2020). Constructive method of increasing the durability of cultivator blades recovered by surface. *Journal of Physics: Conference Series*, 1679, article number 042076.

[20] Apăfăian, A.I., Proto, A.R., & Borz, S.A. (2017). Performance of a mid-sized harvester-forwarder system in integrated harvesting of sawmill, pulpwood and firewood. *Annals of Forest Research*, 60(2), 227-241.

[21] Zhang, X., Zhang, W., & Xu, D. (2020). Life cycle assessment of complex forestry enterprise: A case study of a forest-fiberboard integrated enterprise. *Sustainability*, 12(4147), 1-18.

[22] Crittenden, A.B., Crittenden, V.L., & Crittenden, W.F. (2019). The digitalization triumvirate: How incumbents survive. *Business Horizons*, 62(2), 259-266.

[23] Brown, M., Ghaffariyan, M.R., Berry, M., Acuna, M., Strandgard, M., & Mitchell, R. (2020). The progression of forest operations technology and innovation. *Australian Forestry*, 83, 1-3.

[24] Spinelli, R., Hartsough, B.R., & Magagnotti, N. (2010). Productivity standards for harvesters and processors in Italy. *Forest Production Journal*, 60(3), 226-235.

[25] Hildt, E., Leszczuk, A., Donagh, P., & Schlichter, P. (2019). Time consumption analysis of forwarder activities in thinning. *Croatian Journal of Forest Engineering*, 41(1), 13-24.

[26] Proto, A.R., Macrì, G., Visser, R., Harrill, H., Russo, D., & Zimbalatti, G. (2018). Factors affecting forwarder productivity. *European Journal of Forest Research*, 137(2), 143-151.

[27] Ostanin, V. (2022). Effects of repulsion and attraction between rotating cylinders in fluids. *Scientific Herald of Uzhhorod University. Series "Physics"*, 51, 39-47.

[28] Shynkariuk, Y. (2022). Alternative representation of space and time: Geometric solution of problems of relativity theory. *Scientific Herald of Uzhhorod University. Series "Physics"*, 51, 74-82.

Людмила Леонідівна Тітова[1], Генріх Собчук[2]

[1]Національний університет біоресурсів і природокористування України
03041, вул. Героїв Оборони, 15, м. Київ, Україна

[2]Польська академія наук
00-901, пл. Defilad, 1, м. Варшава, Республіка Польща

Типологічність засобів технічного контролю фізіологічних і ергономічних показників машин для лісотехнічних робіт

Анотація. На сьогоднішній день під час лісосічних, лісотранспортних роботах, в більшості, експлуатується техніка, яку здали на серійне виробництво на початку тисячоліття. Через відсутність власних коштів у підприємств лісового комплексу в останні роки не проводиться оновлення машин для лісотехнічних робіт і устаткування, в яких за термін їх служби зношуються не тільки вихідні зразки, а й цілий комплекс повторно вводиться у ті ж машини змінюваних деталей і інших нетривких елементів. У структурі діючого парку техніки 80 % займає повністю амортизована техніка, яка повинна бути модернізована або списана, а коефіцієнт вибуття в 10 разів перевищує коефіцієнт оновлення. Існуюча ремонтна політика сформувалася в доринкових умовах при відповідних співвідношеннях цін на сировинні ресурси і машини. У той період і була створена діюча до сьогоднішнього дня концепція технічного контролю машин для лісотехнічних робіт: допуски, регламенти, нормативи і т. д. У нинішніх економічних умовах потрібні нові підходи до формування методології технічного контролю і ремонту машин для лісотехнічних робіт. Технічний супровід експлуатації машин для лісотехнічних робіт можна розглядати як інструмент управління запасом їх потенційних можливостей, закладених при виготовленні і поновлених (відновлюваних) при технічному контролі та ремонті. Визначення моменту для проведення робіт по відновленню технічного стану машини залежить від різних чинників, часто суперечать один одному. Мета – виконати аналітичні та експериментальні дослідження з підтвердження існування типологічності засобів технічного контролю фізіологічних і ергономічних показників машин для лісотехнічних робіт шляхом моделювання процесів їх функціонування. Методологія – апробувати засоби системного підходу та системного аналізу типологічності засобів технічного контролю фізіологічних і ергономічних показників машин для лісотехнічних робіт. В статті представлено згенерований результат у вигляді реєструючого алгоритму модуля технічного контроля машин для лісотехнічних робіт. Авторами за результатами експериментальних досліджень представлена графічна інтерпретація інтегральних рівнів шуму на робочому місці водія форвардера в навантаженому стані, в порожньому стані. Висновок – проведені дослідження дають можливість запропонувати оптимальне, з точки зору сприйняття інформації і часу зчитування, розміщення елементів на панелі приладів транспортного засобу. Наукова значимість – підтверджено, що при аналізі впливу періодичності виконання операцій технічного контролю машини для лісотехнічних робіт на перераховані показники доцільно використовувати парний кореляційний аналіз, який полягає у визначенні зв'язку між періодичністю виконання операцій технічного контролю і величиною сумарних питомих витрат, показниками надійності і показниками функціональних властивостей

Ключові слова: ергономіка лісовозних автопоїздів, типологічність засобів технічного контролю, показник надійності, машина для лісотехнічних робіт, технічний контроль та ремонт

Machinery & Energetics
Vol. 13, No. 1. 2022

Journal homepage:
https://technicalscience.com.ua/en

UDC 665.73:54-41
DOI: 10.31548/machenergy.13(1).2022.49-53

Oleksii Kalivoshko[1*], Waclav Romaniuk[2], Mykola Kalivoshko[1]

[1]National University of Life and Environmental Sciences of Ukraine
03041, 15 Heroiv Oborony, Kyiv, Ukraine

[2]Institute of Technological and Natural Sciences of the National Research Institute
05-090, 3 Grabska Alley, Falenty, Republic of Poland

Feasibility study of the efficiency of carbon sorbents based on pine sawdust for removing oil products

Abstract. Oil pollution of the environment in many ways stands out among others. It is known, for example, that a litre of oil deprives oxygen of 40 thousand litres of water, and a tonne of oil pollutes 12 km^2 of the water surface. The content of petroleum products in water above 0.1 mg/l gives fish meat an overwhelming taste and a specific smell of oil during any technological treatments. A wide variety of sorption materials for oil spill response are available on the domestic and global markets. Sorbents are created based on various organic and inorganic materials. Many of them are quite efficient and have a high sorption capacity, but the energy and material costs of their production determine the high cost of the product, which often does not meet consumer requirements. At the same time, promising and cost-effective sorbents can be produced from local secondary raw materials. In recent years, the development of oil sorbents for collecting hydrocarbon leaks based on forest and agricultural industry waste has been actively underway, the use of this type of raw material is conditioned by the rather high absorption capacity of the obtained sorbents, their low cost, availability as a local material, and the possibility of further use. The purpose of the study is to summarise experimental data on the effectiveness of carbon sorbents based on pine sawdust for cleaning petroleum products. The paper presents tabulated data on the structural and sorption characteristics of various fractions of pine sawdust at a humidity of 50-60%. The authors proved experimentally the existence of a dependence of the oil capacity of carbon sorbents from different pine fractions on the duration of carbonation at different temperatures. The paper presents results on the absorption and sorption characteristics of carbon sorbents from different fractions of pine sawdust. Conclusion – at each temperature when carbonation processes were studied, an optimal duration value was obtained at which the oil capacity of the sorbent from different fractions of pine sawdust was the highest, and the yield of the sorbent was maximum. Scientific significance – the authors proved that the carbonation temperature of more than 350°C for pine sawdust of various fractions is not recommended, and for fractions smaller than 1 mm above 300°C, which have a small size and significant burnout and degradation due to the possibility of fire, as a result of which the quantity and quality of carbon sorbent decreases

Keywords: indicators of carbon sorbents, environment, economic indicators, carbonation, petroleum products, sorption capacity, pine fractions

Article's History: Received 06.10.2021; Revised: 27.01.2022; Accepted: 23.02.2022

INTRODUCTION

Petroleum products are a fairly common source of environmental pollution [1]. As indicated in [2], almost 2% of the total amount of fuel and lubricants produced is released into the environment. Both the petroleum products themselves and the impurities they contain are dangerous [3]. In addition, when ingested in soil and water, petroleum products, as a result of physicochemical reactions and biological interactions, turn into toxic substances that cause harmful effects on biota [4]. Water and soil purification from fuel and lubricants by sorption is organisationally, technologically, economically, and environmentally relevant today [5]. Carbon sorbents based on raw materials of the woodworking industry are particularly important and widespread [6]. The study of the essence of carbonation

Suggested Citation:
Kalivoshko, O., Romaniuk, W., & Kalivoshko, M. (2022). Feasibility study of the efficiency of carbon sorbents based on pine sawdust for removing oil products. *Machinery & Energetics,* 13(1), 49-53.

*Corresponding author

processes, physicochemical, absorbing, and structural sorption properties of carbon sorbents, when the raw material is a by-product of the woodworking industry, namely, pine sawdust, the processes of sorption of petroleum products by them, their environmental and economic substantiation and analysis, requires further study and evaluation.

Petroleum products entering the water and soil environment cause significant environmental changes in them [7]. There is a significant and dangerous pollution of the environment with petroleum products and their decomposition products [8]. Sorbents are effective and widespread means for cleaning soil and aquatic ecosystems [9]. Sorbents are known for their absorption properties in cleaning from various kinds of contaminants [10]. In recent decades, sorbents have become increasingly used in all sectors of the national economy, including for soil and water purification from petroleum products [11]. Carbon sorbents obtained on the basis of by-products of agricultural production [12] and the woodworking industry differ significantly in their properties and characteristics [13]. The technology and processes [14] that occur in the production of carbon sorbents have a significant influence on the sorption parameters of sorbents [15]. Carbon sorbents obtained on the basis of sawdust have better sorption and absorption properties, compared to sorbents obtained from tree leaves and straw [16]. The structure [17], properties [18], ways of obtaining [19], and the use of carbon sorbents based on plant raw materials are investigated [20]. However, the nature, properties, sorption characteristics, physicochemical properties and processes of transformation of by-products of the woodworking industry, namely, sawdust, into carbon sorbents, their complex use for cleaning water and soil ecosystems, environmental and economic assessment, are not thoroughly investigated.

The purpose of the study was to investigate: physicochemical, structural, sorption, and absorption properties of pine sawdust and carbon sorbents obtained from it; technological processes, technologies, and transformations in the production of carbon sorbents from pine sawdust; the degree and completeness of purification, environmental and economic feasibility, and advantages of using carbon sorbents obtained from pine sawdust in the purification of the aquatic environment and soils from petroleum products.

RESULTS AND DISCUSSION

Pine sawdust accumulated in the woodworking industry has the best physical, chemical, structural, sorption, and absorption characteristics and properties among other sorbents of plant origin. According to the results of our research, sorbents have good efficiency when their absorption capacity of petroleum products is 2-3 g mg-eq/g or more. They can be directly used to clean the soil and water environment in case of contamination with petroleum products. Pine sawdust, at natural humidity, has an absorption capacity of petroleum products in the range of 2.6-2.8 mg-eq/g, which fully meets these requirements, and therefore, it can be used for sorption in case of contamination. The studies (Table 1) show that the physicochemical, structural, absorption, and sorption properties of various fractions of pine sawdust at a humidity of 60% do not significantly differ from each other. The exception is non-sifted sawdust, the absorption capacity of which is slightly lower compared to other fractions, which is conditioned by the presence of small impurities of wood and bark in it, which have low sorption indicators.

When using pine sawdust at a humidity of 60% for cleaning the water or soil environment from petroleum products, it is not advisable to divide it into fractions. It is enough just to install 5-7 mm sieves directly on sawmills, which will separate the smallest particles of wood and bark from sawdust.

However, such sawdust during long-term storage (even when all requirements are met), due to intensive microbiological processes in a humid environment, can quickly deteriorate, and therefore, requires careful and correct storage conditions.

Table 1. Structural and sorption characteristics of various fractions of pine sawdust at humidity 50-60%

Fraction size	a. g/g	SEC. mg-eq/g	Vs (C_6H_6). g/cm³	Vs (H_2O). g/cm³	S_{pet}.. m²/g
< 1 mm	2.5	2.4	0.07	1.0	8.4
1-3 mm	2.8	2.7	0.07	1.0	8.4
> 3 mm	2.6	2.5	0.07	1.0	8.4
0-5 mm	2.7	2.6	0.07	1.0	8.4
not sifted	2.3	2.2	0.06	0.09	8.0

The structural, physicochemical, absorption and sorption properties of pine sawdust can be improved by the carbonation process.

Carbonation is a method of obtaining carbon sorbents from plant raw materials during heat treatment, which begins when the raw material is heated above 110-120°C. It was established that the carbonation of pine sawdust begins at a temperature of 120-130°C.

Since the hydrocarbon part of pine sawdust consists of cellulose and hemicellulose, and the complex of aromatic compounds – lignin, then during carbonation there are complex processes of destruction of their polymer chains with the release of both resinous substances of complex structure and a large number of volatile compounds. The carbonation process was studied every 50°C, in the range from 100 to 400°C.

It was established that the process of carbonation of pine sawdust begins at a temperature of 120-130°C. Within the temperature range of 200-300°C, the main decomposition reactions of hemicellulose, cellulose, and lignin take place, resulting in the release of simple carbon compounds (carbon dioxide and carbon monoxide), a liquefied mixture, and resins. At different stages of the carbonation process, the intensity and energy of activation of destructive transformations varies significantly, because at different temperature ranges, various components of pine sawdust, hemicellulose, then cellulose and lignin decompose. Therefore, the results obtained indicate the complexity of the process of pine sawdust carbonation.

The study of the process of carbonation of pine sawdust fractions allowed establishing that at each studied temperature of the carbonation process, for each fraction, there is a certain optimal value of its duration, at which the oil capacity of carbonate is the maximum, which is graphically shown in Figure 1.

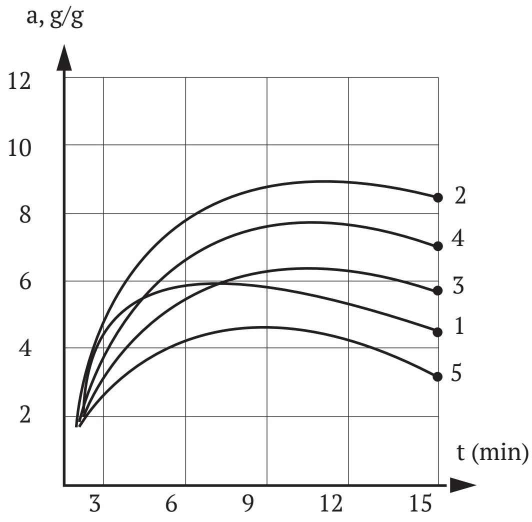

Figure 1. Diagram of links of mobile robot components

The appearance of maxima in Figure 1 is conditioned by changes in the porous structure of sorbents and chemical transformations of the surface of pine sawdust during carbonation. Thus, at the initial stage of the process of carbonation of pine sawdust and its fractions, due to the extraction of moisture, the release of gases, volatile simple substances and resinous compounds, pores are formed, which leads to an improvement in physicochemical and structural parameters, an increase in its sorption capacity of petroleum products to a certain maximum value. This improves the porousity of the carbon material.

According to the studies, the obtained carbon sorbents, due to carbonation of various fractions of pine sawdust, have several times higher oil capacity to petroleum products, better sorption, physicochemical and structural indicators, compared to the initial product (Table 2). Carbon sorbents from sawdust of 1-3 mm fractions have the highest sorption capacity for petroleum products and reach almost 12 g/g. Slightly lower sorption values (almost 10 g/g) for sorbents from sawdust of 0-5 mm fractions. Carbon sorbents made from sawdust fractions larger than 3 mm have a sorption capacity of 8 g/g, while fractions up to 1 mm have a sorption capacity of about 7 g/g. Carbon sorbents made from non-sifted sawdust had the lowest oil capacity, which is conditioned by the presence of small particles of wood and bark in it, which have low sorption properties. After analysing the study results, which characterise carbon sorbents obtained from different fractions of pine sawdust, it can be concluded that sorbents from sawdust fractions of 1-3 mm have the best sorption properties.

However, the oil capacity of the feedstock of sawdust of different fractions did not differ much from each other. The maximum value of the oil capacity of carbon material from pine sawdust of the 1-3 mm fraction is conditioned by the presence of the maximum number of pragmatic centres, since other structural and sorption characteristics for all sorbent fractions are approximately the same.

Special attention should be paid to the analysis of carbon sorbents obtained from different fractions of pine, in matters of their practical use, for cleaning water and soil media from petroleum products (they can be used for cleaning other pollutants). After analysing the sorption, environmental, and economic feasibility and efficiency of carbon sorbents obtained from different fractions of pine, it was concluded that in practical use for cleaning the environment, it is necessary to use carbon sorbents obtained from (without dividing into fractions) sawdust (0-5 mm), from which only wood and bark impurities were separated. That is, sawdust in which all fractions are present (ordinary sawdust). To do this, sawdust on sawmills should be sifted on a sieve of more than 5 mm (up to 10 mm), from which small remnants of wood and bark are removed).

Table 2. Absorption and sorption characteristics of carbon sorbents from various fractions of pine sawdust

Fraction size. mm	a. g/g	SEC. mg-eq/g	Vs(C_6H_6). g/cm^3	Vs(H_2O). g/cm^3	S_{pet}.. m^2/g	Number of PMCs. spin/g
< 1	6-7	3.4	0.11	0.07	14	$10.3 \cdot 10^{18}$
1–3	10-12	3.6	0.12	0.09	13	$13.9 \cdot 10^{18}$
> 3	7-8	3.5	0.11	0.08	12	$12.8 \cdot 10^{18}$
0–5	9.5-10.5	3.5	0.11	0.08	12	$13.1 \cdot 10^{18}$
not sifted	5-6	3.2.	0.10	0.06	11	$9.2 \cdot 10^{18}$

Carbon sorbents obtained from sawdust (without division into fractions), to a certain extent, are inferior in sorption indicators to carbon material obtained from a sawdust of 1-3 mm fraction. However, these advantages do not compensate for the cost of dividing sawdust into fractions, given that the very separation of raw sawdust into fractions is very difficult due to the clogging of the sieve, which requires additional equipment and technology.

Indicators of sorption capacity of sifted pine sawdust and carbon sorbents presented in Tables 1 and 2 indicate that during heat treatment it increases by almost 1.5, and oil capacity by almost 4 times.

At each temperature of carbonation process, an optimal duration value was obtained at which the oil capacity of the sorbent from different fractions of pine sawdust was the highest, and the yield of the sorbent was maximum. The carbonation temperature of more than 350°C for pine sawdust of various fractions is not recommended, and for fractions smaller than 1 mm above 300°C, which have a small size and significant burnout and degradation due to the possibility of fire, as a result of which the quantity and quality of carbon sorbent decreases (Table 3).

Table 3. Weight loss by various fractions of pine sawdust during carbonation

No.	Tk. °C	τ. min.	Weight loss. %
1	250	9.5	55
2	300	9.5	60
3	350	7.0	70
4	400	4.5	75
5	450	4.0	80

The optimal carbonation temperature for all pine sawdust fractions is 300°C with a process duration of 9-9.5 minutes, and for fractions – up to 1 mm 250°C with a duration of 10-10.5 minutes.

CONCLUSIONS

1. Carbonation of pine sawdust should be carried out at a temperature of 200-300°C, for 8-10 minutes, which increases the structural, sorption, and absorption characteristics of carbon sorbents.

2. Carbon sorbents obtained in the process of carbonation of pine sawdust (without admixtures of wood and bark) have a sorption capacity of almost 1.5 times, and oil capacity is almost 4 times higher compared to the corresponding indicators of the initial product.

3. Carbon sorbents obtained from the 1-3 mm pine sawdust fraction have the best physicochemical, structural, sorption, and absorption characteristics.

4. For cleaning water and soil from petroleum products, it is economically and practically advisable to use carbon sorbents obtained directly from pine sawdust without dividing it into fractions (ordinary sawdust from 0-5 mm from which wood and bark impurities are removed). Such sorbents are somewhat inferior in sorption characteristics to sorbents obtained from pine sawdust of 1-3 mm fractions, but they are much cheaper.

REFERENCES

[1] Wychodnik, K., Gałęzowska, G., Rogowska, J., & Wolska, L. (2020). Poultry farms as a potential source of environmental pollution by pharmaceuticals. *Molecules*, 25(5), article number 1031.

[2] Liu, J., Chen, S., Wang, H., & Yan, J. (2016). Evolution of China's urban energy consumption structure – a case study in Beijing. *Energy Procedia*, 88, 88-93.

[3] Sethi, M. (2015). Location of greenhouse gases emissions from thermal power plants in India along the urban-ruralcontinuum. *Journal of Cleaner Production*, 103, 586-600.

[4] Issac, M.N, & Kandasubramanian, B. (2021). Effect of microplastics in water and aquatic systems. *Environmental Science and Pollution Research*, 28, 19544-19562.

[5] Anbumani, S., & Kakkar, P. (2018). Ecotoxicological effects of microplastics on biota: A review. *Environmental Science and Pollution Research*, 25, 14373-14396.

[6] Rogovskii, I.L., Kalivoshko, O.M., Maksimovich, K.Yu., & Maksimovich, E.Yu. (2021). Research of mixed carbon sorbents for removal of oil products from water and soil for preservation of environmental infrastructure. *IOP Conference Series: Earth and Environmental Science*, 720, article number 012108.

[7] Zaborowska, M., Wyszkowska, J., Borowik, A., & Kucharski, J. (2021). Bisphenol A–A dangerous pollutant distorting thebiological properties of soil. *International Journal of Molecular Sciences*, 22, article number 12753.

[8] Gingrich, J., Filipovic, D., Conolly, R., Bhattacharya, S., & Veiga-Lopez, A. (2021). Pregnancy-specific physiologically-based toxicokineticmodels for bisphenol A and bisphenol S. *Environment International*, 147, article number 106301.

[9] Rogovskii, I.L., Kalivoshko, S.M., Voinash, S.A., Korshunova, E. E., Sokolova, V.A., Obukhova, I.A., & Kebko, V.D. (2020). Research of absorbing properties of carbon sorbents for purification of aquatic environment from oil products. *IOP Conference Series: Earth and Environmental Science*, 548, article number 062040.

[10] Mishra, M., Singh, A.P., Kumar, M., & Chand, M. (2021). Investigation of the microwave absorbing properties on polymer sheets. *Journal of Materials Science: Materials in Electronics*, 32(21), 1-10.

[11] Knapik, E. (2020). Separation of BTX fraction from reservoir brines by sorption onto hydrophobizedbiomass in a fixed-bed-column system. *Energies*, 13(1064), 2-15.

[12] Dissanayake, D., Jayasingheb, C., & Jayasinghe, M. (2017). A comparative embodiedenergy analysis of a house with recycledexpanded polystyrene based foam concretewall panels. *Energy and Buildings*, 135, 85-94.

[13] Arezoumandi, M., Smith, A., Volz, J., Khayat, K. (2015). An experimental study on flexuralstrength of reinforced concrete beams with 100% recycled concrete aggregate. *Engineering Structures*, 88, 154-162.

[14] Rogoskii, I., Mushtruk, M., Titova, L., Snezhko, O., Rogach, S., Blesnyuk, O., Rosamaha, Yu., Zubok, T., Yeremenko, O., & Nadtochiy, O. (2020). Engineering management of starter cultures in study of temperature of fermantation of sour-milk drink with apiproducts. *Potravinarstvo Slovak Journal of Food Sciences*, 14, 1047-1054.

[15] Major, M., & Halbiniak, J. (2019). Effect of adhesion between EPS granules and cement matrix on the characteristics of lightweight concretes. *IOP Conference Series Materials Science and Engineering*, 603(3), article number 032054.

[16] Rogovskii, I.L., Polishchuk, V.M., Titova, L.L., Sivak, I.M., Vyhovskyi, A.Yu., Drahnev, S.V., & Voinash, S.A. (2020). Study of biogas during fermentation of cattle manure using a stimulating additive in form of vegetable oil sediment. *ARPN Journal of Engineering and Applied Sciences*, 15(22), 2652-2663.

[17] Smirnova, O.E., & Pichugin, A.P. (2019). Structural and thermal insulation products based on vegetable raw materials. *IOP Conference Series Materials Science and Engineering*, 687(2), article number 022024.

[18] Pichugin, A.P., Denisov, A.S., Khritankov, V.F., & Rubtsova, N.V. (2014). Experience and possibilities of using plant materials in various objects construction. *Innovations and Food Security*, 3(5), 22-28.

[19] Canakci, H., Alak, D., & Celik, F. (2016). Evaluation of shear strength properties of modified expanded polystyrene aggregate. *Procedia Engineering*, 161, 606-610.

[20] Cadere, C., Barbuta, M., Rosca, B., Serbanoiu, A., Burlacu, A., Oancea, I. (2018). Engineering properties of concrete with polystyrene granules. *Procedia Manufacturing*, 22, 288-293.

Олексій Миколайович Калівошко[1], Вацлав Романюк[2], Микола Федотович Калівошко[1]

[1]Національний університет біоресурсів і природокористування України

03041, вул. Героїв Оборони, 15, м. Київ, Україна

[2]Інститут технологічних і природних наук Національного дослідницького інституту
05-090, алея Грабська, 3, с. Фаленти, Республіка Польща

Техніко-економічне обґрунтування ефективності вуглецевих сорбентів на основі тирси сосни для очищення нафтопродуктів

Анотація. Нафтові забруднення довкілля багато в чому виділяються серед інших. Відомо, наприклад, що літр нафти позбавляє кисню 40 тисяч літрів води, тонна нафти забруднює 12 км^2 водяної поверхні. Вміст у воді нафтопродуктів вище 0,1 мг/л надає м'ясу риб непереборний при жодних технологічних обробках присмак і специфічний запах нафти. На вітчизняному та світовому ринках є велика різноманітність сорбційних матеріалів для ліквідації нафтових розливів. Сорбенти створюються на основі різних органічних та неорганічних матеріалів. Багато з них є досить ефективними і мають високу сорбційну ємність, проте енергетичні та матеріальні витрати на їх виробництво визначають високу вартість продукту, що часто не задовольняє вимог споживачів. Водночас перспективні та економічно вигідні сорбенти є можливим виготовляти з місцевої вторинної сировини. В останні роки активно ведуться розробки з отримання нафтових сорбентів для збору проток вуглеводнів на основі відходів лісової та сільськогосподарської промисловості, використання цього типу сировини обумовлено досить високою поглинаючою здатністю одержуваних сорбентів, їх низькою вартістю, доступністю як місцевого матеріалу та можливістю подальшого застосування. Мета статті – узагальнення експериментальних досліджень з ефективності вуглецевих сорбентів на основі тирси сосни для очищення нафтопродуктів. В статті представлені табульовані дані про структурні та сорбційні характеристики різних фракцій тирси сосни при вологості 50–60 %. Авторами доведено експериментальним шляхом існування залежності величини нафтоємності вуглецевих сорбентів із різних фракцій сосни від тривалості карбонізації при різних температурах. В статті подано результати про поглинальні та сорбційні характеристики вуглецевих сорбентів із різних фракцій тирси сосни. Висновок – при кожній температурі, коли досліджувалися процеси карбонізації, маємо оптимальне значення тривалості, при якому нафто ємність сорбенту з різних фракцій тирси сосни є найвищою, а вихід сорбенту максимальний. Авторами доведено, що температура карбонізації тирси сосни різних фракцій більше 350°С не рекомендується, а для фракції менше 1 мм понад 300°С, яка має малі розміри та значне вигоряння і деградацію, через можливість загоряння, внаслідок чого знижується кількість та якість вуглецевого сорбенту

Ключові слова: показники вуглецевих сорбентів, довкілля, економічні показники, карбонізація, нафтопродукти, сорбційна ємність, фракції сосни

Machinery & Energetics
Vol. 13, No. 1. 2022

Journal homepage:
https://technicalscience.com.ua/en

UDC 331.45
DOI: 10.31548/machenergy.13(1).2022.54-59

Oleksandr Voinalovych[1*], Andrzej Marczuk[2], Tetyana Zubok[1]

[1]National University of Life and Environmental Sciences of Ukraine
03041, 15 Heroiv Oborony, Kyiv, Ukraine

[2]University of Life Sciences in Lublin
20400, 7 Stanislav Leshchynskyi Str., Lublin, Republic of Poland

Principles of development of occupational safety business games

Abstract. According to modern researchers, the professional qualities of employees and their social orientation are formed in socially significant labour activities, which are collective in nature. Therefore, for the development of independence, activity, and other important qualities, it is necessary to give the opportunity to participate in a holistic work process. This means analysing the labour task, identifying the goal, drawing up a plan and organising its implementation, current and final control, and self-assessment. As practice shows, these tasks can be most fully implemented by implementing business games. The relevance of the study is determined by the existing contradictions between: the requirements of the labour market for the quality of labour and the weak preparation of employees for work in the new socio-economic conditions; conservatism of forms and methods of professional training of employees and the need to activate labour training; the needs of employees in social protection through employment and the low level of establishment of basic professional knowledge and skills necessary for the performance of occupational safety professional functions. The goal is to present the basics of developing business games in occupational safety disciplines, adapting them to the problems of occupational safety, and evaluate the effectiveness of their application in the educational process. Methodology – the business game was considered as a simulation of the real activity of an employee in various created occupational safety situations. The paper structures the results of the morphology of stages and the sequence of conducting an occupational safety business game. The authors substantiate the structural representation of the functions (tasks) of the head of a business game. Analytical research is presented in the form of a synthesis of the function of occupational safety business games with criteria for evaluating their effectiveness. The existence of a correlation between the average scores of responses from the training module on a 100-point system for different methods of teaching the discipline against the background of the overall score of academic groups for the academic year is confirmed: control (training in the form of lectures and practical works); research (training in the form of lectures and business games)

Keywords: active training methods, occupational safety business game, modelling of production situations, occupational safety, industrial safety

Article's History: Received: 01.10.2021; Revised: 10.01.2022; Accepted: 23.02.2022

INTRODUCTION

The relevance of this study is conditioned by the need to search for new methodically appropriate ways to train specialists when students study the disciplines of the "occupational safety" complex. In particular, the use of occupational safety business games in the educational process is promising [1].

Educational business games involve modelling a certain organisational activity in the presence of problematic situations at the enterprise, the solution of which during the game lesson develops practical thinking in students, allowing them to develop the ability to analyse the conditions and consequences of decisions made [2]. The main goal of the occupational safety business game is to prepare students to solve technological and organisational situations related to the safety of work at the enterprise [3]. At the same time, the principles on which occupational safety business games are developed are not yet sufficiently substantiated.

Suggested Citation:
Voinalovych, O., Marczuk, A., & Zubok, T. (2022). Principles of development of occupational safety business games. *Machinery & Energetics,* 13(1), 54-59.

*Corresponding author

Currently published developments in the field of business games on occupational safety concern only certain occupational safety topics [4], and their application does not sufficiently contribute to the development of a logical approach among students to coordinate the use of normative occupational safety documents of various levels [5]. It also does not create a consistent transition from some sections of "occupational safety" to others [6]. Therefore, it is relevant to introduce the study of individual sections of "occupational safety" in the form of business games. The most common are business games that are designed for the construction industry and fire safety [7].

In particular, the development of occupational safety business games for industrial situations in agriculture, as one of the most traumatic sectors of the economy, is relevant [8].

But the main attention is now paid to the introduction of computerised occupational safety games into the educational process, which is advisable for training workers [9]. It is business games, in which workers are introduced in a playful way to the main dangers in the workplace and occupational safety requirements, that account for the main number of publications [10]. To improve the skills of enterprise officials, it is useful to use business games of the organisational plan [11], when game participants model algorithms for actions of officials of various levels of management [12].

The cornerstone laid down for the functioning of the occupational safety management system at the enterprise [13] should be the participation of all employees in occupational safety work [14]. Under this condition, the occupational health and safety management system will be effective [15], because the majority of employees of the enterprise will be involved in maintaining a proper high level of occupational health and safety [16], and not just a few officials [17]. This substantiates the possibility of joining the occupational safety business game in various roles of many of its participants [18], such as all students of individual subgroups [19], who must perform separate laboratory and practical work (tasks) on occupational safety [20].

Purpose of the study. Present the basics of developing business games in occupational safety disciplines, adapting them to the problems of occupational safety, and evaluate the effectiveness of their application in the educational process.

RESULTS AND DISCUSSION

The introduction of business games of the organisational plan to occupational safety training leads to the fact that the student must work out (analyse) various sources of information related to the activities of the enterprise to gain the necessary knowledge. The student's participation in the occupational safety business game leads to the activation of their thinking, forces (even regardless of their desire) to be active during the lesson for a long time. This contributes to independent decision-making, increases the degree of motivation of the student and their emotionality. In occupational safety business games, it is possible to combine collective and individual forms of assimilation of occupational safety principles, considering information about the state of production based on previously obtained theoretical generalisations.

An occupational safety business game should be based on simulation and game models that can be characterised by a certain sequence (Fig. 1). As the subject of the occupational safety business game, it is necessary to consider a certain order of activity of participants in accordance with a given professional activity.

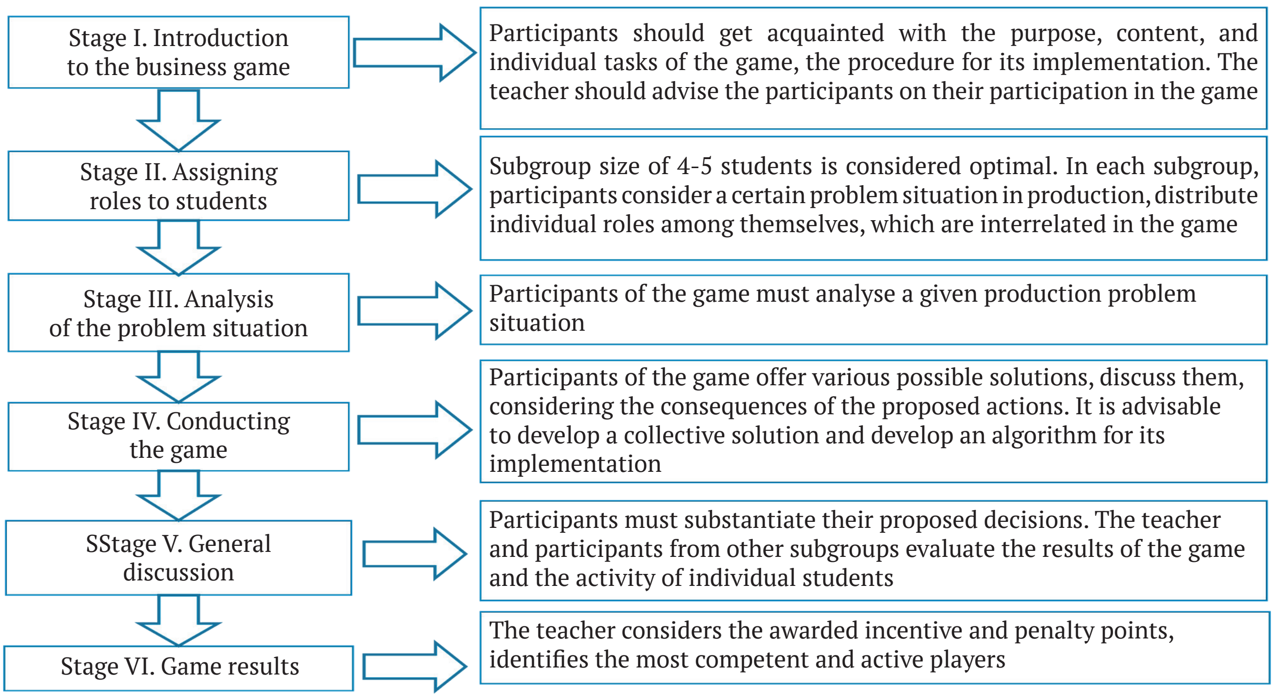

Figure 1. Stages and sequence of conducting the occupational safety business game

The development of the occupational safety business game of an organisational plan involves the use of the following research methods:

– modelling of production situations;

– structuring materials of the occupational safety regulatory framework;

– search for information

The simulation and game models used in the occupational safety business game are characterised differently. The simulation model should determine the content of activities on occupational safety issues of officials of the enterprise, as a certain part of occupational safety work. A simulation model is considered as a prototype of a model or an object of simulation. The game model should describe the activities of participants in a business game according to the simulation model. The game model shows the actions of participants in accordance with the duties of occupational safety officials of the enterprise. During the occupational safety business game, the teacher can allow participants to suggest their own (even erroneous) actions to solve an industrial problem related to occupational safety, and give a certain freedom of action to the participants of the game. The task of the teacher, as the head of the occupational safety business game, is shown in the form of a diagram (Fig. 2).

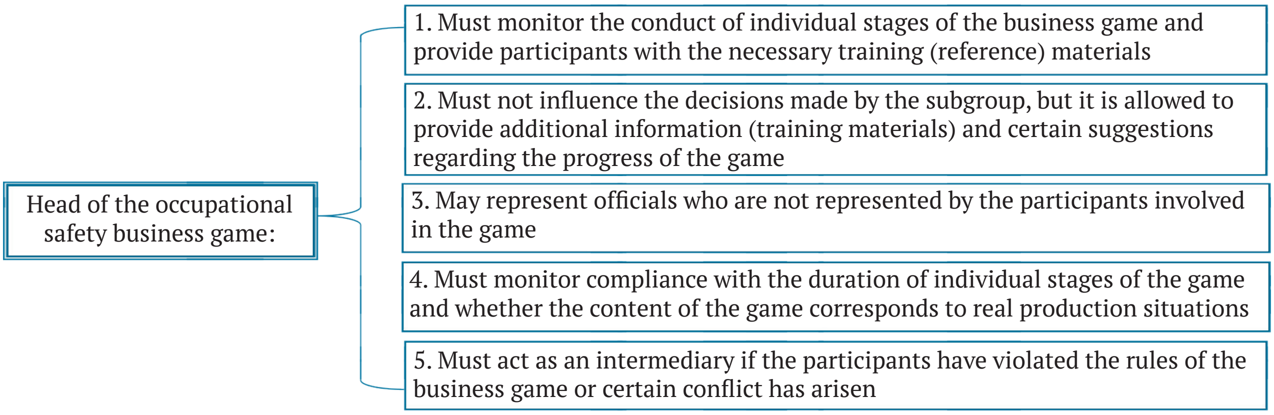

Figure 2. Structural representation of the functions (tasks) of the business game manager

The analysis of the possibilities of game technologies for solving occupational safety issues at the enterprise, which will increase the effectiveness of occupational safety training of officials, identifies the following functions of business games (Fig. 3) and offers criteria for evaluating their effectiveness.

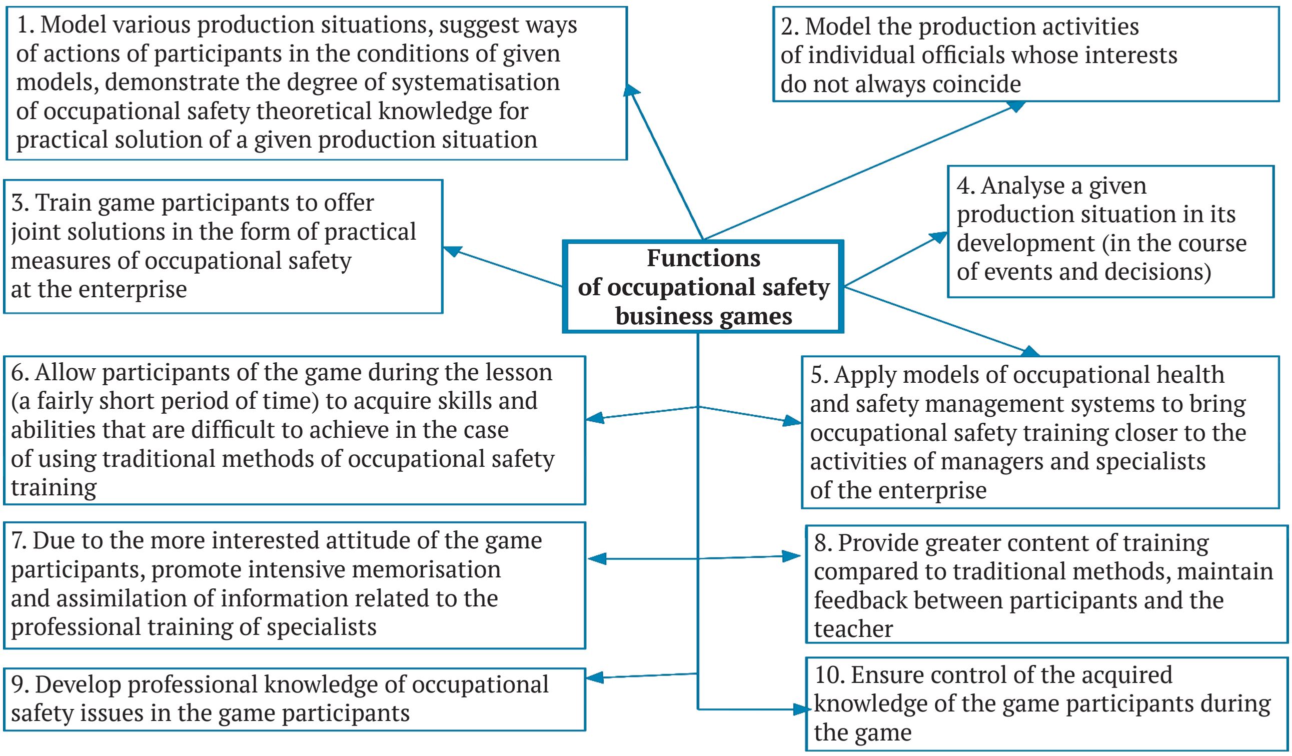

Figure 3. Functions of occupational safety business games with criteria for evaluating their effectiveness

The complex of occupational safety business games should provide for the transfer of game functions between participants, so that each participant (student of the subgroup) can perform duties in each of the multi-level positions of the enterprise – head, occupational safety engineer, head of the division, chief specialist, insurance expert of the Social Insurance Fund of Ukraine, State Labour inspector, inspector of fire supervision, etc. The variety of topics on occupational safety, on which occupational safety training is conducted, allows implementing such a distribution and interchangeability of the functions of participants.

During the occupational safety business games, students will be able to:

– get acquainted with the occupational safety duties of the company's officials;

– acquire the ability to interact with managers and subordinates, and use the regulatory documents on occupational safety used at the enterprise;

– learn how to find out the hidden causes of injuries and occupational diseases based on the analysis of dangerous and harmful factors at work;

– learn how to offer effective measures to prevent occupational risks in the workplace.

The results of evaluating the work in the game classes of participants of occupational safety business games allow the teacher to get an objective idea of the acquired professional knowledge of the participants of the game, about the readiness for further occupational safety management activities, in particular, regarding the practical solution of complex industrial situations related to occupational safety.

Research on the effectiveness of business games on occupational safety is characterised by certain methodological difficulties. But as a result of the analysis of the academic performance of students, for whom certain sections of the discipline "Occupational safety" were taught in the form of occupational safety business games, allowed drawing a conclusion about a significant increase in the level of academic performance, and therefore, the professional readiness of future specialists

Before introducing occupational safety business games into the educational process, it is necessary to substantiate their place and scope in the curriculum, and formulate recommendations for their implementation. First of all, the occupational safety business game should become a practical embodiment of the previously mastered educational material. In the structure of a business game, it is necessary to adhere to the following main stages: a) preparatory; b) conduct of the game; c) analysis and summarisation of its results. Considering two aspects of the goal of a business game (motivational and didactic), the success of a business game depends on the participants' awareness of the goal and objectives of the game, and the requirements for each of the participants.

To find out the degree of effectiveness of conducting occupational safety business games, the results of modular control of experimental groups of students from game classes were compared with the results of similar certification of students of control groups for whom traditional practical classes were conducted. The study compared the average response scores on a 100-point system for experimental and control groups, considering the overall performance score of the groups for the academic year.

The obtained data showed that the level of knowledge of students in the groups where practical classes were conducted in the form of a business game was significantly higher compared to the results of students in the control groups (Fig. 4).

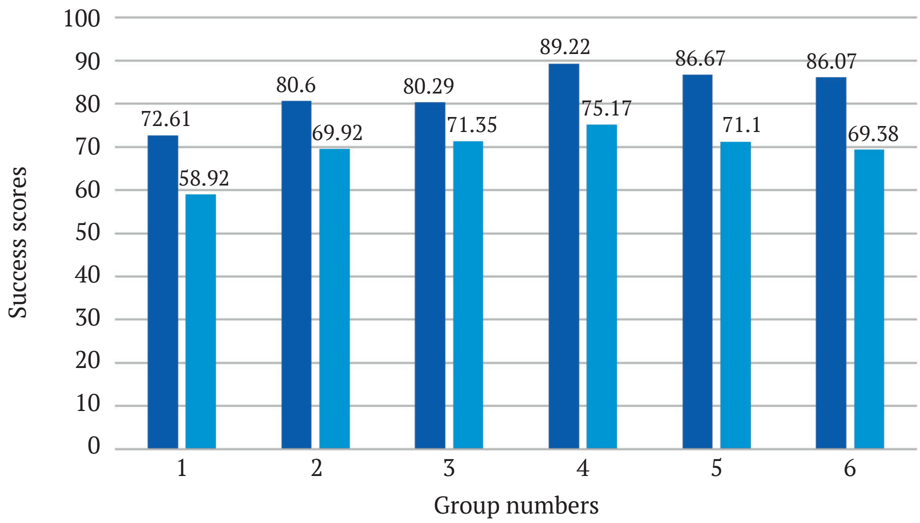

Figure 4. Comparison of average scores of responses (left columns) from the training module on a 100-point system for different methods of teaching the discipline against the background of the overall score of academic groups (right columns) for the academic year: groups 1, 2, 3 – control (training in the form of lectures and practical works); groups 4, 5, 6 – research (training in the form of lectures and business games)

Comparing the data of averaged response scores from the student control module on a 100-point system with the overall group performance score for the academic year, a direct correlation was established between the two data sets. The strength of the correlation was 0.708, which according to the scale is a strong relationship, as evidenced by the level of significance.

CONCLUSIONS

1. Methodological approaches to the use of occupational safety business games are described, which would allow activating independent creative activity in the case of training students and improving the occupational safety skills of officials of agro-industrial enterprises. The application of the formulated principles allows acquiring the ability to make optimal decisions on occupational safety in production conditions and in case of non-standard situations.

2. Insufficient attention of researchers to substantiate the theoretical foundations of business games on occupational safety is noted. It is also important to improve the practice of using business games as an active occupational safety method of training. The structure of business games is proposed, which concerns the detection of violations of occupational safety at the enterprise and other issues, which allows modelling elements of future professional activity.

3. The described principles of preparing and conducting the occupational safety business game can be used as one of the active teaching methods that allow students to act independently for a certain time in a simulated situation. Analysis of the development of the situation, various ways to solve it, actions, methods, and ways out of critical situations regarding labour safety improves the quality of the educational process and contributes to the accumulation of experience.

4. On the example of the use of business games in the educational process on certain topics of the "Occupational safety" discipline, their effectiveness is shown, evaluated by the results of the following testing.

REFERENCES

[1] Asplund, T., Neset, T.S., & Käyhkö, J. (2019). Benefits and challenges of serious gaming – the case of the Maladaptation Game. *Open Agriculture*, 4, 107-117.

[2] Li, H., Chan, G., & Skitmore, M. (2012). Visualizing safety assessment by integrating the use of game technology. *Automation in Construction*, 22, 498-505.

[3] Cierniak-Emerych, A., & Pietroń-Pyszczek, A. (2019). Gamification as a tool to improve the level of occupational safety and health in company. *Scientific Journal of Silesian University of Technology. Organization and Management Series*, 136, 87-96.

[4] Vigoroso, L., Caffaro, F., Cremasco, M.M., & Cavallo, E. (2021). Innovating occupational safety training: A scoping review on digital games and possible applications in agriculture. *International Journal of Environmental Research and Public Health*, 18(4), article number 1868.

[5] Mohd, N.I., Ali, K.N., & Ebrahimi, S.S. (2021). Understanding the level of self-directed learning and decision-making style of construction-related workers. *International Association of Online Engineering: Limoges, France*, 2, 44-53.

[6] Din, Z.U., & Gibson, G.E. (2019). Serious games for learning prevention through design concepts: An experimental study. *Safety Science*, 115, 176-187.

[7] Pisarenko, G., Voinalovych, O., Rogovskii, I., & Motrich, M. (2019). Probability of boundary exhaustion of resources as factor of operational safety for agricultural aggregates. *Engineering for Rural Development*, 18, 291-298.

[8] Gao, Y., Gonzalez, V.A., & Yiu, T.W. (2019). The effectiveness of traditional tools and computer-aided technologies for health and safety training in the construction sector: A systematic review. *Computers & Education*, 138, 101-115.

[9] Williams-Bell, F.M., Kapralos, B., & Hogue, A. (2014). Using serious games and virtual simulation for training in the fire service: A review. *Fire Technology*, 51, 553-584.

[10] Ma, Q., Yang, Z., & Chen, H. (2012). A serious game for teaching and learning agricultural machinery driving. *International Conference on Artificial Intelligence and Soft Computing*, 12, 56-62.

[11] Caffaro, F., Cremasco, M.M., Roccato, M., & Cavallo, E. (2020). Drivers of farmers' intention to adopt technological innovations in Italy: The role of information sources, perceived usefulness, and perceived ease of use. *Journal of Rural Studies*, 76, 264-271.

[12] Voinalovych, O.V., & Holopura, S.M. (2020). Justification of the risk-based approach of operation of mobile agricultural equipment on the example of details of separate units of tractors. *Machinery & Energetics. Journal of Rural Production Research*, 11(3), 173-179.

[13] Carrillo, D.L., García, A.C., & Laguna, T.R. (2019). Using gamification in a teaching innovation project at the university of Alcalá: A new approach to experimental science practices. *Electronic Journal of e-Learning*, 17, 93-106.

[14] Leba, M., Ionicã, A., & Apostu, D. (2014). Educational software based on gamification techniques for medical students. In *Recent advances in information and communication technology: Proceedings of the 10th international conference* (pp. 225-230). Phuket: Prince of Songkla University.

[15] Voinalovych, O., Hnatiuk, O., Rogovskii, I., & Pokutnii, O. (2019). Probability of traumatic situations in mechanized processes in agriculture using mathematical apparatus of Markov chain method. *Engineering for Rural Development*, 18, 563-269.

[16] Day, L., Voaklander, D., & Sim, M. (2008). Risk factors for work-related injury among male farmers. *Occupational and Environmental Medicine*, 66, 312-318.
[17] Rogovskii, I.L., Titova, L.L., Voinash, S.A., Sokolova, V.A., Tarandin, G.S., & Polyanskaya, O.A. (2021). Modeling the weight of criteria for determining the technical level of agricultural machines. *Earth and Environmental Science*, 677, article number 022100.
[18] Hall, J., Wyeth, P., & Johnson, D. (2016). Creating authentic experiences within a serious game context: Evaluation of engagement and learning. In *Joint international conference on serious games* (pp. 55-66).Cham: Marsh Springer.
[19] Kuindersma, E., Van Der Pal, J., Van Den Herik, J., & Plaat, A. (2017). Building a game to build competencies. In *Games and learning alliance* (pp. 14-24). Cham: Marsh Springer.
[20] Holopura, S.M., & Chmara, P.O. (2020). Business game as a way to increase the efficiency of the educational process in study topics providing of first aid to victims in accidents. *Machinery & Energetics. Journal of Rural Production Research*, 11(4), 49-56.

Олександр Володимирович Войналович[1], Анджей Марчук[2], Тетяна Олександрівна Зубок[1]

[1]Національний університет біоресурсів і природокористування України
03041, вул. Героїв Оборони, 15, м. Київ, Україна

[2]Університет наук про життя в Любліні
20400, вул. Станіслава Лещинського, 7, м. Люблін, Республіка Польща

Засади розроблення працеохоронних ділових ігор

Анотація. Як зазначають сучасні дослідники, професійні якості працівників, їхня громадська спрямованість формуються у соціально значущій трудовій діяльності, колективній за своїм характером. Тому для розвитку самостійності, активності, а також інших необхідних якостей потрібно дати можливість брати участь у цілісному процесі праці. Мається на увазі аналіз трудового завдання, виявлення мети, складання плану та організація його виконання, поточний та підсумковий контроль, самооцінка. Як показує практика, найповніше ці завдання можна реалізувати шляхом впровадження ділових ігор. Актуальність дослідження визначається існуючими протиріччями між: вимогами ринку праці до якості робочої сили та слабкою підготовкою працівників до трудової діяльності у нових соціально-економічних умовах; консерватизмом форм та методів професійного навчання працівників та необхідністю активізації трудової підготовки; потребами працівників у соціальному захисті шляхом працевлаштування та низьким рівнем сформованого базових професійних знань та умінь, необхідних для виконання працеохоронних професійних функцій. Мета – представити засади розроблення ділових ігор з працеохоронних дисциплін, адаптувавши їх до проблематики безпеки праці, та оцінити ефективність їх застосування у навчальному процесі. Методологія – ділову гру розглядали як моделювання реальної діяльності працівника в різних створених працеохоронних ситуаціях. В статті структуровано результати морфології етапів і послідовності проведення працеохоронної ділової гри. Авторами обґрунтовано структурне представлення функцій (завдань) керівника ділової гри. Аналітичні дослідження представлені у вигляді синтезу функції працеохоронних ділових ігор з критеріями оцінення їх ефективності. Підтверджено існування кореляційного зв'язку усереднених оцінок відповідей з навчального модуля за 100-бальною системою за різних методик викладання дисципліни на фоні загального балу успішності навчальних груп за навчальний рік: контрольні (навчання у вигляді лекцій та практичних робіт); дослідні (навчання у вигляді лекцій та ділових ігор)

Ключові слова: активні методи навчання, працеохоронна ділова гра, моделювання виробничих ситуацій, охорона праці, виробнича безпека

Machinery & Energetics
Vol. 13, No. 1. 2022

Journal homepage:
https://technicalscience.com.ua/en

UDC 631.1.004
DOI: 10.31548/machenergy.13(1).2022.60-66

Denys Mozharivskyi[1*], Liudmyla Titova[1], Oleksandr Nadtochiy[1], Petr Dasic[2]

[1]National University of Life and Environmental Sciences of Ukraine
03041, 15 Heroiv Oborony, Kyiv, Ukraine

[2]Higher Technical School of Mechanics
21000, 1 Shkilna Str., Novi Sad, Serbia

Aspects of expert system of engineering management of technical condition of combine harvesters

Abstract. Ensuring the country's food independence is one of the most important tasks, the successful solution of which depends on the effective functioning of the agro-industrial complex. The main condition for solving the issues of technical support of agricultural enterprises is the high quality and competitiveness of Ukrainian agricultural machinery, in particular, combine harvesters. Engineering management plays an important role in improving the efficiency of using combine harvesters, timely detection and prevention of technological and technical failures. In practice, when using complex harvesting equipment, one of the most important tasks is the technological regulation of the machine in the field. This task belongs to the class of time-consuming engineering problems. Basically, the solution of the problem of engineering management of combine harvesters is assigned to the operator and depends on their qualifications. Difficulties in solving the problem of technological regulation are associated with the uncertainty of information about the factors of the external environment in which the combine operates and the complexity and insufficient study of the relationships between harvesting factors, regulatory parameters, and indicators of the quality of the combine. Therefore, special attention should be paid to the development of information support systems for the operator's intellectual activities, which help it during harvesting operations. One of these promising areas is the development of expert systems for the subject area under consideration. The purpose is to substantiate aspects of engineering management of the technical condition of the combine harvester and the functions of practical application in information technology. Methodology – an expert system of engineering management of the technical condition of combine harvesters can operate in two modes: acquiring knowledge and solving problems. The paper presents the results of communication synthesis in the system "combine harvester – combine operator – master diagnostician". According to the results of production tests, failures of hydraulic equipment and electrohydraulics of combine harvesters of the Slavutych model were tabulated. Conclusion – the use of an expert system has reduced the time spent on collecting and analysing information about the technical condition and making decisions – they are more than four times less than the time spent on troubleshooting. Scientific relevance – the validity of existence at the level of significance α=0.05 of the null hypothesis that the duration of technical diagnostics is equal to the duration of repair has been proven, and the competing hypothesis that the duration of diagnostics of a combine harvester is less than the duration of repair

Keywords: intellectual aspect, engineering, diagnostics, combine operation

Article's History: Received: 20.09.2021; Revised: 06.01.2022; Accepted: 23.02.2022

INTRODUCTION

The efficiency of agricultural production is largely determined by the degree of mechanisation of technological operations and the technical level of machines [1]. A means of mechanising the harvesting of grain, sunflower, corn, and other crops is a combine harvester, one of the most complex machines in modern agricultural production [2]. The majority, namely 83%, of grain harvesting equipment in Ukraine is made up of John Deere, Class, New Holland, and Slavutych combines [3].

Management of the technical condition of machines, in particular, combine harvesters, can be considered in

Suggested Citation:
Mozharivskyi, D.M., Titova, L.L., Nadtochiy, O.V., & Dasic, P. (2022). Aspects of expert system of engineering management of technical condition of combine harvesters. *Machinery & Energetics,* 13(1), 60-66.

*Corresponding author

three aspects [4]: informational, intellectual, and physical (Fig. 1). In the information aspect, this is the collection and processing of data on the technical condition of the machine. Information about the technical condition can be obtained by the organoleptic method [5] or with the help of technical diagnostic tools – built-in control and measuring devices or standard diagnostics [6], special measuring devices, information and measuring diagnostic complexes [7]. Intellectual aspect – development of a diagnostic algorithm, analysis of information about the technical condition, and making a management decision [8]. Physical aspect – implementation of the control effect of technical service, regulation, and inclusion of backup elements [9].

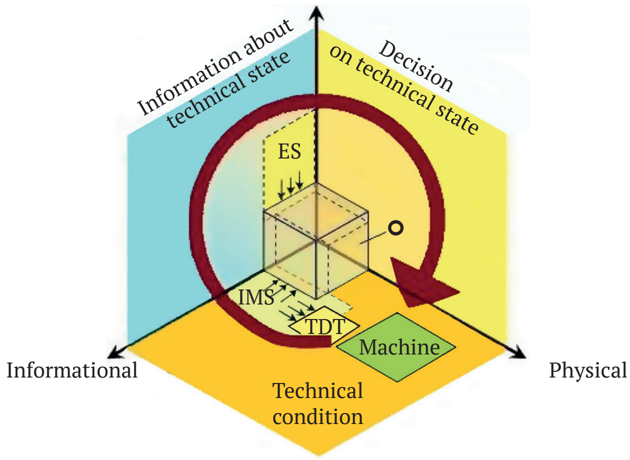

Figure 1. Operator in coordinates:
O – operator; TDT – traditional diagnostic tools; IMS – information and measurement system; ES – expert system

The security and professional level of machine operators, driver managers and specialists of the engineering and technical service of agricultural enterprises are the most important factors for the effective use of equipment and, unfortunately, current problems of the industry [10]. The most qualified and active specialists left the village in the 1990s [11]. Currently, the situation is not improving [12]. The number of machine operators is reduced by 3-5% annually [13]. The share of machine operators of the first and second classes in their total number decreases and is less than 60% [14]. Young people entering the agricultural sector of the economy are not only not professional machine operators, but also in the vast majority are poorly trained and cannot conduct technological processes in conditions adequate to the environment [15]. Of the total number of employees of the engineering service of agricultural enterprises, 70-75% have professional education, and only 30-35% have higher education [16].

In the absence of a centralised system of training and improving the effectiveness of qualifications, the main means of maintaining the competence of specialists engaged in maintenance is the availability and constant updating of technical documentation at the level of individual agricultural farms [17]. Technical documentation mainly comes with a new machine, or with new equipment [18]. Considering the specifics of the work carried out, methodological manuals, route maps, and user manuals made in the form of printed publications quickly fall into disrepair [19]. This explains the insufficient amount of necessary technical documentation [20]. On the other hand, printed publications (books, posters, etc.) do not provide ease of editing and adding knowledge [21]. At the same time, the technical documentation required for the organisation of maintenance is practically absent for free sale [22].

In this regard, it is necessary to provide support for the operator in information and intellectual aspects, or even exclude it from these areas of technical condition management [23]. That is, it is necessary to automate the process of generating information about the technical condition and provide support for making managerial decisions [24].

In the physical aspect, technical condition management can be carried out by low-skilled personnel [25]. But even in this aspect, the technical condition can be managed automatically, for example, by enabling backup elements [26]. However, this approach is unlikely to be widely used in agricultural machinery.

Thus, it is necessary to "shift" the operator to the origin along the "axes" of the intellectual and information aspects [11], transferring its functions to intelligent and information-measuring systems (Fig. 2). Diagnostics of the technical condition of the combine harvester and its components as objects of technical diagnostics during operation are in various technical conditions [6]. The change in technical condition is characterised by an external feature [21].

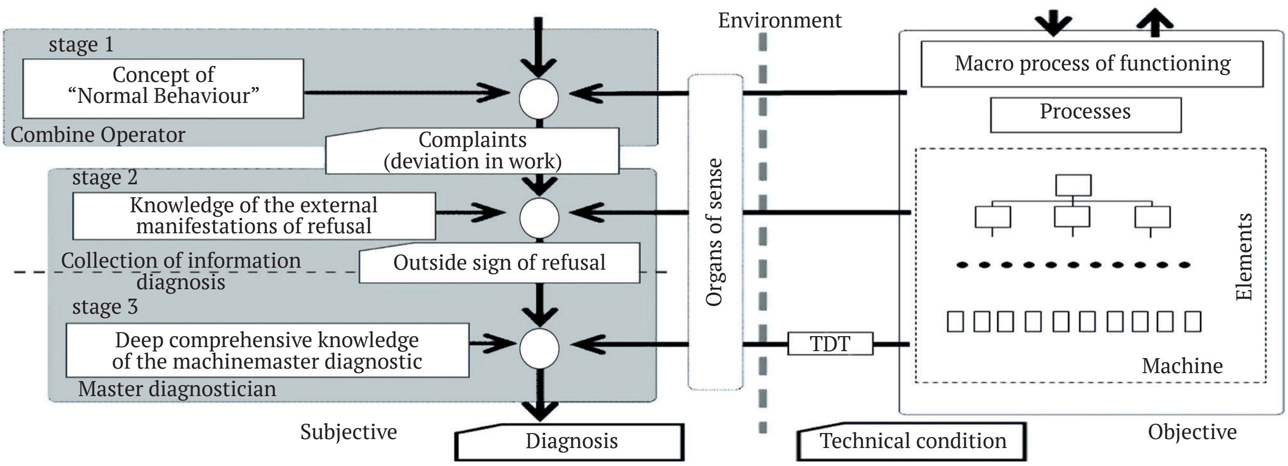

Figure 2. Communication scheme in the system "combine harvester – combine operator – master diagnostician"

Next, the study considers the process of generating information about the technical condition of the combine in the "combine harvester – combine operator – master diagnostician" system. The information generation process can be divided into two parts: collecting a priori information (stages 1 and 2 in Fig. 2) and actually diagnosing it (stage 3 in Fig. 2).

At the first stage, the operator informs the master diagnostician of their complaints about the machine [9]. Complaint is a description of a deviation perceived by the operator in the behaviour of the machine, or a clear sign of failure [3]. Examples of complaints: the header does not rise, the harvester valve does not close, instead of turning the discharge screw, the header is lowered, oil leaks along the hydraulic cylinder rod [16]. This is a clear sign of failure.

At the second stage of diagnostics (Fig. 2), the diagnostician analyses the operator's complaint and begins to collect additional information about the condition of the machine [7]. First of all, the diagnostician must make sure that the deviation recorded by the operator is caused by an objective failure of the machine, and not by subjective reasons [1]. For example, a deviation of the unloading device drive that does not turn on has been recorded, in order to recognise it as a manifestation of a combine failure, it is necessary to verify the truth of the following statements:

– the engine is running;

– the inclined discharge screw is in the working position;

– the power button of the discharge device drive is in the ON position.

At this stage of diagnosis, it is also necessary to link the external manifestations of deviations with specific elements of the object [20]. At the same time, object elements are understood as components of the object parts, assembly units, aggregates, the object as a whole and the rules for their installation, adjustment parameters, parameters of the state of components (if in specific conditions it is advisable to separate them from the corresponding parts).

The external failure sign is input information for the third stage (Fig. 2) – determining a non-working element with the required depth [14]. This stage involves the implementation of the traditional diagnostic procedure for elements whose failures may cause the appearance of an external sign.

The purpose of the study – to substantiate aspects of engineering management of the technical condition of the combine harvester and the functions of practical application in information technology.

RESULTS AND DISCUSSION

The authors of this study have developed and are improving an expert system that implements the following functions: description of the design of the combine harvester; preliminary configuration of the working bodies of the machine; adjustment of technological parameters; troubleshooting in the units and systems of the machine; explanation of the results obtained; addition and editing of knowledge; assistance to the user when working with the expert system. The expert system can work in two modes: acquiring knowledge and solving problems. In the knowledge acquisition mode, the knowledge engineer forms a knowledge base together with an expert. In problem solving mode, the user communicates with the expert system. The dialogue box for entering information provides a natural language interface for the user. The interface is one of the most complex components of any software product designed for wide application. The main problem with interface development is related to the user's lack of computer skills. Thus, the organisation of qualified help tips becomes a key issue from an additional service. In addition to traditional static information, the expert system uses multimedia elements that significantly increase visibility and make it easier for users who are not familiar with using computers.

The updated version of the expert bounce search system has a number of features. When used in the expert advisor mode, the expert system provides the maximum amount of information about the technical condition of the combine harvester based on the external features observed by the operator. Moreover, the expert system allows the operator to move from passive observation to setting up "experiments" to obtain new external features. For example, when registering an external feature, the "lifting/lowering of the harvester" button is in the lifting position and the motor is running and the harvester is not in the topmost position and the harvester position relative to the ground has not become higher than it was, the expert system can ask the operator to move the key to rotate the discharge auger to the transfer position to the working position and then ask: "Is the inclined discharge auger being transferred to the working position?". The answer to this question would allow the expert system to adjust the list and sequence of elementary checks, and therefore, increase the effectiveness of diagnostics.

Figure 3 shows the view of the prototype window of the expert system for a situation in which the operator complains about the combine: they chose the interested unit from the list on the left side of the programme window, the unit can be selected by pointing to the corresponding area on the 3D image of the combine: not all combine operators know the names of the units; from the list of deviations proposed by the system, the operator indicated a failure to rise, although the combine lift is a function of the hydraulic system, but many combine operators in the text of the complaint prefer to mention the element that visualises the failure, and such features must be considered when developing the programme interface); after indicating deviations in operation the expert system starts interviewing the operator to establish external manifestations of the technical condition of the combine. As a result of communication with the expert system, the operator will receive a list and sequence of basic checks and necessary explanations.

During the period of harvesting grain and leguminous crops in 2021 in the Bilotserkivskyi District of the Kyiv Oblast, data were collected on failures of Slavutych KZS 9-1 (18 vehicles), John Deere (21 vehicles), and Claas (3 vehicles) combine harvesters.

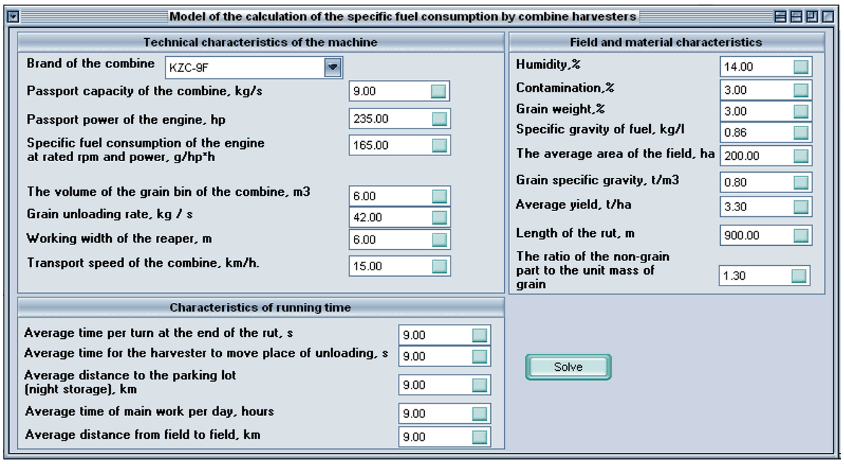

Figure 3. Interface of the expert system window

The following data was registered:
– complaint;
– technical diagnosis;
– duration of diagnosis;
– duration of repairs.

The expert system described above was used for diagnostics and repairs.

The duration of diagnostics was adopted as an indicator of the effectiveness of the technical diagnostics process. Generally speaking, the time spent on completing work can be considered as a complex indicator of its complexity, labour intensity, and responsibility.

In this paper, only failures of hydraulic equipment and electrohydraulics of combine harvesters of the Slavutych model are considered. During the observation period, 21 failures of these systems were recorded (Table 1).

Table 1. Failures of combine harvesters of the Slavutych model

No.	Complaint	Diagnosis	τ_d, hours	τ_r, hours
1	"The entire hydraulic system does not work"	Clogged overflow valve seat	0.12	0.13
2	"The discharge auger is not removed and unloading is not turned on"	No "mass" on HEC	0.10	0.08
3	"The speed of the reel is falling"	Failure of the valve of the shut-off device of the CVT control section of the reel 5PE	0.02	0.17
4	"Steering failure"	Failure of the steering unit AR–125	0.10	2.50
5	"When the header drive is turned on, the electrohydraulic fuse blows"	Closing of the control circuit for switching on the drive of the header part 3PE to "ground"	0.17	0.08
7	"The entire hydraulic system does not work"	Failure of SOV	0.28	1.12
8	"Slow lowering of the header"	The risks on the spindle and the disc mower housing are not combined	0.05	0.02
9	"The threshing drum speed does not increase"	CVT hydraulic cylinder failure	0.18	1.30
10	"Spontaneous lowering of the header"	Failure of the locking device of the lifting/lowering section of the header part 5PM	0.02	3.00
11	"Uploading is not enabled"	DO-13-1 sensor failure blocking switching on of the discharge device drive	0.12	0.08
12	"The header drive does not turn on"	1. Open circuit of the control section for switching on the drive of the header part of 3PE. 2. Mechanical part failure	0.38	0.43
13	"The entire hydraulic system does not work"	Failure of HEC	0.27	0.45
14	"The entire hydraulic system does not work"	NSH-32 pump drive failure	0.22	1.90
15	"The discharge auger cannot be removed"	The hole of the seat of the electromagnet needle of the 3PE discharge screw rotation section is clogged	0.08	0.25
16	"Uploading is not enabled"	Incorrect connection of wires on 2PE	0.18	0.02
17	"The speed of the threshing drum is falling"	Failure of the valve of the shut-off device of the threshing drum speed control section of 3PE	0.03	0.17
18	"Spontaneous lowering of the header"	Failure of the valve of the shut-off device of the lifting/lowering section of the header part of 5PE	0.02	0.17
19	"When lifting the header, the discharge auger is removed"	Worn rubber ring of the seat of the electromagnet of the section of rotation of the discharge screw of 3PE	0.10	0.13
20	"The header and reel do not rise/fall"	5PM failure (worn parts)	0.38	3.05
21	"Uploading is not enabled"	1. DO-13-1 sensor failure blocking the activation of the discharge device drive 2. Mechanical part failure	0.25	0.48

In Table 1, the following abbreviations are applied: 2PE, 3PE, 4PE, 5PE – electro-hydraulic distributors of 2-, 3-, 4-, and 5-sections; 5PM – muscle distributor; SOV – safety overflow valve (pressure hydraulic valve); HEC – hydraulic valve with electromagnetic control (flow control distributor).

During the observation period, not a single diagnostic error was registered, that is, the effectiveness of diagnostics is maximum.

For clarity, data on the duration of diagnostics and repairs are presented as a diagram in Figure 4.

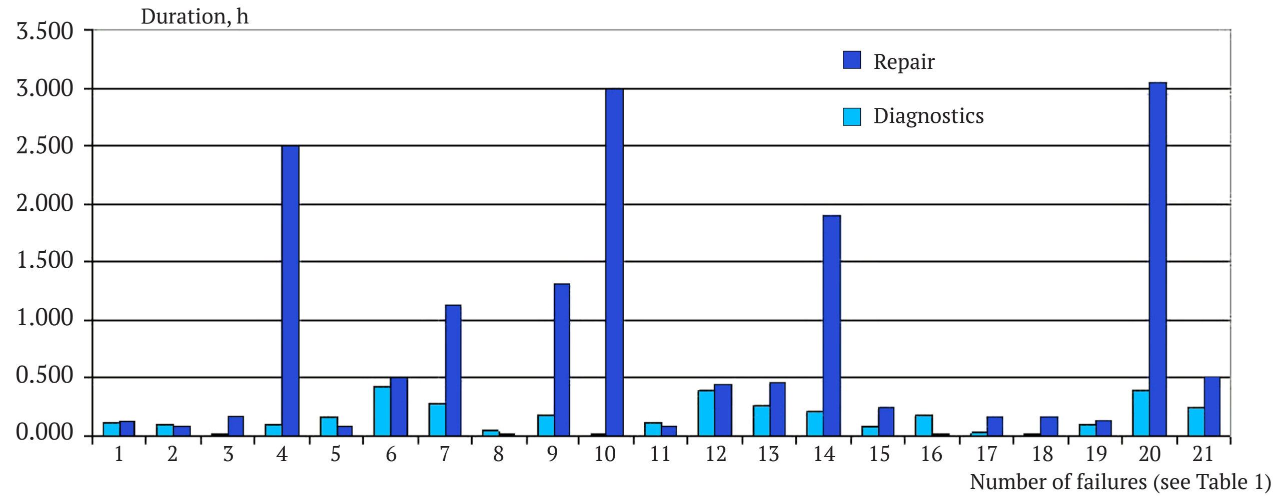

Figure 3. Interface of the expert system window

Based on the obtained data, the average values of the duration of diagnostics and repair of the combine harvester were determined, which amounted to $\bar{\tau}_d$= 0.17 hours and $\bar{\tau}_r$= 0.76 hours.

For a comparative assessment of the duration of diagnosis and repair, a statistical hypothesis about the equality of average normal general populations was tested.

The considered hypothesis has the form:

$$H_0{:}M(\bar{\tau}_d)=M(\bar{\tau}_r)H_1{:}M(\bar{\tau}_d)<M(\bar{\tau}_r),\ (\alpha=0.05) \qquad (1)$$

that is, at the level of significance α=0.05, the null hypothesis that the duration of technical diagnostics is equal to the duration of repairs is considered. A competing hypothesis is that the duration of diagnosis of a combine harvester is less than the duration of repair.

As a criterion for testing the null hypothesis (1), the value of:

$$KI = \frac{\bar{\tau}_d - \bar{\tau}_r}{\sqrt{D(\bar{\tau}_d)+D(\bar{\tau}_r)}}, \qquad (2)$$

where $D(\bar{\tau}_d)$+$D(\bar{\tau}_r)$ – variances of arithmetic mean diagnostic and repair durations, respectively.

The criterion value calculated by equation (2) Z_{obs}=-2,72, a critical point Z_{cr}=1,64, that is Z_{obs}<-Z_{cr}, therefore, the null hypothesis is rejected. At the significance level of 0.05, it can be argued that the duration of diagnosis is less than the duration of repair. Diagnostics of machines is mostly related to the information and intellectual aspects of managing the technical condition, while repair is related to the physical one. The results obtained indicate that the use of an expert system has reduced the time spent on collecting and analysing information about the technical condition and making decisions – they are more than four times less than the time spent on repairs. Data on the duration of diagnostics of a combine harvester without the use of an expert system are given in [7, 19]. Moreover, as practice shows, combine operators are often not able to independently diagnose the machine at all, especially in terms of electrical equipment and hydraulics.

Therefore, the use of an expert system significantly expands the range of tasks solved by the combine operator, without increasing the information load on them.

CONCLUSIONS

1. The proposed expert system contains aspects of engineering management of the technical condition of the combine harvester and implements the following functions: description of the design of the combine harvester; preliminary configuration of the working bodies of the machine; adjustment of technological parameters; troubleshooting in the units and systems of the machine; explanation of the results obtained; addition and editing of knowledge; assistance to the user when working with the expert system.

2. The expert system can work in two modes: acquiring knowledge and solving problems. In the knowledge acquisition mode, the knowledge engineer forms a knowledge base together with an expert. In problem solving mode, the user communicates with the expert system.

3. It was established empirically that the average values of the duration of diagnostics and repair of a combine harvester of the 2021 season were $\bar{\tau}_d$= 0.17 hours and $\bar{\tau}_r$= 0.76 hours.

REFERENCES

[1] Beier, G., Ullrich, A., Niehoff, S., Reibig, M., & Habich, M. (2020). Industry 4.0: How it is defined from a sociotechnical perspective and how much sustainability it includes – A literature review. *Journal of Cleaner Production*, 259, article number 120856.

[2] Dubbini, M., Pezzuolo, A., De Giglio, M., Gattelli, M., Curzio, L., & Covi, D. (2017). Last generation instrument for agriculture multispectral data collection. *CIGR Journal*, 19, 158-163.

[3] Bevly, D.M., Gerdes, J.C, & Parkinson, B.W. (2002). A new yaw dynamic model for improved high speed control of a farm tractor. *Journal of Dynamic Systems, Measurement, and Control*, 124(4), 659-667.

[4] Nazarenko, I., Mishchuk, Y., Mishchuk, D., Ruchynskyi, M., Rogovskii, I., Mikhailova, L., Titova, L., Berezovyi, M., & Shatrov, R. (2021). Determiantion of energy characteristics of material destruction in the crushing chamber of the vibration crusher. *Eastern-European Journal of Enterprise Technologies*, 4(7(112), 41-49.

[5] Aldoshin, N., & Didmanidze, O. (2018). Harvesting lupines albus axial rotory combine harvesters. *Research in Agricultural Engineering*, 64(4), 209-214.

[6] Brown, R., & Richards, A. (2018). Engineering principles of agricultural machinery. *ASABE*, 84(2), 1120-1132.

[7] Chen, S., Zhou, Y., Tang, Z., & Lu, S. (2020). Modal vibration response of rice combine harvester frame under multi-source excitation. *Biosystems Engineering*, 194, 177-195.

[8] Awasthi, S., Sarsaiya, S., Awasthi, M., Liu, T., Zhao, J., Kumar, S., & Zhang, Z. (2020). Changes in global trends in food waste: Research challenges and opportunities. *Bioresource Technology*, 299, 428-438.

[9] Golovkov, A., Moskovskiy, M., & Khamuev, V. (2019). Justification of the type of combine harvester for farms. *E3S Web of Conferences*, 126(2), article number 00029.

[10] Azizi, S., Sanaye-Pasand, M., & Paolone, M. (2019). A modified formula for distance relaying of tapped transmission lines with grounded neutrals. *IEEE Trans on Power Delivery*, 34(2), 690-699.

[11] Ebrahimi, R., Esfahanian, M., & Ziaei-Rad, S. (2013). Vibration modeling and modification of cutting platform in a harvest combine by means of operational modal analysis. *Measurement*, 4(6(10), 3959-3967.

[12] Kuzmich, I.M., Rogovskii, I.L., Titova, L.L., & Nadtochiy, O.V. (2021). Research of passage capacity of combine harvesters depending on agrobiological state of bread mass. *IOP Conference Series: Earth and Environmental Science*, 677, article number 052002.

[13] Guerrero, J.W., Toscano, A., Pacheco, L.V., & Tovar, J. (2018). Analysis of the energetic and productive effects derived by the installation of a conveyor belt in the metal-mechanic industry. *International Journal of Energy Economics and Policy*, 8(6), 196-201.

[14] Isaac, N., Quick, G., Birrell, S., Edwards, W., & Coers, B. (2006). Combine harvester econometric model with forward speed optimization. *Applied Engineering in Agriculture*, 22, 25-31.

[15] Matindi, R., Masoud, M., Hobson, P., Kent, G., & Liu, S. (2018). Harvesting and transport operations to optimise biomass supply chain and industrial biorefinery processes. *International Journal of Industrial Engineering Computations*, 9(3), 265-288.

[16] Rogovskii, I.L., Titova, L.L., Gumenyuk, Yu.O., & Nadtochiy, O.V. (2021). Technological effectiveness of formation of planting furrow by working body of passive type of orchard planting machine. *IOP Conference Series: Earth and Environmental Science*, 839, article number 052055.

[17] Šotnar, M., Pospíšil, J., Mareček, J., Dokukilová, T., & Novotný, V. (2018). Influence of the combine harvester parameter settings on harvest losses. *Acta Technologica Agriculturae*, 3, 105-108.

[18] Xidias, E.K. (2018). Time-optimal trajectory planning for hyper-redundant manipulators in 3D workspaces. *Robotics and Computer-Integrated Manufacturing*, 50, 286-298.

[19] Miu, V. (2016). Combine harvesters: Theory, modeling and design. *CRC*, 6, 208-242.

[20] Szpica, D. (2019). New Leiderman–Khlystov coefficients for estimating engine full load characteristics and performance. *Chinese Journal of Mechanical Engineering*, 32(1), 94-107.

[21] Yezekyan, T., Marinello, F., Armentano, G., Trestini, S., & Sartori, L. (2020). Modelling of harvesting machines' technical parameters and prices. *Agriculture*, 10(6), 194-204.

[22] Rogovskii, I.L., Titova, L.L., Voinash, S.A., Troyanovskaya, I.P., & Sokolova, V.A. (2021). Change of technical condition and productivity of grain harvesters depending on term of operation. *IOP Conference Series: Earth and Environmental Science*, 720, article number 012110.

[23] Yata, V.K., Tiwari, B.C., & Ahmad, I. (2018). Nanoscience in food and agriculture: Research, industries and patents. *Environmental Chemistry Letters*, 16, 79-84.

[24] Xu, L., Chai, X., Gao, Z., Li, Y., & Wang, Y. (2019). Experimental study on driver seat vibration characteristics of crawler-type combine harvester. *International Journal of Agricultural and Biological Engineering*, 12(2), 90-97.

[25] Toledo, M., Siles, J., Gutiérrez, M., & Martín, M. (2018). Monitoring of the composting process of different agroindustrial waste: Influence of the operational variables on the odorous impact. *Waste Management*, 76, 266-274.
[26] Zhang, X. (2018). Vibration control method for a crawler-type combine harvester. *Emirates Journal of Food and Agriculture*, 30, 873-882.

Денис Миколайович Можарівський[1], Людмила Леонідівна Тітова[1], Олександр Васильович Надточій[1], Петр Дасіч[2]

[1]Національний університет біоресурсів і природокористування України
03041, вул. Героїв Оборони, 15, м. Київ, Україна

[2]Вища технічна школа механіки
21000, вул. Шкільна, 1, м. Новий Сад, Сербія

Аспекти експертної системи інженерного менеджменту технічним станом зернозбиральних комбайнів

Анотація. Забезпечення продовольчої незалежності країни – одне з найважливіших завдань, успішне вирішення якого залежить від ефективного функціонування галузей агропромислового комплексу. Основною умовою у вирішенні питань технічного забезпечення аграрних підприємств є висока якість та конкурентоспроможність української сільськогосподарської техніки, зокрема зернозбиральних комбайнів. У підвищенні ефективності використання зернозбиральних комбайнів, своєчасному виявленні та запобіганні технологічним і технічних відмовам велика роль належить інженерному менеджменту. На практиці при використанні складної збиральної техніки одним з найважливіших завдань є технологічне регулювання машини в польових умовах. Це завдання належить до класу трудомістких інженерних завдань. В основному вирішення проблеми інженерного менеджменту зернозбиральних комбайнів покладається на оператора та залежить від його кваліфікації. Труднощі з вирішенням завдання технологічного регулювання пов'язані з невизначеністю інформації про фактори зовнішнього середовища, в якій функціонує зернозбиральний комбайн, а також складністю та недостатньою вивченістю взаємозв'язків між факторами збирання, регулювальними параметрами та показниками якості роботи комбайна. Тому на особливу увагу заслуговують питання розробки систем інформаційної підтримки інтелектуальної діяльності оператора, які допомагають йому при проведенні збиральних робіт. Одним з таких перспективних напрямів є розробка експертних систем для предметної галузі, що розглядається. Мета – обґрунтувати аспекти інженерного менеджменту технічним станом зернозбирального комбайна і функції практичного застосування в інформаційній технології. Методологія – експертна система інженерного менеджменту технічним станом зернозбиральних комбайнів може працювати в двох режимах: набуття знань та рішення задач. В статті представлено результати синтезу спілкування в системі "зернозбиральний комбайн – комбайнер – майстер діагност". За результатами виробничих випробування табульовано відмови гідрообладнання та електрогідравліки комбайнів сімейства Славутич. Висновок - застосування експертної системи дозволило скоротити витрати часу на збір та аналіз інформації про технічний стан і прийняття рішення – вони більш ніж в чотири рази менше витрат часу на усунення несправностей. Наукова значимість – доведена правмірність існування на рівні значущості α=0,05 нульової гіпотези про те, що тривалість технічного діагностування дорівнює тривалості ремонту, та конкуруючої гіпотези – тривалість діагностування зернозбирального комбайна менша тривалості ремонту

Ключові слова: інтелектуальний аспект, інженерія, діагностування, робота комбайна

Machinery & Energetics
Vol. 13, No. 1. 2022

Journal homepage:
https://technicalscience.com.ua/en

UDC 6631.1.004
DOI: 10.31548/machenergy.13(1).2022.67-76

Ivan Rogovskii[1*], Bohdan Lyubarets[1], Kinga Borek[2]

[1]National University of Life and Environmental Sciences of Ukraine
03041, 15 Heroiv Oborony, Kyiv, Ukraine

[2]Institute of Technological and Natural Sciences of the National Research Institute
05090, 3 Grabska Alley, Falenty, Republic of Poland

Analyticity of non-stationary processes of change in diagnostic parameters of hydrostatic transmissions of harvesters

Abstract. The creation of competitive agricultural machinery on the world market is an urgent task. And the solution of this problem is primarily related to the issues of improving reliability. This is especially relevant for complex and therefore expensive agricultural machinery. It becomes an unacceptable luxury to operate combine harvesters where 50% of all working time is spent on downtime. These downtimes are associated with insufficient technical level and low reliability. Especially noteworthy is the low reliability of the drive elements. One of the ways to increase the energy saturation of complex agricultural machines is to replace mechanical gears for driving working bodies with hydraulic ones. The increase in the initial cost of the machine due to this can be compensated by reducing the cost of spare parts in further operation and reducing downtime. In the designs of Ukrainian and foreign manufacturers of agricultural machinery, a promising area today is the creation of a multifunctional hydro-mechanical drive. The purpose of the study is to confirm the existence of analytical approaches to describing non-stationary processes of changing the diagnostic parameters of hydrostatic transmissions of combine harvesters. The methodology is based on the Lagrange principle, developed elements of the fundamental provisions of the mechanics of continuous media with movable boundaries in relation to hydraulic drive systems of hydrostatic transmissions of combine harvesters, which allow expanding the field of research and modelling of diagnostics of these systems. The paper proves that in the field under study, the Bless method is a more effective method for numerically solving such systems of equations. It is shown that for one-dimensional motions of incompressible liquid media moving in the channel and bounded by mobile boundaries, the calculation is reduced to solving the equation $a(x, t)\ \ddot{x}=b(x, t)\ \dot{x}^2+c(x, t)$. Where $x=x(t)$ is the coordinate of the anterior or posterior boundary of the liquid medium moving in the channel. The authors of this study prove that this equation is a generalised Bernoulli equation for the case of motion of incompressible liquid media with moving boundaries. The proposed method allows calculating the dynamics of starting an ampulised hydraulic drive system for hydrostatic transmissions of combine harvesters with minimal volumes of 1...10% of gas cavities for storing the drive working fluid. The elements of the theory described above and the developed calculation methods allow expanding the field of research of dynamic modes of operation of hydraulic systems of the power drive of hydrostatic transmissions of combine harvesters in the process of filling the working fluid of hydraulic system channels with branches and hydraulic supports

Keywords: methodology, transmission, hydrostatics, efficiency, hydraulic systems

Article's History: Received: 13.10.2021; Revised: 10.01.2022; Accepted: 23.02.2022

INTRODUCTION

The operation of hydraulic systems of hydrostatic transmissions of combine harvesters in severe operating conditions is accompanied by complex high-speed hydrodynamic processes caused by the movement of liquid and gas-liquid media in the hydraulic channels and working cavities of hydraulic machines of these systems [1]. One of the most complex phenomena is the processes caused by the movement of these media, which have mobile boundaries [2]. These phenomena are mainly associated with the removal and filling of hydraulic channels and working cavities of hydraulic drive systems of hydrostatic transmissions of combine harvesters with working fluid [3]. They

Suggested Citation:
Rogovskii, I., Lyubarets, B.S., & Borek, K. (2022). Analyticity of non-stationary processes of change in diagnostic parameters of hydrostatic transmissions of harvesters. *Machinery & Energetics,* 13(1), 67-76.

*Corresponding author

are typical for dynamic modes of operation of hydraulic systems: during overloads, during transient modes, during adjustment, refuelling, starting, and stopping [4]. They constantly accompany the operation of volumetric hydraulic units of hydraulic drive systems of hydrostatic transmissions of combine harvesters [5]. In general, these processes are typical for the operation of hydraulic systems of hydrostatic transmissions of combine harvesters operating on the principle of displacement of working fluids [6].

Complex problems of hydromechanics of liquid media with moving boundaries arise when studying the phenomena of not complete, but partial filling with working fluid of the cavities of hydraulic cylinders of volumetric units of hydraulic systems of hydrostatic transmissions of combine harvesters [7]. These phenomena take place during cavitation, which occurs due to a decrease in fluid pressure anywhere in the channel [8]. They can appear, for example, when the gas pressure drops in the gas cavities of tanks for storing working fluids of hydraulic systems [9]. They occur when starting the hydraulic pump drive or in transient modes of their operation, when the speed of rotation of the pump shaft exceeds the calculated values [10]. In this case, the liquid does not have time to fill the channels of the hydraulic cylinders due to the high speed of rotation of the cylinder block or the low pressure at the pump inlet [11].

The considered processes of hydraulic systems of drives of hydrostatic transmissions of combine harvesters are characterised by a sharp release of gases dissolved in liquid, flow continuity breaks, they are accompanied by the phenomena of incomplete water hammer, flow separation from the walls of the main channels and their incomplete filling [12].

In general, the study of the processes of motion of liquid and gas-liquid media with moving interface of media such as: "liquid-gas" or "liquid-solid", "liquid-piston" refers to the tasks of hydromechanics with contact breaks of media [13]. The main content of these tasks is to determine the laws of motion of mobile boundaries of discontinuities [14]. After that, the calculation of other flow parameters does not cause significant difficulties [15]. As already noted [16], the phenomena and processes described above significantly affect the technical condition of hydrostatic transmissions of combine harvesters, but they are poorly understood. This is conditioned by their physical complexity, difficulties in calculating and modelling them, and limited possibilities for observing the features of these phenomena and measuring their physical parameters [17].

In addition, the scope of setting and solving problems of hydromechanics with moving boundaries of media for hydraulic drive systems is limited by the Euler principle traditionally used in hydraulics [18]. Studies show that here, along with the Euler principle, it is necessary to apply the Lagrange principle, which is more general in physical and mathematical terms, since it allows setting and solving problems of hydromechanics with moving boundaries of the medium [19]. Its use would allow developing the fundamental provisions of the mechanics of continuous media with moving boundaries in relation to dynamic problems of changing the diagnostic parameters of hydrostatic transmissions of combine harvesters [20]. This would significantly expand the areas of research and solving problems of hydromechanics of changing the diagnostic parameters of hydrostatic transmissions of combine harvesters, improve the quality, accuracy and reliability of calculations, and the adequacy of modelling real processes that accompany their work [21].

The purpose of the study is to confirm the existence of analytical approaches to describing non-stationary processes of changing the diagnostic parameters of hydrostatic transmissions of combine harvesters.

RESULTS AND DISCUSSION

The study considers the problem of calculating the characteristics of processes of one-dimensional unsteady motion of liquid media with moving boundaries in channels of complex geometric shapes. It is assumed that the area $\sigma(s)$ of the channel cross-section is a given function of the curved coordinate s counted along the channel axis. A liquid medium moves in the channel, bounded by two moving surfaces and the side surface of the channel: the boundaries of the medium. The areas of moving surfaces are equal to $\sigma_1(t)=\sigma[s_1(t)]$ and $\sigma_2(t)=\sigma[s_2(t)]$, the area of the side surface of the channel is equal to $\sum(t)$ (Fig. 1).

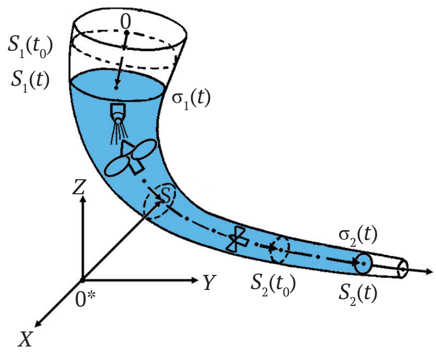

Figure 1. Movement of liquid media with movable boundaries in the channels of pipelines of hydraulic systems of drives of hydrostatic transmissions of combine harvesters

It is assumed that the pressure of a liquid medium on moving surfaces is given. Since the liquid medium considered here consists of the same liquid particles, and the boundary conditions of the problem are set at the moving boundaries of the medium, the Lagrange approach can be used as the most appropriate research principle in such cases.

The position of moving surfaces in the channel is determined by Euler curved coordinates $s_0(t)=s(\xi_1, t)$ and $s_2(t)=s(\xi_2, t)$, where ξ_1 and ξ_2 – Lagrange coordinates indicating the state of the surfaces under consideration at the initial time t=0. The movement of the liquid is carried out under the action of mass and surface forces. The main relations describing the patterns of movement of these surfaces in these channels are obtained. It is assumed that the pressure $p_1=p(s_1, t)$ and $p_2=p(s_2, t)$ on the surfaces of these boundaries are known functions of Euler coordinates s_1 and s_2, and time t.

The theory and calculation methods are based on general integral relations expressing the basic laws of mechanics of continuous media with moving boundaries (Fig. 1), namely, the laws of change: masses $m(t)$ of medium, its kinetic energy $E(t)$, the amount of movement $\bar{K}(t)$ of environment, and the moment $\bar{L}(t)$ of its quantities of motion are represented as equations:

$$\frac{dm}{dt} = \frac{d}{dt}\int_{V(t)} \rho dV = \int_{V(t)} \frac{d\rho}{dt} dV + \int_{\sigma_2(t)} \rho v_n d\sigma - \\ - \int_{\sigma_1(t)} \rho v_n d\sigma = \sum_{(i,j)} \dot{m_{i,J}} \tag{1}$$

$$\frac{dE}{dt} = \frac{d}{dt}\int_{V(t)} \rho \frac{1}{2} v^2 dV = \int_{V(t)} \frac{d}{d(t)} \\ [\rho \frac{1}{2} v^2] dV + + \int_{\sigma_2(t)} \rho \frac{1}{2} v^2 v_n d\sigma \\ - \int_{\sigma_1(t)} \rho \frac{1}{2} v^2 v_n d\sigma = \int_{V(t)} \rho \cdot \bar{f} \cdot \bar{v} dV + \\ \int_{\sigma_1(t)} \rho \cdot \overline{v_n} d\sigma - \int_{\sigma_2(t)} \rho \cdot \overline{v_n} d\sigma - \dot{D} + \sum_{(i,j)} \dot{E}_{i,j} \tag{2}$$

$$\frac{d\bar{K}}{dt} = \frac{d}{dt}\int_{V(t)} \rho \bar{v} dV = \int_{V(t)} \frac{d}{dt} \\ (\rho \bar{v}) dV + + \int_{\sigma_2(t)} (\rho \bar{v}) v_n \cdot d\sigma - \int_{\sigma_1(t)} (\rho \bar{v}) v_n \cdot d\sigma = \\ \int_{V(t)} \bar{f} \rho dV + \int_{\sigma_1(t)} \bar{p}_n d\sigma - \int_{\sigma_2(t)} \bar{p}_n d\sigma - \int_{\Sigma(t)} \bar{\tau}_n d\sigma + \sum_{(i,j)} \dot{\bar{K}}_{i,j} \tag{3}$$

$$\frac{dL}{dt} = \frac{d}{dt}\int_{V(t)} (\bar{r} \, x \, \rho \bar{v}) dV = \int_{V(t)} \frac{d}{dt} \\ (\bar{r} \, x \, \rho \bar{v}) dV + \int_{\sigma_2(t)} (\bar{r} \, x \, \rho \bar{v}) \bar{v}_n d\sigma - \int_{\sigma_1(t)} \\ (\bar{r} \, x \, \rho \bar{v}) \bar{v}_n d\sigma = \int_{V(t)} (\bar{r} \, x \, \rho \bar{f}) dV + \int_{\sigma(t)} \\ (\bar{r} \, x \, \bar{p}_n) \, d\sigma + \sum_{(i,j)} \dot{\bar{L}}_{i,j} \tag{4}$$

where: $\bar{v}$ – vector of the absolute velocity of movement of a given particle of the medium, m/s; ρ, kg/m^3 – density of the medium; $\bar{f}$, m/s^2 and $\bar{\rho}=\bar{\rho}_n+\bar{\rho}_\tau$, N/m^2 – respectively, vectors of stresses of mass and surface forces acting on the particle of the medium and its surface; $\sum_{(i,j)} \dot{m}_{i,j}$, kg/s, $\sum_{(i,j)} \dot{E}_{i,j}$, W – the sum of the capacities of additional sources and effluents of mass and mechanical energy, respectively, located inside the moving medium; $\sum_{(i,j)} \dot{\bar{K}}_{i,j}$, kg·M/s^2, $\sum_{(i,j)} \dot{\bar{L}}_{i,j}$, kg·m^2/s^2 – the sum of the capacities of additional sources and drains and the moment of the amount of movement, respectively, located inside the moving medium; $\bar{r}$ – radius-vector drawn to a given point of the medium from point O* – the centre of its rotation (Fig. 1).

Notably, the integration region is mobile and depends on time t, s. Integral relations (1)-(4) will be used in deriving equations describing the processes of motion of incompressible liquid media with moving boundaries in the channels of hydraulic drive systems by vane and volumetric hydraulic machines, and with jet devices.

In the one-dimensional case for movement in the channel of a compressed liquid medium bounded by mobile surfaces $\sigma_1(t)$ and $\sigma_2(t)$ (Fig. 1), the above relations will take the form:

$$\int_{S_1}^{S_2} \frac{d\rho(s,t)}{dt} \sigma(s) \, ds + \rho(s_{2,},t) \, v(s_{2,},t) \sigma(s_2) - \\ - \rho(s_{1,},t) \, v(s_{1,},t) \sigma(s_1) = \sum_{(i,j)} m_{i,j} \tag{5}$$

$$\int_{S_1(t)}^{S_2(t)} \frac{d}{dt} [\rho(s,t)\bar{v}(s,t)] \sigma(s) ds + \rho(s_2,t)\bar{v}(s_2,t) v(s_2(t)\sigma(s_2) - \\ \rho(s_1,t)\bar{v}(s_1,t) v(s_1(t)\sigma(s_1) = \int_{S_1(t)}^{S_2(t)} \rho(s,t)\bar{f}(s,t)\sigma(s) ds + \\ \int_{\sigma_1(t)} \bar{p}_n d\sigma - \pi \cdot \int_{S_1(t)}^{S_2(t)} \bar{\rho}_\tau \cdot \delta(s) ds + \sum_{(i,j)} \bar{K}_{i,j} \tag{6}$$

$$\int_{S_1(t)}^{S_2(t)} \frac{d}{dt} \left[\frac{1}{2} \rho(s,t) v^2(s,t)\right] \sigma(s) ds + \\ \frac{1}{2} \rho(s_2,t) v^3(s_2,t) \sigma(s_2) - \frac{1}{2} \rho(s_1,t) v^3(s_1,t) \sigma(s_1) = \\ \int_{S_1(t)}^{S_2(t)} \rho(s,t) \bar{f}(s,t) \bar{v}(s,t) \sigma(s) ds + \\ p(s_1,t) v(s_1,t) \sigma(s_1) - p(s_2,t) v(s_2,t) \sigma(s_2) - \dot{D} + \sum_{(i,j)} N_{i,j} \tag{7}$$

$$\int_{S_1(t)}^{S_1(t)} \frac{d}{dt} [\bar{r}(s,t) \, x \, \rho(s,t) \bar{v}(s,t)] \sigma(s) ds + \\ [\bar{r}(s_2,t) \, x \, \rho(s_2,t) \, x \, \bar{v}(s_2,t)] \, \sigma(s_2) - \\ [\bar{r}(s_1,t) \, x \, \rho(s_1,t) \, x \, \bar{v}(s_1,t)] \, \sigma(s_1) = \\ \int_{S_1(t)}^{S_2(t)} [\bar{r} \, x \, \rho(s,t) \bar{f}(s,t)] \sigma(s) ds + \\ \int_{\sigma_1(t)} (\bar{r} \, x \, \bar{p}) d\sigma - \int_{\sigma_2(t)} (\bar{r} \, x \, \bar{p}) d\sigma + \sum_{(i,j)} L_{i,j} \tag{8}$$

where: $Y(s, t)$, m/s – the average absolute velocity of liquid particles in section s at time t; $p(s_1, t)$, $p(s_2, t)$, Pa –average pressure on moving surfaces; $\dot{D}$, W – the rate of dissipation of mechanical energy of the medium due to friction and eddy formation, equal to:

$$\dot{D} = \frac{1}{2} \lambda Q^3(t) \rho \int_{S_1(t)}^{S_2(t)} \frac{ds}{\sigma^2(s)\delta(s)} sign \, v \tag{9}$$

where: λ – coefficient of fluid energy loss in the Darcy-Weisbach equation; δ(s) – channel diameter, m.

Equation (9) can be used for all currents satisfying the condition $\lambda=\lambda(Re,\Delta_{III}/\delta)$, where Re – the Reynolds criterion, ΔW, m – height of the roughness bumps of the channel walls.

Notably, the form of writing conservation laws in the above form (5)-(8) is general, both in the Euler approach and in the Lagrange approach. The difference is as follows.

If the liquid medium moving in the channel has movable boundaries with coordinates $s=s_1(t)$ and $s=s_2(t)$, and consists of the same particles (Lagrange approach), then in this case $v\,(s_1 t) = \frac{ds_1}{dt}, v\,(s_2 t) = \frac{ds_2}{dt}$. If the area of the channel through which the liquid moves is bounded by fixed boundaries with coordinates $s_1=const=l_1$ and $s_2=const=l_2$ (Euler approach), then $v(s_1,(t)=v(l_1, t)$ and $v(s_2,(t)=v(l_2, t)$.

This form of notation is also valid in the case of the movement of a liquid medium bounded on one side by a stationary surface with a coordinate $s_1=const=l_1(v(s_1, t)=v_1(l_1, t))$, and on the other side – a movable surface with a coordinate $s_2(t), \left(v(s_2,t) = \frac{ds_2}{dt}\right)$. This case corresponds to filling in the channel.

This recording form is also valid if the channel is empty. In this case, the liquid medium is bounded, on the one hand, by a mobile surface with a coordinate $s_1(t)$, ($v(s_1, t)=\frac{ds_1}{dt}$), and on the other – a fixed surface with coordinates $const=l_2(v(s_2, t)=v_2(l_2, t))$.

For one-dimensional problems with moving boundaries of media $s_1(t)$ and $s_2(t)$ the relations for conservation laws, written as (6)-(8), can be obtained by formal time differentiation of the values $m(t)$ of the mass of a liquid, its kinetic energy $E(t)$, and the amount of motion $\bar{K}(t)$ of liquid, and the moment $\bar{L}(t)$ of its number of movements, represented, respectively, in the form of:

$$m(t) = \int_{S_1(t)}^{S_1(t)} \rho(s,t)\sigma(s) ds \tag{10}$$

$$E(t) = \frac{1}{2}\int_{S_1(t)}^{S_1(t)} \rho(s,t) v^2(s,t)\sigma(s) ds \tag{11}$$

$$\bar{K}(t) = \int_{s_1(t)}^{s_1(t)} \rho\,(s,t)\bar{v}(s,t)\sigma(s)ds \tag{12}$$

$$\bar{L}(t) = \int_{s_1(t)}^{s_1(t)} [\bar{r}(s,t) \text{x}\, \rho(s,t)\bar{v}\,(s,t)]\sigma(s)ds \tag{13}$$

Here the property of the derivative of the integral is used, which depends on the parameter t, when the integrand and the integration limits depend on this parameter:

$$\frac{d}{dt}\int_{s_1(t)}^{s_2(t)} f(s,t)ds = \int_{s_1(t)}^{s_2(t)} \frac{df(s,t)}{dt}ds + \frac{ds_2(t)}{dt} f(s_2(t),t) - \frac{ds_1(t)}{dt} f(s_1(t),t) \tag{14}$$

For incompressible liquid media, the law of conservation and energy conversion, considering the viscosity of the medium and the mobility of its boundaries, can be written in the form:

$$\frac{1}{2}\rho \int_{s_1(t)}^{s_2(t)} \frac{dv^2(s,t)}{dt}\sigma(s)ds + \frac{1}{2}\rho[v^2(s_2,t)\sigma(s)v(s_2,t) - v^2(s_1,t)\sigma(s_1)v(s_1 t)] = \rho \int_{s_1(t)}^{s_2(t)}[\cos(\bar{v},\bar{X}) \cdot f_x(t) + \cos(\bar{v},\bar{Y})\cdot f_Y(t) + \cos(\bar{v},\bar{Z})\cdot f_z(t)]v(s,t)\sigma(s)ds + p(s_1,t)v(s_1,t)\sigma(s_1) - p(s_2,t)v(s_2,t)\sigma(s_2) + \sum_{(i,j)} N_{i,j} - \frac{1}{2}\lambda \int_{s_1(t)}^{s_2(t)} \frac{ds}{\sigma^2(s)\delta(s)} Q^3(t) signv \tag{15}$$

For this case, the relations are valid:

$$\int_{s_1(t)}^{s_2(t)} \frac{dv^2(s,t)}{dt}\sigma(s)ds = \int_{s_1(t)}^{s_2(t)} \frac{d}{dt}\left[\frac{Q^2(t)}{\sigma(s)}\right]ds = \frac{dQ^2(t)}{dt}\int_{s_1(t)}^{s_2(t)} \frac{ds}{\sigma(s)} \tag{16}$$

Provided that mass forces manifest themselves only in the form of gravity forces:

$$f_x = f_y = 0,\ f_z = -g \tag{17}$$

$$\int_{s_1(t)}^{s_2(t)}[\cos(\bar{v},\bar{Z})\cdot f_z]\cdot v(s,t)\sigma(s)ds = g[Z(s_1) - Z(s_2)]Q(t) \tag{18}$$

where $[Z(s_1)\text{-}Z(s_2)]$ – the difference in the heights of the centres of the surfaces of movable borders above an arbitrary horizontal plane (Fig. 1). Considering the above ratios:

$$\frac{1}{2}\rho\frac{dQ^2}{dt}\int_{s_1(t)}^{s_2(t)}\frac{ds}{\sigma(s)} + \frac{1}{2}\rho\left[\frac{1}{\sigma^2(s_2)} - \frac{1}{\sigma^2(s_1)}\right]\cdot Q^3(t) = [p(s_1,t) - p(s_2,t)]\cdot Q(t) + g\rho[Z(s_1) - Z(s_2)]\cdot Q(t) - \frac{1}{2}\rho\left[\lambda\int_{s_1(t)}^{s_2(t)}\frac{ds}{\sigma^2(s)\sigma(s)} + \sum_{(k)}\frac{\zeta_k}{\sigma_k^2}\right]\cdot Q^3(t) + \sum_{(i,j)} N_{i,j} \tag{19}$$

where ζ_k – in general, the time-dependent coefficient ofk-th local hydraulic resistance located at some point in the channel. For $Q(t)\neq 0$:

$$\rho\frac{dQ}{dt}\int_{s_1(t)}^{s_2(t)}\frac{ds}{\sigma(s)} + \frac{1}{2}\rho\left[\frac{1}{\sigma^2(s_2)} - \frac{1}{\sigma^2(s_2)}\right]\cdot Q^2(t) = p(s_1,t) - p(s_2,t) + g\rho[Z(s_1) - Z(s_2)] - \frac{1}{2}\rho\left[\lambda\int_{s_1(t)}^{s_2(t)}\frac{ds}{\sigma^2(s)\sigma(s)} + \sum_{(k)}\frac{\zeta_k}{\sigma_k^2}\right]\cdot Q^2(t) + \sum_{(i,j)}\Delta p_{i,j} \tag{20}$$

where $\sum_{(i,j)}\Delta p_{i,j} = \frac{1}{Q}\sum_{(i,j)} N_{i,j}$.

Counting (for certainty) in this equation $Q = \frac{ds_2}{dt}\sigma(s_2)$ and given that:

$$\frac{d}{dt}\sigma(s_2) = \frac{d}{dt}\sigma[s_2(t)] = \sigma'(s_2)\frac{ds_2}{dt},\ \sigma'(s_2) = \frac{d\sigma}{ds}, s = s_2 \tag{21}$$

and also that:

$$\frac{dQ}{dt} = \frac{d}{dt}\left[\frac{ds_2}{dt}\sigma(s_2)\right] = \frac{d^2 s_2}{dt^2}\sigma(s_2) + \sigma'(s_2)\left(\frac{ds_2}{dt}\right)^2 \tag{22}$$

obtain:

$$\rho\sigma(s_2)\int_{s_1(t)}^{s_2(t)}\frac{ds}{\sigma(s)}\ddot{s}_2 + \frac{1}{2}\rho\sigma^2(s_2)\left[\frac{1}{\sigma^2(s_2)} - [\frac{1}{\sigma^2(s_1)} + 2\frac{\sigma'(s_2)}{\sigma^2(s_2)}\int_{s_1(t)}^{s_2(t)}\frac{ds}{\sigma(s)}\right]\cdot \dot{s}_2^2 = p(s_1,t) - p(s_2,t) + \rho g[Z(s_1) - Z(s_2)] - \frac{1}{2}\sigma^2(s_2)\left[\lambda\int_{s_1(t)}^{s_2(t)}\frac{ds}{\sigma^2(s)\sigma(s)} + \sum_{(k)}\frac{\zeta_k}{\sigma_k^2}\right]\cdot\dot{s}_2^2\, sign\,\dot{s}_2 + \Delta P \tag{23}$$

If it is accepted that $Q(t) = \frac{ds_1}{dt}\sigma(s_1)$, then the equation written above will have the form:

$$\rho\sigma(s_1)\int_{s_1(t)}^{s_2(t)}\frac{ds}{\sigma(s)}\ddot{s}_1 + \frac{1}{2}\rho\sigma^2(s_1)\left[\frac{1}{\sigma^2(s_2)} - \frac{1}{\sigma^2(s_1)} + 2\frac{\sigma'(s_1)}{\sigma^2(s_1)}\int_{s_1(t)}^{s_2(t)}\frac{ds}{\sigma(s)}\right]\cdot\dot{s}_1^2 = p(s_1,t) - p(s_2,t) + \rho g[Z(s_1) - Z(s_2)] - \frac{1}{2}\sigma^2(s_1)\left[\lambda\int_{s_1(t)}^{s_2(t)}\frac{ds}{\sigma^2(s)\sigma(s)} + \sum_{(k)}\frac{\zeta_k}{\sigma_k^2}\right]\cdot\dot{s}_1^2\, sign\,\dot{s}_1 + \Delta P \tag{24}$$

From equation (1) for the law of conservation of mass of a moving medium, in the absence of sources and drains of mass inside the liquid:

$$\frac{ds_1}{dt}\sigma(s_1) = \frac{ds_2}{dt}\sigma(s_2) \tag{25}$$

In this case, the acceleration of the boundaries of the moving medium is related by the equations:

$$\frac{d^2 s_1}{dt^2}\sigma(s_1) + \sigma'(s_1)\left(\frac{ds_1}{dt}\right)^2 = \frac{d^2 s_2}{dt^2}\sigma(s_2) + \sigma'(s_2)\left(\frac{ds_2}{dt}\right)^2$$

Relations (11) and (12) allow switching in equation (10) to a single variable, for example, $x(t)=s_2(t)$. The coordinate of the movable border is indicated by a lowercase letter x, in contrast to the X-axis designation, which is capitalised in Figure 1.

It follows from (11) that $\sigma(s_1)ds_1 = \sigma(s_2)ds_2$, hence, after integrating the left side of this equation within the range of ζ_1 to s_1 and the right one – within the limits of up to ζ_2 to s_2, obtain:

$$f(s_1) = f(\zeta_1) + f(s_2) - f(\zeta_2), \tag{26}$$

where:

$$f(y) = \int\sigma(y)dy,\ y = s_1, \zeta_1, s_2, \zeta_2. \tag{27}$$

Equations (13), (14) determine the relationship between the coordinates s1 and s2 in the form of:

$$s_1 = s_1(s_2) = s_1(\underline{x}) \tag{28}$$

or

$$s_2 = s_2(s_1) = s_2(x). \tag{29}$$

In case of a minor change in the area $\sigma'(s)$ of cross-section of the channel, components containing the derivative of the area along the coordinate, i.e., the value of $\sigma'(s)$, can be ignored. In the case of filling or emptying tanks with a spherical or conical surface, the value of $\sigma(s)$ should be considered.

Now equation (10) can be written for a single variable, for example, $x(t)=s_2(t)$, i.e., relative to the coordinate x anterior fluid boundary:

$$\rho\sigma(x)f_1(x)\ddot{x} + \frac{1}{2}\rho\left[1 - \frac{\sigma^2(x)}{\sigma^2[s_1(x)]} + 2f_1(x)\sigma'(x)\right]\dot{x}^2 = p[s_1(x),t] - p(x,t) + g\rho\{Z[s_1(x)] - Z(x)\} - \frac{1}{2}\rho\sigma^2(x)\left[\lambda f_2(x) + \sum\frac{I_k}{\sigma_k^2}\right]\dot{x}^2 + \Delta p \tag{30}$$

where:

$$f_1(x) = \int_{s_1(x)}^{x}\frac{ds}{\sigma(s)},\ f_2(x) = \int_{s_1(x)}^{x}\frac{ds}{\sigma^2(s)\delta(s)}$$

$$f_1(x) = \int_{s_1(x)}^{x} \frac{ds}{\sigma(s)},\ f_2(x) = \int_{s_1(x)}^{x} \frac{ds}{\sigma^2(s)\delta(s)}. \quad (31)$$

If equation (31) uses the independent variable $x(t)=s_1(t)$ using relation (30), which establishes the relation $s_2=s_2(s_1)=s_2(x)$, then the equation with respect to the coordinate x posterior fluid boundary is obtained:

$$\rho\sigma(x)k_1(x)\ddot{x} + \frac{1}{2}\rho\left[\frac{\sigma^2(x)}{\sigma^2[s_2(x)]} - 1 + 2k_1(x)\sigma'(x)\right] \dot{x}^2 = p(x,t) - p[s_2(x),t] + \rho g\{Z(x) - Z[s_2(x)]\} - \frac{1}{2}\rho\sigma^2(x)\left[\lambda k_2(x) + \sum_k \frac{\zeta_k}{\sigma_k^2}\right]\dot{x}^2 sign\,\dot{x} + \Delta p \quad (32)$$

where:

$$k_1(x) = \int_{x}^{s_2(x)} \frac{ds}{\sigma(s)},\ \ k_2(x) = \int_{x}^{s_2(x)} \frac{ds}{\sigma^2(s)\delta(s)}. \quad (33)$$

In the case when one of the intersections s_1 or s_2 is stationary (for example, when liquid is released through cross-section $s_2=l$ of channel), $x=s$ should be taken as the desired variable $x=s_1(t)$, that is, the coordinate of the posterior boundary. In this case, the equation (32) should use $s_2(x)=l$:

$$\rho\sigma(x)k_1(x,l)\ddot{x} + \frac{1}{2}\left[\frac{\sigma^2(x)}{\sigma^2(l)} - 1 + 2\sigma'(x)k_1(x,l)\right] \dot{x}^2 = p(x,t) - p(l,t) + \rho g[Z(x) - Z(l)] - \frac{1}{2}\rho\sigma^2(x) \left[\lambda k_2(x,l) + \sum \frac{\zeta_k}{\sigma_2^2}\right]\dot{x}^2 \mathrm{sign}\dot{x} + \Delta p \quad (34)$$

where:

$$k_1(x,l) = \int_{x}^{l} \frac{ds}{\sigma(s)},\ \ k_2(x,l) = \int_{x}^{l} \frac{ds}{\sigma^2(s)\delta(s)}. \quad (35)$$

In this general form, equation (34) can be used to determine the function $p=p(l, t)$. This function can be used to calculate the time change in pressure at an arbitrary (stationary) point l of the channel filled with working fluid. To do this, the expression for $p=p(l, t)$ is used, defined by equation (30), substituting the value $x(t)$, $\dot{x}(t)$, $\ddot{x}(t)$, found as a result of solving general equations, for example, (28) or (29).

Thus, the calculation of parameters that characterise the dynamics of motion of liquid media with moving boundaries in channels of complex geometric shapes can be reduced to solving the Cauchy problem for some ordinary nonlinear second-order differential equation with respect to the coordinate $x(t)$ one of the movable boundaries and allowed relative to the highest derivative. This equation can be reduced to the form:

$$\ddot{x}_i = f(x_i, \dot{x}_i, t) \quad (36)$$

It can be shown that the calculation of parameters that determine the dynamics of motion of liquid media with moving boundaries in branched channels with the number of moving boundaries equal to n+1 for example, when filling hydraulic lines with working fluid, it is reduced to solving the Cauchy problem for systems n of ordinary second-order differential equations with respect to coordinates xi of movable borders: $\ddot{x}_i=f(x_i, \dot{x}_i, t)$ $i=1...n$.

The equations obtained here are generalisations of the Bernoulli equation for the case of motion of liquid media with moving boundaries in channels of complex geometric shapes. Here is an example of using the Lagrange approach to calculate the motion characteristics of liquid media with moving boundaries in spherical coordinates. This approach is applied to constructing a model of the dynamics of a gas bubble in a gas-liquid medium. It was shown above that the main dynamic characteristics of the processes of one-dimensional motion of incompressible liquid media with moving boundaries in the channels of hydraulic lines, elements, and aggregates of hydraulic drive systems are described by ordinary nonlinear second-order differential equations of the form (34).

This type of equation allows directly determining the coordinates of the moving boundaries of a liquid medium, for example, the liquid flow front, the boundaries of the medium with a moving piston of a hydraulic cylinder, and the position of the surface of any other moving element bordering the liquid. The appearance of these equations also allows using the efficient methods specifically adapted to solve them.

The equations used in this paper, however, also have a specific feature due to the presence of discontinuous coefficients in them. The presence of such coefficients is determined by the need to consider (in the calculation process) in these equations additional terms that appear or "disappear" from the composition of this equation at a certain time. In this system of equations, new equations may appear or "disappear". This can be caused by the opening of valves, abrupt changes in the cross-sectional areas of hydraulic distributor channels during adjustment, and during transient modes of operation of hydraulic systems. Additional equations appear, for example, when starting injectors, vane, or volumetric pumps, and in other similar cases, when calculations need to take into account new sources or drains of mass, energy, amount of movement, or moment. This also happens when branches from the main lines of hydraulic systems are filled with liquid, in cases where new local hydraulic supports appear.

These features make it difficult to use standard programmes for solving systems of ordinary differential equations, for example, in the currently widely used MathCad mathematical environment. This is explained by the following.

The presence of discontinuous coefficients in the right-hand sides of ordinary differential equations written in Cauchy form makes it inefficient to apply many well-known methods for numerical integration of these equations. Thus, the use of one-step Runge-Kutta methods implies sufficient smoothness of the right-hand sides of equations and their derivatives. In addition, in these methods, to calculate the desired functions in the next step, it is necessary to calculate the value of the right side of equation (20) several times. This significantly increases the calculation time, since the right-hand sides of the equations described by the processes under study usually have cumbersome expressions. The Euler method is applicable in this case, but requires small integration steps, while providing little accuracy. The so-called k-step methods, which include methods based on finite-difference schemes of the Milne method, are not convenient in these cases, since when the coefficients of these equations are abruptly changed, it is necessary to calculate the beginning of the integration table fairly accurately each time, while, as a rule, one-step methods of the Runge-Kutta type are used. Evidently, all this significantly complicates the algorithm and the numerical calculation process itself, while increasing the calculation time.

The requirements for the device of mathematical support of CAD hydraulic drive systems lead to the need to search for such methods of numerical integration of equations that would have sufficient simplicity and efficiency in solving the problems described above. It is known that in the formal approach to the question of numerical integration, the Cauchy problem for equations of order above the first and their systems is reduced to the Cauchy problem for systems of first-order equations. However, methods specifically adapted to solve higher-order equations often turn out to be more rational.

These problems have led to the need to look for new ways and methods for solving systems of differential equations with ordinary derivatives containing discontinuous coefficients. Studies have shown that the Bless method was quite effective here. Its advantages are as follows. Firstly, this method is specifically designed for solving second-order differential equations. Secondly, this method has a very high accuracy: its error is about $0(h^6)$. Thirdly, in this method, at each step of numerical integration, it is enough to calculate the right-hand side of the differential equation only once, and only at the fifth step is refinement performed with high accuracy.

The essence of this method is explained by the example of solving a system of equations of the form (20). The essence of the method is to calculate in the next step (at the point t_{e+1}) of the desired vector function $\bar{x}(t)$ and its derivatives $\dot{\bar{x}}(t)$ and $\ddot{\bar{x}}(t)$ using relations:

$$\bar{x}(t_{k+1}) \approx \bar{x}(t_k) + h\cdot\dot{\bar{x}}(t_k) + \frac{1}{2}h^2\cdot\ddot{\bar{x}}(t_k).$$

$$\bar{x}(t_{k+1}) \approx \bar{x}(t_k) + h\ddot{\bar{x}}(t_k).$$

$$\ddot{\bar{x}}(t_{k+1}) = \bar{f}\left(\bar{x}(t_{k+1}), \dot{\bar{x}}(t_{k+1}), t_{k+1}\right),$$

where $t_{k+1}=t_k+h$; h – integration step.

In order to avoid a significant accumulation of errors in the calculation process, this method provides for updating vector functions every 5 steps $\bar{x}(t)$ and $\dot{\bar{x}}(t)$ with high accuracy (about $0(h^6)$). This is done using inequalities:

$$\bar{x}(t_{k+5}) \approx \bar{x}(t_{k+5}) + \frac{5}{24}h^2\cdot\frac{1}{2}(9\cdot\ddot{\bar{x}}(t_{k+4}) + 20\cdot\ddot{\bar{x}}\left(t_{k+1} - 29\cdot\ddot{\bar{x}}(t_k)\right) \tag{37}$$

$$\dot{\bar{x}}(t_{k+5}) \approx \dot{\bar{x}}(t_{k+5}) + \frac{1}{24}h\cdot\left(11\cdot\ddot{\bar{x}}(t_{k+5}) + 5\cdot\ddot{\bar{x}}(t_{k+1}) - 16\cdot\ddot{\bar{x}}(t_k)\right) \tag{38}$$

Thus, in the calculation process, at each step of calculating the values of coordinates and velocities of movement of the moving boundary, the right-hand sides of the system of equations (37) and (38) are calculated only once. This significantly reduces the calculation time compared to other methods, where it is necessary to calculate the right-hand sides of the system of equations several times before taking the next step in time.

As already noted, this circumstance is very large with cumbersome expressions for the right-hand sides of the above system of equations. Given the importance of this circumstance, it is the latter feature that is characteristic of systems of equations describing the dynamics of the hydraulic systems under study.

A comparative analysis of the known methods for numerically solving ordinary second-order differential equations shows that the most widely used method for solving them, the Runge-Kutta method, is a method of only the fourth order of accuracy, it gives an error of the solution of order $0(h^4)$. Here, to take the next step in time, it is necessary to calculate the value of the right-hand side of the system of equations (38) four times. Although the Runge-Kutta method meets the most demanding requirements for the accuracy of numerical methods, its use, however, implies sufficient smoothness of the right-hand sides of equations and their derivatives. It is these conditions that are not met when calculating the characteristics of the processes studied here.

Comparison with other methods of numerical integration of second-order differential equations, for example, with the "polyline" method, shows the disadvantages of this method, since it also requires sufficient smoothness of the obtained solutions. Therefore, it is the Bless method that meets the highest requirements for the accuracy of calculation and the cost of machine time. It also has clear advantages over other methods in terms of universality and applicability to solving systems of second-order equations with discontinuous coefficients.

All these arguments allowed recommending the Bless method for numerically solving problems of dynamics of one-dimensional motion of incompressible liquid media with moving boundaries in the channels of hydraulic lines and machines of the hydraulic systems under study. A deeper and more comprehensive analysis of this method would allow applying it in the future for CAD of promising hydraulic systems as the most accurate, simple, and effective method.

In the introduction, it was noted that when filling channels with narrowing and branches with liquid, phenomena occur in the liquid that significantly affect the dynamics of the filling process of these channels [106, 108]. These phenomena are mainly associated with a narrowing of the fluid flow when filling these channels. When studying these phenomena, difficulties arise in determining the compression ratio ε of the liquid jet in these channels. For local hydraulic resistances of complex geometric shapes with narrowing of channels, this value is necessary to determine the pressure increase at the time of water hammer associated with flow inhibition due to narrowing of the channel when it is filled.

For local hydraulic resistances of complex geometric shapes, difficulties are determined by the fact that the value of the abrupt decrease in the fluid velocity due to impact when filling a channel with this resistance is unknown. The value of the compression ratio of the jet formed at the moment of incomplete hydraulic impact is also not known (Fig. 2). These circumstances do not allow the Zhukovsky formula for incomplete hydraulic shock to be used directly for this case. The simplest scheme of the process under consideration is shown in Figure 2.

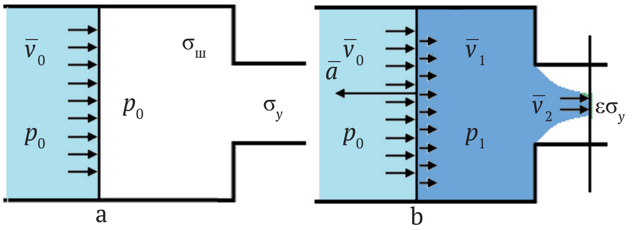

Figure 2. Calculation scheme of incomplete water hammer when filling a channel with a narrowing: a – before the impact, liquid parameters with the number 0; b – after the impact, parameters with the numbers 1 and 2

Figure 2 shows $\bar{a}$ vector of the speed of a water hammer sound wave. The area of fluid after impact is bounded by sections 1 and 2.

Next, the study considers the basic physical picture of the process under study and builds its mathematical model. The necessary relations are obtained for calculating the value ε of the compression ratio of the liquid jet, and the value ΔP of the shock pressure increase when filling a main line with hydraulic resistance in the form of narrowing of the channel with a gas-liquid medium. It is assumed that when filling a compressed liquid or gas-liquid medium of a channel with local hydraulic resistance (in the form of a sharp narrowing of the channel, see Figure 2) the flat front of the liquid flow (before it hits the local hydraulic resistance) moves at a speed of v_0 (Fig. 2a; cross-section 0-0). The pressure of the medium, in this case – air, in front of the liquid flow front is equal to p_0. When the liquid front hits the local hydraulic resistance under study, an increased pressure wave occurs in the liquid p_1 (Fig. 2b; cross-section 1-1). This wave begins to propagate against the current at the speed of sound a. In this case, the speed of movement of liquid particles behind the shock wave decreases by a jump to the value of v_1. Shock pressure increase $\Delta p=p_1-p_0$ in this case, is determined by the Zhukovsky formula for incomplete hydraulic shock:

$$\Delta p=\rho a(v_0-v_1), \tag{39}$$

where ρ – liquid density, kg/m^3.

Speed v_1 is not known. It is known that due to the short duration of the impact, the flow of compressed fluid in the obstacle area with a good approximation can be considered non-viscous and weightless ($Re\to\infty$, $Fr\to\infty$). Therefore, its flow through the narrowing of the channel can be considered in a one-dimensional approximation as a jet with a flat front (Figure 2b, cross-section 1-1, 2-2). The speed v_2 of the flow front is determined by the fluid parameters R_1 and v_1 by the compression wave in Figure 2b this area is more darkened, and also – the value of the coefficient ε of jet compression and pressure R_2 on the free surface of the jet. Therefore, in the region of a compressed liquid, the energy equation can be used in the form of the well-known Bernoulli relation, which here is an expression of the law of conservation and transformation of energy for an ideal liquid:

$$p_1-p_2=\rho(v_2^2-v_1^2)/2. \tag{40}$$

Speed v_1 and v_2 are related here by the ratio of continuity of the liquid flow in the form of equality:

$$v_1\sigma_1=\varepsilon v_2\sigma_2, \tag{41}$$

where σ_1 and σ_2 – the area of the corresponding cross-sections of the channel.

The latter relation is the law of conservation of the mass of the liquid flow for the case under consideration. It should be noted, however, that the front of the fluid filling the trunk is usually frothy and blurry. In addition, with strong geometric narrowing of the channels in local hydraulic resistances at the flow front, even before the impact, a gradual increase in pressure is observed, due to the fact that (as the front approaches the obstacle) the gas in front of the flow front is compressed. These features of the filling process can significantly smooth out impact phenomena. Here, however, for the sake of simplicity of consideration, this is ignored and it is considered that $p_2=p_0$.

To calculate the value ε of the compression ratio of the jet (liquid or gas-liquid flow) at the moment of impact of the flow front on the resistance, and to determine the value Δp in the above cases, the results of experimental studies of ordinary operation of combine harvesters can be used.

Here, the value ε of the compression ratio of the flow jet at the time of incomplete hydraulic impact is proposed to be calculated using the speed values established experimentally from the experiment v_0 at the moment when the front approaches this local hydraulic resistance, and the value Δp of incomplete hydraulic shock. The calculation of the value ε here is proposed to be performed using the equation obtained from the equality, which expresses the well-known laws of conservation of energy and mass, written above. Equation for calculating ε has the form:

$$\varepsilon = \bar\sigma\cdot\left[1+\frac{2\Delta\bar p}{M_0(1-\Delta\bar p)^2}\right]^{-\frac{1}{2}}, \tag{42}$$

where:

$$\Delta\bar p=\frac{\Delta p}{\rho a v_0};\ M_0=\frac{v_0}{a};\ \lambda=\left(\frac{\bar\sigma^2}{\varepsilon^2}-1\right)^{-1};\ \bar\sigma=\sigma_1/\sigma_2.$$

Studies have shown that if the value of ε is known in advance (for example, when it is already predefined visually or becomes known from at least one reliable experience, and obtained theoretically or calculated in the above way from experimental data), then it can be used in the future to determine the value Δp of hydraulic shock in a reasonably wide range of changes in full-scale conditions and the above values M_0 and ε.

In this case, the calculation $\Delta\bar p$ can use the equation:

$$\Delta\bar p=1+\frac{\lambda}{M_0}-\left[\left(1+\frac{\lambda}{M_0}\right)^2-1\right]^{\frac{1}{2}}, \tag{43}$$

where $\lambda=\left(\frac{\bar\sigma^2}{\varepsilon^2}-1\right)^{-1}$.

Evidently, the above equation is a converted Zhukovsky formula to a form that makes it possible to determine the impact pressure increase Δp in the main line at known values of the flow front velocity v_0 at the moment of impact, the speed of sound a in a liquid, the geometric characteristic of the resistance $\bar\sigma=\sigma_1/\sigma_2$ of coefficient ε of jet compression.

Additional studies have shown that the method described above and the calculation equations (42) and (43) can also be used to determine the parameters of incomplete hydraulic shock in the event of a sudden partial overlap of a channel already filled with liquid or gas-liquid medium, for example, by a hydraulic distributor of the working fluid of a volumetric one (Fig. 3).

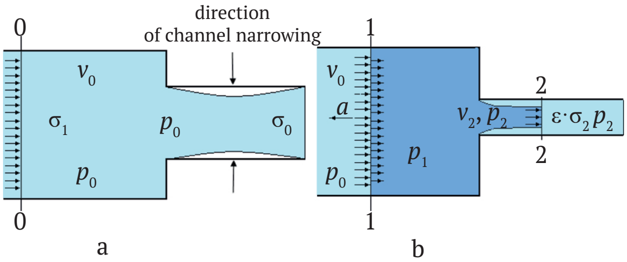

Figure 3. Diagram of fluid movement when the channel is partially blocked:
a – before the overlap (before the impact); b – after the overlap (after the impact)

It is important to note that the coefficient ε, according to the calculation, can be determined using any values of M_0 and $\Delta\bar{p}$ taken from a single experiment for a given local resistance. However, in this case, the question arises about the possible dependence ε from the change of M_0 and $\Delta\bar{p}$.

The studies described in this paper have shown that the values of ε determined experimentally by the equation (42) for washers, practically do not depend on the change of M_0 and $\Delta\bar{p}$. At the same time, the most significant circumstance for practice is that the definition of ε in this way, can be performed on small-sized laboratory models. For example, the value ε obtained for throttle washers with geometric characteristics $\bar{\sigma}$=3.04 and $\bar{\sigma}$=3.31 did not differ by more than 5 % from the above value ε=0.64.

These circumstances allowed determining experimentally (at the second stage of research) the values of ε for complex geometric resistances such as small-sized axial pumps or vane turntables of flow meters. In particular, the value ε for two different types of pumps were determined for small-size laboratory models. They turned out to be equal to 0.50 for the pump with $\bar{\sigma}$=2.53 and 0.56 – for the pump with $\bar{\sigma}$=2.26.

Studies have also shown that the value of the coefficient ε and for small-sized pump models, are practically independent of M_0 and $\Delta\bar{p}$, and can be taken as constant values for the studied values R_e. The values of the jet compression coefficients obtained in this way were used for theoretical calculations of shock pressure increases in various cases of filling with ordinary liquid and liquid containing undissolved gas bubbles.

Using values ε=*const*, dependencies were also calculated for $\Delta\bar{p}=\Delta\bar{p}(M_0)$, which were compared with experimental values $\Delta\bar{p}$. Analysis of these comparisons indicates that the accuracy of calculations of shock pressure increases, in this case, is acceptable for practice (Figure 4).

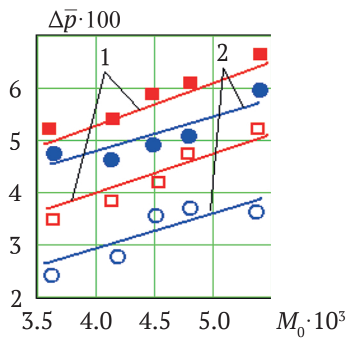

Figure 3. Calculation and experiment data

Note: ■ *– pump,* $\bar{\sigma}$*=2.53;* □ *– pump,* $\bar{\sigma}$*=2.26;* ○ *– washer,* $\bar{\sigma}$*=3.31;* ● *– washer,* $\bar{\sigma}$*=3.04; 1 – calculation for augers; 2 – calculation for washers.*

Thus, as a result of the research described above, elements of the theory were developed and a method for calculating the processes of incomplete water hammer that occurs when filling channels with local hydraulic resistances of complex geometric shapes with liquid or gas-liquid media was created. The developed method allows determining the coefficient ε of liquid jet compression and value Δp^{-} of relative impact pressure increase in case of incomplete hydraulic impact on local hydraulic resistance of complex geometric shape.

CONCLUSIONS

1. Coefficient ε can be defined using any values of M_0 and $\Delta\bar{p}$ taken from a single experiment for a given local resistance. However, in this case, the question arises about the possible dependence ε from the change of M_0 and $\Delta\bar{p}$.

2. The most significant circumstance for practice is that the definition of ε in this way, can be performed on small-sized laboratory models. For example, the value ε obtained for throttle washers with geometric characteristics $\bar{\sigma}$=3.04 and $\bar{\sigma}$=3.31 did not differ by more than 5% from the above value ε=0.64. These circumstances allowed determining experimentally, at the second stage of research, the values of ε for complex geometric resistances such as small-sized axial pumps or vane turntables of flow meters. In particular, the value ε for two different types of pumps were determined for small-size laboratory models. They turned out to be equal to 0.50 for the pump with $\bar{\sigma}$=2.53 and 0.56 – for the pump with $\bar{\sigma}$=2.26.

3. A method of engineering calculation is proposed. The method allows determining the coefficient ε of liquid jet compression and value $\Delta\bar{p}$ of relative impact pressure increase in case of incomplete hydraulic impact on local hydraulic resistance of complex geometric shape hydrostatic transmissions of combine harvesters.

REFERENCES

[1] Yezekyan, T., Marinello, F., Armentano, G., Trestini, S., & Sartori, L. (2020). Modelling of harvesting machines' technical parameters and prices. *Agriculture*, 10, 194-203.

[2] Diemer, R. (2019). Transport in the European Union – current trends and issues. *Mobility and Transport*, B-1049, 143-191.

[3] Isaac, N., Quick, G., Birrell, S., Edwards, W., & Coers, B. (2006). Combine harvester econometric model with forward speed optimization. *Applied Engineering in Agriculture*, 22, 25-31.

[4] Biaou, O., Moreira, J., Hounhouigan, J., & Amponsah, S. (2016). Effect of threshing drum speed and crop weight on paddy grain quality in axial-flow thresher (ASI). *Journal of Multidisciplinary Engineering Science and Technology*, 3(1), 3716-3721.

[5] Rogovskii, I.L., Titova, L.L., Voinash, S.A., Sokolova, V.A., Pushkov, Yu.L., Krivonogova, A.S., & Kokieva, G.E. (2020). Modeling the distribution of internal stresses in surface strengthened layer of steel parts after cementation and hardening. *Journal of Physics: Conference Series*, 1679, article number 042069.

[6] Dubbini, M., Pezzuolo, A., De Giglio, M., Gattelli, M., Curzio, L., Covi, D., Yezekyan, T., & Marinello, F. (2017). Last generation instrument for agriculture multispectral data collection. *CIGR Journal*, 19, 158-163.

[7] Nazarenko, I., Mishchuk, Y., Mishchuk, D., Ruchynskyi, M., Rogovskii, I., Mikhailova, L., Titova, L., Berezovyi, M., & Shatrov, R. (2021). Determiantion of energy characteristics of material destruction in the crushing chamber of the vibration crusher. *Eastern-European Journal of Enterprise Technologies*, 4(7(112), 41-49.

[8] Masek, J., Novak, P., & Jasinskas, A. (2017). Evaluation of combine harvester operation costs in different working conditions. *Engineering for Rural Development*, 16, 1180-1185.

[9] Xu, L., Wei, C., Liang, Z., Chai, X., & Li, Y. (2019). Development of rapeseed cleaning loss monitoring system and experiments in a combine harvester. *Biosystems Engineering*, 178, 118-130.

[10] Kavka, M., Mimra, M., & Kumhála, F. (2016). Sensitivity analysis of key operating parameters of combine harvesters. *Research in Agricultural Engineering*, 62(3), 113-121.

[11] Rogovskii, I.L., Titova, L.L., Voinash, S.A., Maksimovich, K.Yu., Galimov, R.R., Sokolova, V.A., Parfenopulo, G.K., & Taraban, M.S. (2020). Constructive method of increasing the durability of cultivator blades recovered by surface. *Journal of Physics*, 1679, article number 042076.

[12] Mráz, M., Urbanovičová, O., Findura, P., & Prístavka, M. (2019). Use of information systems to support decision making according to analysis machines. *Agricultural Machinery*, 2, 89-93.

[13] Partko, S.A., & Sirotenko, A.N. (2020). Self-oscillation in agricultural mobile machine units. *Journal Physics*, 1515, article number 042084.

[14] Šotnar, M., Pospíšil, J., Mareček, J., Dokukilová, T., & Novotný, V. (2018). Influence of the combine harvester parameter settings on harvest losses. *Acta Technologica Agriculturae*, 3, 105-108.

[15] Brown, R., & Richards, A. (2018). Engineering principles of agricultural machinery. *Journal of the ASABE*, 84(2), 1120-1132.

[16] Aldoshin, N., & Didmanidze, O. (2018). Harvesting lupines albus axial rotory combine harvesters. *Research in Agricultural Engineering*, 64(4), 209-214.

[17] Rogovskii, I.L., Titova, L.L., Voinash, S.A., Troyanovskaya, I.P., & Sokolova, V.A. (2021). Change of technical condition and productivity of grain harvesters depending on term of operation. *Earth and Environmental Science*, 720, article number 012110.

[18] Miu, V. (2016). Combine harvesters: Theory, modeling and design. *International Journal of Education and Research*, 6, 208-224.

[19] Yousif, A.L., Dahab, H.M., & El-Ramlawi, R.H. (2013). Crop-machinery management system for field operations and farm machinery selection. *Journal of Agricultural Biotechnology and Sustainable Development*, 5, 84-90.
[20] Bawatharani, R., Jayatissa, D., Dharmasena, D., & Bandara, M. (2013). Impact of reel index on header losses of paddy and performance of combine harvesters. *Tropical Agricultural Research*, 25(1), 1-13.
[21] Mimra, M., Kavka, M., & Kumhála, F. (2017). Risk analysis of the business profitability in agricultural companies using combine harvesters. *Research in Agricultural Engineering*, 63, 99-105.

Іван Леонідович Роговський[1], Богдан Святославович Любарець[1], Кінга Борек[2]

[1]Національний університет біоресурсів і природокористування України
03041, вул. Героїв Оборони, 15, м. Київ, Україна

[2]Інститут технологічних і природних наук Національного дослідницького інституту
05090, Grabska Alley, 3, с. Фаленти, Республіка Польща

Аналітичність нестаціонарних процесів зміни діагностичних параметрів гідростатичних трансмісій зернозбиральних комбайнів

Анотація. Створення конкурентоспроможних на світовому ринку сільськогосподарських машин є актуальним завданням. І вирішення цього завдання насамперед пов'язане із питаннями підвищення надійності. Особливо це поширюється на складну, а отже, і дорогу сільськогосподарську техніку. Стає недозволеною розкішшю експлуатувати комбайни, у яких 50 % всього робочого часу припадає на простої. Ці простої пов'язані з недостатнім технічним рівнем та низькою надійністю. Особливо слід зазначити низьку надійність елементів приводів. Одним із напрямів підвищення енергонасиченості складних сільськогосподарських машин є заміна механічних передач для приводу робочих органів на гідравлічні. Збільшення первісної вартості машини за рахунок цього може бути компенсовано зменшенням витрати запасних частин у подальшій експлуатації та скороченням часу простоїв. У конструкціях українських та зарубіжних виробників сільськогосподарської техніки перспективним напрямом на сьогоднішній день є створення багатофункціонального гідромеханічного приводу. Мета дослідження – підтвердити існування аналітичних підходів опису нестаціонарних процесів зміни діагностичних параметрів гідростатичних трансмісій зернозбиральних комбайнів. Методологія основана на принципі Лагранжа, розвинених елементів фундаментальних положень механіки суцільних середовищ з рухомими межами стосовно гідравлічних систем приводів гідростатичних трансмісій зернозбиральних комбайнів, що дозволяють розширити область досліджень і моделювання діагностування зазначених систем. В статті доведено, що в досліджуваній області більш ефективним методом чисельного рішення таких систем рівнянь є метод Блесса. Показано, що для одновимірних рухів нестискуваних рідких середовищ, що переміщаються в каналі і обмежених рухомими межами, розрахунок зводиться до вирішення рівняння $a(x, t)\ \ddot{x}=b(x, t)\ \dot{x}^2+c(x, t)$. Тут $x=x(t)$ – координата переднього або заднього кордону рідкого середовища, що переміщається в каналі. Авторами обґрунтовано, що це рівняння є узагальненим рівнянням Бернуллі на випадок руху нестискуваних рідких середовищ з рухомими межами. Запропонований метод дозволяє здійснити розрахунки динаміки запуску ампулізованої гідросистеми приводу гідростатичних трансмісій зернозбиральних комбайнів з мінімальними обсягами 1...10 % газових порожнин для зберігання робочої рідини приводу. Описані вище елементи теорії і створені методи розрахунку дозволяють розширити область дослідження динамічних режимів роботи гідросистем силового приводу гідростатичних трансмісій зернозбиральних комбайнів в процесі заповнення робочою рідиною каналів гідросистем з відгалуженнями і гідравлічними опорами

Ключові слова: методологія, трансмісія, гідростатика, ефективність, гідравлічні системи

ЗМІСТ

CONTENTS

ТЕХНІКА ТА ЕНЕРГЕТИКА

Науковий журнал

Том 13, № 1. 2022

Заснований у 2010 р. Виходить чотири рази на рік

Оригінал-макет видання виготовлено у відділі науково-технічної інформації
Національного університету біоресурсів і природокористування України

Відповідальний редактор:
Г. Івченко

Редагування англомовних текстів:
С. Воровський, К. Касьянов

Комп'ютерна верстка:
К. Сосєдко

Підписано до друку 29 квітня 2022 р. Формат 60*84/8
Умов. друк. арк. 9,3
Наклад 50 прим.

Адреса видавництва:
Національний університет біоресурсів і природокористування України
вул. Героїв Оборони, 15, м. Київ, 03041, Україна
E-mail: info@technicalscience.com.ua
www: https://technicalscience.com.ua/uk

MACHINERY & ENERGETICS

Scientific Journal

Volume 13, No. 1. 2022

Founded in 2010. Published four times per year

The original layout of the publication is made in the Department of Scientific and Technical Information of National University of Life and Environmental Sciences of Ukraine

Managing editor:
H. Ivchenko

Editing English-language texts:
S. Vorovsky, K. Kasianov

Desktop publishing:
K. Sosiedko

Signed for print of April 29, 2022. Format 60*84/8
Conventional printed pages 9.3
Circulation 50 copies

Editors Office Address:
National University of Life and Environmental Sciences of Ukraine
03041, 15 Heroiv Oborony, Kyiv, Ukraine
E-mail: info@technicalscience.com.ua
www: https://technicalscience.com.ua/en